Automated solid phase synthesis of oligosaccharides as tools for structural and functional analysis

Inaugural-Dissertation
to obtain the academic degree
Doctor rerum naturalium (Dr. rer. nat.)

submitted to the Department of Biology, Chemistry and Pharmacy
of Freie Universität Berlin

by

Alonso Pardo Vargas

2020

Supervisor: Prof. Dr. Peter H. Seeberger

Second examiner: Prof. Dr. Matthew Hopkinson

Date of defense: 04.03.2020

My thesis was independently composed/authored by myself, using solely the referred sources and support. I additionally assert that this thesis has not been part of another examination process.

The work in this dissertation was performed between January 2016 and December 2019 in the Department of Biomolecular Systems, Max Planck Institute of Colloids and Interfaces under the supervision of Prof. Dr. Peter H. Seeberger

Acknowledgements

First, I am grateful to my supervisor Prof. Peter Seeberger for his supervision and support throughout my Ph.D., also for giving me the possibility to work in the Biomolecular Systems department at the Max Planck Institute of Colloids and Interfaces.

I thank Prof. Dr. Matthew Hopkinson for kindly agreeing to review this thesis.

I thank current and former members of the Automation group, in particular to Dr. Kim Le Mai Hoang, Dr. Chandradhish Ghosh, Dr. Eric Sletten, Dr. Yuntao Zhu, Dr. José Danglad Dr. Abragam Joseph*, Mauro Sella* and Monica Guberman* for their friendship and their scientific support. I would also like to thank all members of Carbohydrate Materials group Dr. Martina Delbianco, Yang Yu, Dr. Vittorio Bordoni, Theodore Tyrikos, Giulio Fittolani, and Soeun Gim, not only for the valuable scientific discussion but for making a nice working atmosphere in the lab. I would like to express my gratefulness to Dr. Kim Le Mai Hoang, Dr. Martina Delbianco and Dr. Deborah Senf for proofreading my thesis.

My special thanks are extended to Eva Settels for her help with the HPLC and Dorothee Böhme for making sure everything worked as it should.

I thank all members of the Biomolecular Systems Department for the enjoyable working atmosphere, especially to sandwich Freitag group and the coffee people: Sandra Pinzon, Mara Guidi, Dr. Pietro Dallabernardina, Dr. Marco Mende, Jasmin Heidepriem, Alexandra Tsouka, Elena Shanina, Amiera Madani, Agata Baryzewska, Uwe Osswald, Grigori Paris, Cristian Cavedon, Antonella Rella, Ignacio Álvarez, Dr. Bartholomäus Pieber, and Dr. Jamal Malik who made lunch so much fun.

I´m deeply grateful to all my colleagues and friends that are no longer at MPI; Matthew Plutschack, Ankita Malik, Priya Bharate, Renee Roller, Sebastian Simonetti, Andrew Kononov, for a great time together. I would like to thank the Colombian community: Daniel Varon, Daniel Cruz, Viviana Correa, Lorena Ruiz and Sandra Pinzon for making me feel like at home being 9000Km away.

Finally, my gratitude goes to my family, especially to my mom Stella, Juan Pablo, Papá and abuelita for their constant support and love.

*Honorary members of automation group

Table of Contents

Summary

Automated Glycan Assembly (AGA) is introduced in chapther 1. AGA is a powerful technique for the solid-phase synthesis of oligosaccharides. These glycans have potential as analytical standards and as substrates for structural and functional analysis of different carbohydrate-degrading enzymes. AGA is based on the addition of different building blocks (BB) to a functionalized solid support; oligosaccharides of different lengths and branching patterns can be produced after iterative cycles of AGA. In chapter 2 AGA was employed to prepare the core structure of arabinomannosides (AM) from *M. tuberculosis*, containing α-(1,6)-Man, α-(1,5)-Ara and α-(1,2)-Man linkages. The introduction of a capping step after each glycosylation and further optimized reaction conditions (time and temperature) allowed for the synthesis of a series of oligosaccharides, ranging from hexa- to branched dodecasaccharides. These improvements towards a more robust AGA platform ensure high coupling efficiencies over long sequences. In a collaboration work with Dr. Abragam, the limits of AGA were surpassed, granting access to a 100-mer α-(1,6) polymannoside. The flexibility of AGA in the synthesis of long structures was demonstrated by the convergent block coupling. A set of oligosaccharide fragments prepared by AGA gave a multiple-branched 151-mer polymannoside, the largest polysaccharide prepared by any synthetic method to date. This collection of arabinomannosides was used as standards for the developing of a new analytical technique, namely, direct imaging of single glycan molecules with sub-nanometer resolution using scanning tunneling microscopy (STM). In collaboration with Dr. Xu Wu, direct visualization of mannosides at sub-nanometer resolution permitted the differentiation of α-(1,2) and α-(1,6) linkages together with the localization of the branching point at a single-molecule scale. This technique is expected to be useful for the identification of recurrent structural features of glycans with biological importance.

In Chapter 3 AGA was employed to synthesize a collection of six linear α-(1,6)-mannosides and seven β-(1,3)-glucans with specific β-(1,6) and β-(1,4) substitution patterns containing a free reducing end, using two different traceless photolabile linkers. These compounds were used to characterize carbohydrate-degrading enzymes obtained from marine sources. Synthetic α-(1,6)-mannosides permitted the characterization of the putative mannanase GH76A from *Salegentibacter sp*.. In collaboration with Dr. Solanki, a detailed 3D structure of the active site of GH76A was obtained after the co-crystallization of synthetic mannose tetramer

with mutant mannanase GH76. Incubation of these synthetic α-(1,6)-mannosides with GH76A generated hydrolyzed glycans, this suggested that the enzyme GH76A functions as an endo α-(1,6)- mannanase.

Zusammenfassung

Die automatisierte Oligosaccharidsynthese (AGA) ist eine leistungsstarke Technik für die Festphasensynthese von Oligosacchariden. Diese Glykane können als analytische Standards und als Substrate für die strukturelle und funktionelle Analyse von verschiedenen Kohlenhydrat-abbauenden Enzymen dienen. AGA basiert auf der Verknüpfung von verschiedenen Bausteinen (BB) an eine funktionalisierte Festphase; Oligosaccharide von verschiedenen Längen und Verzweigungen können durch iterative AGA Zyklen produziert werden. In Kapitel 2 wurde AGA angewendet, um die Kernstruktur von Arabinomannosiden (AM) aus *M. tuberculosis* herzustellen, die α-(1,6)-Man-, α-(1,5)-Ara- und α-(1,2)-Man-Verknüpfungen enthalten. Die Verwendung eines *Capping*-Schrittes nach jeder Glykosylierung und zusätzlich optimierte Reaktionsbedingungen (Zeit und Temperatur) haben die Synthese von einer Reihe von Oligosacchariden ermöglicht, die von Hexa- bis hin zu verzweigten Dodecasacchariden reichen. Diese Steigerung hin zu einer robusteren AGA-Plattform gewährleistet hoch effiziente Verknüpfungsschritte über lange Sequenzen. In Zusammenarbeit mit Dr. Abragam wurden die Grenzen der AGA übertroffen, wodurch der Zugang zu einem 100-mer α-(1,6) Polymannosid möglich wurde. Die Flexibilität der AGA in der Synthese von langen Strukturen wurde durch konvergente Synthese durch Blockverknüpfungen demonstriert. Ein Set von Oligosaccharid Fragmenten, welches mittels AGA hergestellt wurde, ergab ein mehrfach verzweigtes 151-mer Polymannosid, welches das bis heute größte Polysaccharid ist, das durch synthetische Methoden hergestellt wurde. Diese Bibliothek von Arabinomannosiden wurde als Standards für die Entwicklung von einer neuen analytischen Methode verwendet, nämlich der Bildgebung von einzelnen Glykanmolekülen mit sub-nanometer Auflösung durch die Verwendung von Rastertunnelmikroskopie (RTM, engl. STM). In Kollaboration mit Dr. Xu Wu war die direkte Visualisierung von Mannosiden in sub-nanometer Auflösung möglich und dadurch die Unterscheidung von α-(1,2)- und α-(1,6)-Verknüpfungen und die Lokalisation der Verzweigungen auf der Skala von einzelnen Molekülen. Diese Technik kann dafür benutzt werden, wiederkehrende strukturelle Merkmale von Glykanen zu identifizieren, die eine biologische Bedeutung haben.

In Kapitel 3 wurde die AGA verwendet, um eine Sammlung herzustellen, die sechs lineare α-(1,6)-Mannoside und sieben β-(1,3)-Glukane mit spezifischen β-(1,6) β-(1,4)-Substitutionsmustern mit einem freien reduzierenden Ende umfasst. Dafür wurden zwei

verschiedene photolabile Linker eingesetzt. Diese Verbindungen fanden Anwendung in der Charakterisierung von Kohlenhydrat-abbauenden Enzymen aus dem Meer. Synthetische α-(1,6)-Mannoside erlaubten die Charakterisierung der vermeintlichen Mannanase GH76A aus *Salegentibacter sp*.. In Kollaboration mit Dr. Solanki konnte nach Co-Kristallisierung des synthetischen Mannose Tetramers mit einer mutierten mannanase GH76 eine detaillierte 3D Struktur vom aktiven Zentrum von GH76A erhalten werden. Durch Inkubation der synthetischen α-(1,6)-Mannoside mit GH67A wurden hydrolysierte Glykane generiert, was darauf hinweist, dass das Enzym GH76A als endo α-(1,6)- Mannanase fungiert.

List of Publications

Publications

Pardo-Vargas A., Bharate P., Delbianco M., Seeberger P.H. **Automated Glycan Assembly of Arabinomannan Oligosaccharides from Mycobacterium tuberculosis**. *Beilstein Journal of Organic Chemistry*. **2019,** 15, 2936-2940. DOI: 10.3762/bjoc.15.288

Le Mai Hoang K., Pardo-Vargas A., Zhu Y., Yu Y., Loira M., Delbianco M., Seeberger P.H. **Traceless Photolabile Linker Expedites the Chemical Synthesis of Complex Oligosaccharides by Automated Glycan Assembly** *J. Am. Chem. Soc.* **2019**, 141, 22, 9079-9086. DOI: 10.1021/jacs.9b03769

Pardo-Vargas A., Delbianco M., Seeberger P.H. **Automated glycan assembly as an enabling technology**. *Current Opinion in Chemical Biology*. **2018**, 46:48-55. DOI: 10.1016/j.cbpa.2018.04.007

Patents

Pardo-Vargas A., Le Mai Hoang K., Angel J., Sletten E., Seeberger P.H. "Device for Rapid Automated Synthesis of Oligo- and Polysaccharides". Patent pending.

Pardo-Vargas A., Le Mai Hoang K., Angel J., Sletten E., Seeberger P.H. "Microwave-assisted Method for Synthesis of Oligo- and Polysaccharides on solid phase " Patent pending.

Conference Presentations

Pardo-Vargas A., Bharate P., Delbianco M., Seeberger P.H. **Automated Glycan Assembly of Arabinomannan Oligosaccharides from Mycobacterium tuberculosis.** Oral presentation delivered at Immunoshape international Symposium on glycoimmunology, San Sebastian, Spain, July 2018.

Pardo-Vargas A., Seeberger P.H. **A hybrid approach to sialylated glycan synthesis: combination of automated solid-phase and enzymatic synthesis.** Oral presentation delivered at 29th International Carbohydrate Symposium, Lisbon, Portugal, 2018.

Pardo-Vargas A., Le Mai Hoang K., Seeberger P.H. **Defined glycan structures as substrates to study hydrolases from marine bacteria.** Oral presentation delivered at Immunoshape meeting, Manchester, United Kingdom, December 2018.

Abbreviations

Ac: acetyl

ACN: acetonitrile

AM: arabinomannosides

AGA: Automated Glycan Assembly

Ar: aryl

Ara: arabinose

BB: building block

Bn: benzyl

Bu: butyl

Bz: benzoyl

Cbz: Carboxylbenzyl

CIP: contact ion pair

DABCO: 1,4-diazabicyclo[2.2.2]octane

DCE: 1,2-dichloroethane

DCM: dichloromethane

DIC: *N*,*N'*-diisopropylcarbodiimide

DMAP: dimethylaminopyridine

DMF: *N*-*N*-dimethylformamide

DBU: 1,8-diazabicyclo[5.4.0]undec-7-ene

ELSD: evaporative light scattering detector

ESI: electronspray ionization

ESI-IBD: electrospray ion beam deposition

Et: ethyl

EtOAc: ethyl acetate

FID: flame ionization detector

Fmoc: fluorenylmethyloxycarbonyl

FTIR: fourier transform infrared

GH: glycosyl hydrolase

Hex: hexane

HPLC: high performance liquid chromatography

HRMS: high resolution mass spectrometry

HSQC: heteronuclear single quantum coherence spectroscopy

HPAEC-PAD: high-performance anion-exchange chromatography coupled with pulsed amperometric detection

LC: liquid chromatography

Lev: levulinoyl

LevOH: levulinic acid

LG: leaving group

MALDI-TOF: matrix-assisted laser desorption/ionization-time of flight

Man: mannose

Me: methyl

MPIKG: Max-Planck-Institute for Colloids and Interfaces

MS: mass spectrometry

m/z: mass-to-charge ratio

NIS: *N*-iodosuccinimide

NMR: nuclear magnetic resonance

NP: normal phase

PG: protecting group

Ph: phenyl

rt: room temperature

RP: reversed phase

STM: scanning tunneling microscopy

TFA: trifluoroacetic acid

TfOH: triflic acid

THF: tetrahydrofuran

TMSOTf: trimethylsilyl triflate

UHV: ultra-high vacuum

UV: ultraviolet

WT: wild type

Symbols

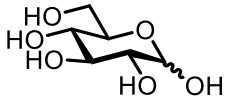

D-Glucose
(Glc)

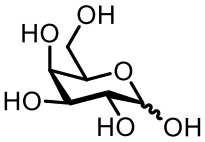

D-Galactose
(Gal)

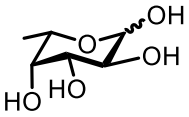

L-Fucose
(Fuc)

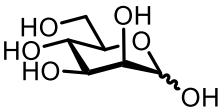

D-Mannose
(Man)

Solid Support

1. Introduction

This chapter has been modified in part from the following article:

Pardo-Vargas A, Delbianco M, Seeberger PH: **Automated glycan assembly as an enabling technology**. *Current Opinion in Chemical Biology* 2018, **46**:48-55. DOI: 10.1016/j.cbpa.2018.04.007

Carbohydrates are the most abundant biopolymers on earth.[1,2] Early perceptions propose glycan functions barely as structural support and energy reservoirs; however current studies reveal many critical functions of glycans regarding cell-glycans interactions[3] and their roles as regulatory switches,[4,5] cell-cell communication,[6] host-pathogen interactions,[7] among many others. Human cells are covered with glycans, many are found conjugated to proteins and lipids[1] with *N*- glycosylated and *O*- glycosylated proteins, the most well-studied. *N*- and *O*- glycosyl modifications affect the structure, function and stability of the protein. For example, *N*-glycan sites promote proper folding of newly synthesized polypeptides in the endoplasmatic reticulum (ER).[8] *O*-glycosylations in mucins act as lubricants in mucus.[9] Mixed *N*- and *O*-glycans are crucial to oocyte fertilization and embryogenesis development.[10]

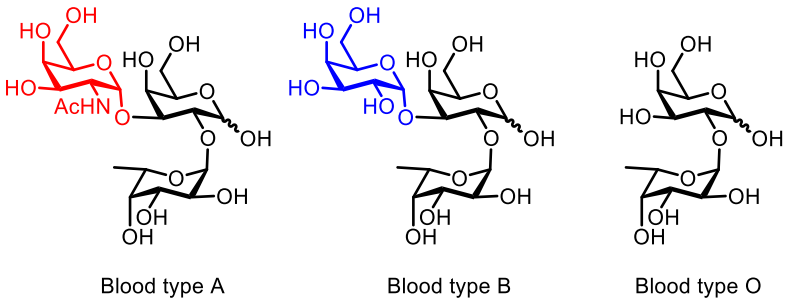

Figure 1.1 Antigenic glycan structures present on red blood cells determine the human blood groups.

1 Introduction

Glycolipids such as glycosylphosphatidylinositol (GPI) connect glycoproteins to membrane lipids and are involved in membrane trafficking.[11] Human blood group antigens are determined by small changes on the surface glycans of red blood cells (Figure 1.1).[1]

Deep and precise knowledge of the glycans biological functions is crucial for the development of pharmacological agents, such as the discovery of bacterial vaccines. Bacteria are covered by a dense outer layer of glycans called capsular polysaccharides (CPS).[12] CPS provide bacteria with a physical barrier for protection. Inducing an immune response against those specific bacterial glycans, e.g. CPS from *S. pneumonia* led to the development of Pneumovax® 23 and Prevnar®13 vaccines.[13,14] Current efforts to improve the vaccine include the incorporation of more *S. pneumonia* serotypes either via semisynthetic or fully synthetic routes.[15,16] Anticancer vaccines based on glycans are isolated under development after the discovery of tumor-associated carbohydrate antigens (TACAs) from many different forms of cancer like breast, colon, and lung. TACAs are glycans markers associated with cancer level of invasion and metastasis due to glycosylation changes in *N*-linked and *O*-linked glycans.[17-20] An anticancer vaccine including Globo H antigen, (Figure 1.2) targets CD1d receptors on the dendritic and NKT cell surfaces and is currently under clinical phase III studies against prostate and breast cancer.[21] Glycans can be used to boost the immune response in vaccines, for instance, the compound galactolipid KRN7000[22] (Figure 1.2) and they have been used as an adjuvant and an immune stimulator to boost the efficacy of the Globo H vaccine.[23]

Glycans have also been modified to generate synthetic drugs called glycomimetic. For example, Glucose glycomimetic 2-[^{18}F]Fluoro-2-deoxyglucose (^{18}F-FDG)[24] is transported into cells, where it accumulates as FDG-6-phosphate. The molecule acts as an indicator of glucose uptake, metabolism, and cell viability, for oncology PET imaging. Inhibitors of α-glucosidase like Glucobay, which decreases absorption of glucose is used for the treatment of type 2 diabetes mellitus.[25] Heparin glycomimetic Arixtra containing low molecular weight heparin and heparin sulfate serves as anticoagulants. The molecule binds to the anti-coagulant factor antithrombin (AT),[26] which inactivates several enzymes of the coagulation system, and now it is used in the treatment of patients with deep vein thrombosis and pulmonary embolism.

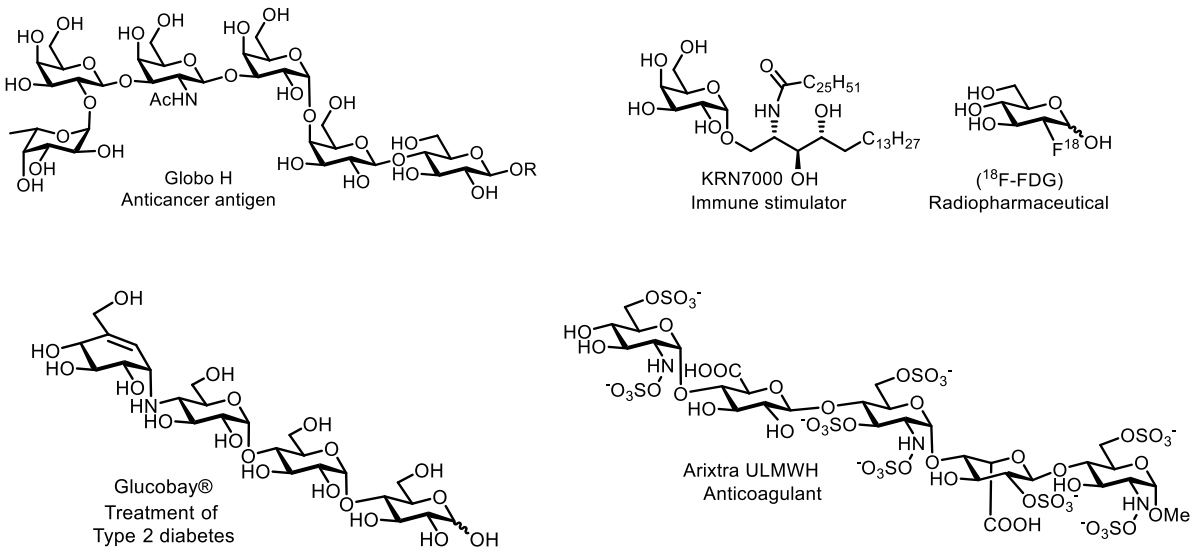

Figure 1.2 Glycan with relevant pharmacological activity.

1.1. Challenges in Carbohydrate Syntheses

Other biopolymers such as oligonucleotides (DNA and RNA) and proteins are well understood at the molecular level. For these biopolymers, automated sequencing and synthesis have fueled rapid progress in the development of molecular biology tools. The easy manipulation of polynucleotides in concert with gene expression technologies made pure proteins accessible, thereby advancing proteomics and genomics. [27] In contrast, knowledge of oligosaccharides in research fields such as molecular glycobiology is still in its infancy, in part, due to the inherent complexity of glycoproteins present in a single cell. Each protein can be glycosylated, often in multiple sites. Furthermore, a new stereogenic center is formed with each glycosidic linkage, creating a virtually endless number of possible structures.

The great glycan diversity makes purification from natural sources extremely challenging and not always feasible.[1] Hence access to structurally diverse and complex carbohydrate structures is either achieved by chemical or enzymatic synthesis. Enzymatic synthesis preparation of polysaccharides using glycosyltransferases or glycosynthases give high yields, with high regio- and stereo-specificity without the use of any protecting groups.[29] However, enzymes technology is not widespread and it is limited to some laboratories, further limits its flexibility. Thus, chemical synthesis is frequently the only way to obtain pure glycans. The total synthesis of glycans is based on the formation of glycosidic linkages and protecting group manipulations.[30] The synthetic chemical knowledge has improved to the point, where complex structures, such as a 92 unit arabinogalactan, can be prepared on a milligram scale. This reliable

but labor-intensive process often becomes a research project itself, since the overall synthesis takes many months or years to complete.[31, 32]

1.2. The Glycosylation Reaction

Complex oligosaccharides are made of monosaccharides, which are connected via glycosidic bonds. The precise formation of glycosidic bond is likewise a challenge in chemical synthesis since the reaction between a glycosylic donor and the hydroxyl group of the acceptor generates an additional stereocenter. The mechanism of a chemical glycosylation reaction is shown in Figure 1.3.

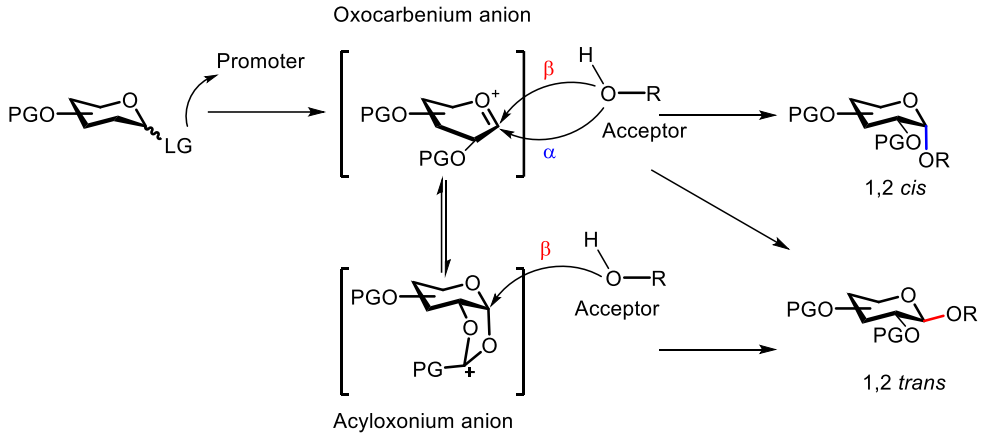

Figure 1.3 Mechanism of the glycosylation reaction without participating group (top) and with (bottom) a participating group.

The mechanism of the glycosylation reaction is not fully understood; however, certain pathways have been established. It is assumed that the glycosylic donor forms an oxocarbenium ion after activation with an electrophilic promoter which leads to irreversible elimination of the leaving group.[33] Recently, such oxocarbenium ion intermediate has been detected by IR spectroscopy under cryogenic conditions (Figure 1.3).[34] A new glycosidic bond is formed when the oxocarbenium ion is attacked by a hydroxyl group of the glycosylic acceptor. The acceptor can approach from either the upper face giving the 1,2-*trans* product (often β) or from the lower face, to give the 1,2-*cis* product (often α). Side-reactions increase the complexity of the glycosylation reaction; glycosylic donors can undergo elimination, hydrolysis, rearrangements, or orthoester formation.[35] Normally a mixture of both α and β isomers are obtained; however, several strategies have been developed to take control over the stereoselectivity. Group participation effect can influence the stereoselectivity. High 1,2-*trans* stereoselectivity is accessible using neighboring group participation at C-2 (Figure 1.3- Acyloxonium ion).

Typically, an ester protecting group is installed at C-2, which forms an acyloxonium ion complex with C-1. This intermediate blocks the α-face and leaves only the β-face free for the following attack of the glycosyl acceptor. As a result, 1,2-*trans* product is formed with high selectivity.[33, 36] Other ways to use protecting groups to influence the stereochemistry include the use of ester protecting groups at the C-6 position of the donor to remotely hinder the β-face through either sterical or electronic interactions.[37] This effect favors the attack on the α-face to promote the selective formation of 1,2-*cis* glycosidic bonds. Protecting groups can also lock the conformation of the donor and influence the stereochemical outcome of the reaction. For example, a 4,6-*O*-benzylidine ring can lock the conformation of mannoside donors to favor the challenging β-*cis*-mannoside linkage.[38] Temperature can influence the stereoselectivity of the glycosylation since the α-anomer is thermodynamically favored due to the anomeric effect. The anomeric effect stabilizes the axial configuration at C-1, via hyperconjugation between the unshared electron pair on the ring oxygen atom and the σ* orbital of the axial C-O bond at *cis*-C-1.[39] The solvent choice affects the stereoselectivity since glycosylation occurs through contact ion pair.[40] For example, the use of acetonitrile favors the formation of the β-product, since the solvent forms an adduct at the α-face, whereas ethereal solvent such as THF, diethylether, and 1,4-dioxane promote the α-product.[41,42]

A deep understanding of the glycosylation reaction has led to the successful synthesis of many complex oligosaccharides. However, obtaining pure natural and non-natural structures is a time-consuming process. Automated methods such as Automated Glycan Assembly (AGA) technologies were developed to facilitate reliable access to oligosaccharides, which provides users with valuable materials to better understand glycan structure-activity relationship for the development of molecular glycobiology and material science.

1.3. **Automated Solution-Phase Methods**

Most solution-based methods, aiming to accelerate the synthetic process by reducing the number of purification steps in between, are not fully automated and remain labor-intensive. The semi-automated computer-based one-pot synthesis is based on the sequential addition of building blocks (BBs) according to the difference in their reactivity as calculated by the OptiMer software. [43] (Figure 1.4-A) This conceptually attractive methodology requires many different mono-, di- and trisaccharide BBs. Another one-pot method is based on the anodic oxidation of the glycosylic donor in the presence of tetrabutylammonium triflate (Bu_4NOTf) in an electrolysis cell to generate the corresponding triflate donor. The thioglycoside acceptor is

then added and, upon glycosylation, the oxidation process is repeated. [44] An instrument was developed to control temperature, delivery of reagents, and the electrical potential of the reaction cell. DFT calculations are performed prior to synthesis to estimate the oxidation potentials of the building blocks. Recently, the synthesis of the GPI anchor core trisaccharide[45] and a TMG-chitotriomycin precursor [46] were reported.

Another method uses a fluorous tag linker that is coupled to the desired glycan to simplify purification. After, deprotection and chain elongation, the tagged compound is separated from the reaction mixture by fluorous solid-phase extraction (FSPE). (Figure 1.4-B) A robot can handle the solutions autonomously.[47] Linear and branched β-oligomannosides were synthesized using a β-directing C-5 participation strategy.[48, 49] Recently, automated fluorous-assisted synthesis using hypervalent iodonium as glycosylation promoter at ambient temperatures permitted the synthesis of a β(1,6)-glucan tetramer.[50] A renewable benzyl-type fluorous tag was prepared to reduce costs.[51] To date, FSPE technique can be applied only to the synthesis of short oligomers. Similar to the fluorous tag methodology, the hydrophobically assisted switching phase method (HASP) uses a hydrophobic tag to simplify the separation of the desired oligosaccharide from the reaction mixture. This strategy was illustrated in the context of a nonamannoside synthesis.[52]

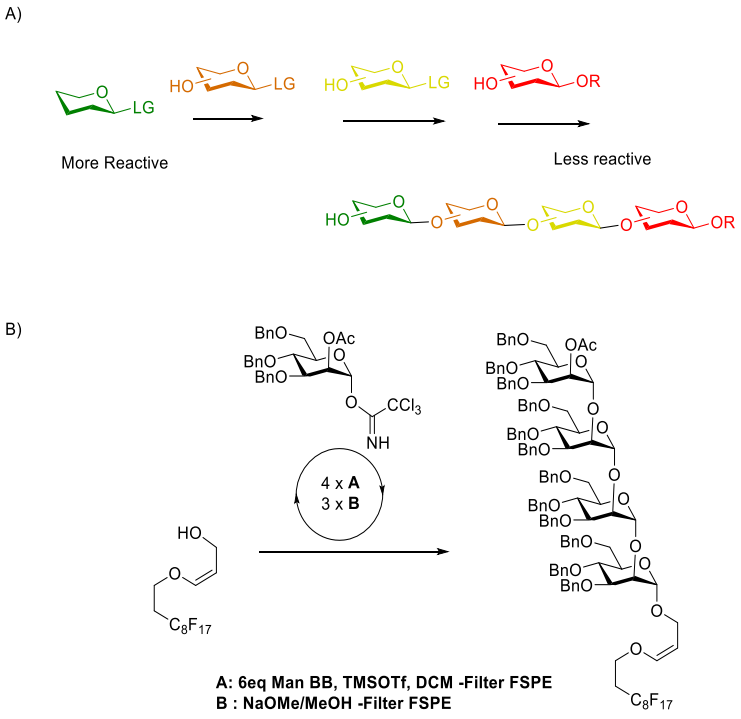

Figure 1.4 A) Scheme of one-pot synthesis of glycans B) Oligosaccharide Synthesis using fluorous tag.

1.4. **Solid-phase Methods**

Glycan solid phase synthesis is based on the peptide solid-phase synthesis principles introduced by Merrifield.[53] Glycosylation occurs in the interphase between the resin and the solution, afterward, the excess of reagents is removed by filtration, facilitating purification of the intermediates. Although solid supports were used also in carbohydrate synthesis since 1985[54] the first automated solid-phase oligosaccharide synthesis (Automated Glycan Assembly- AGA) was reported in 2001 by Seeberger, based on an adapted peptide synthesizer.[55] The desired oligosaccharide is assembled using repeating cycles of glycosylation, capping and deprotection steps on a polystyrene Merrifield resin. Iterations of the homemade synthesizer led to the development of the commercial version Glyconeer 2.1™ in 2015.[55-57]

1.4.1. The Linkers

In AGA the glycan is attached to the solid support via a linker that is cleaved upon completion of the assembly, affording the target compound. The linker has to tolerate the reaction conditions during the assembly process and permit the easy liberation of the final product. Following metathesis labile linker **1**[58] and base-labile linker **2,**[59] the photocleavable linkers were developed for their orthogonality to a wide range of reaction conditions (Figure 1.5). Photocleavable linkers are stable in both acidic and basic conditions and compatible with a wide variety of protecting groups including Nap, Fmoc, Lev, Bn and Bz. Aminoalkyl linker **3** affords conjugation-ready glycans.[60] Traceless linker **4** affords a free reducing end after the final deprotection.[61,62] The current challenge involves further development of the photocleavage efficiency, currently around 60-70%, to improve overall yields for AGA.

1.4.2. AGA Coupling Cycle

The glycosylation reaction is the key step during AGA. A collection of "approved" building blocks was developed and many BBs are now commercially available.[57] For each BB, key reaction parameters, such as activators, reaction temperatures, and equivalents of BB per cycle were optimized. To minimize the formation of deletion sequences, a large excess of sugar donor (ten equiv. per coupling step over two glycosylation cycles) was traditionally used to drive the reaction to completion.[57] An optimized reaction temperature and concentration permit the completion of the reaction with only one glycosylation cycle (five to eight equiv. of BB).[63]

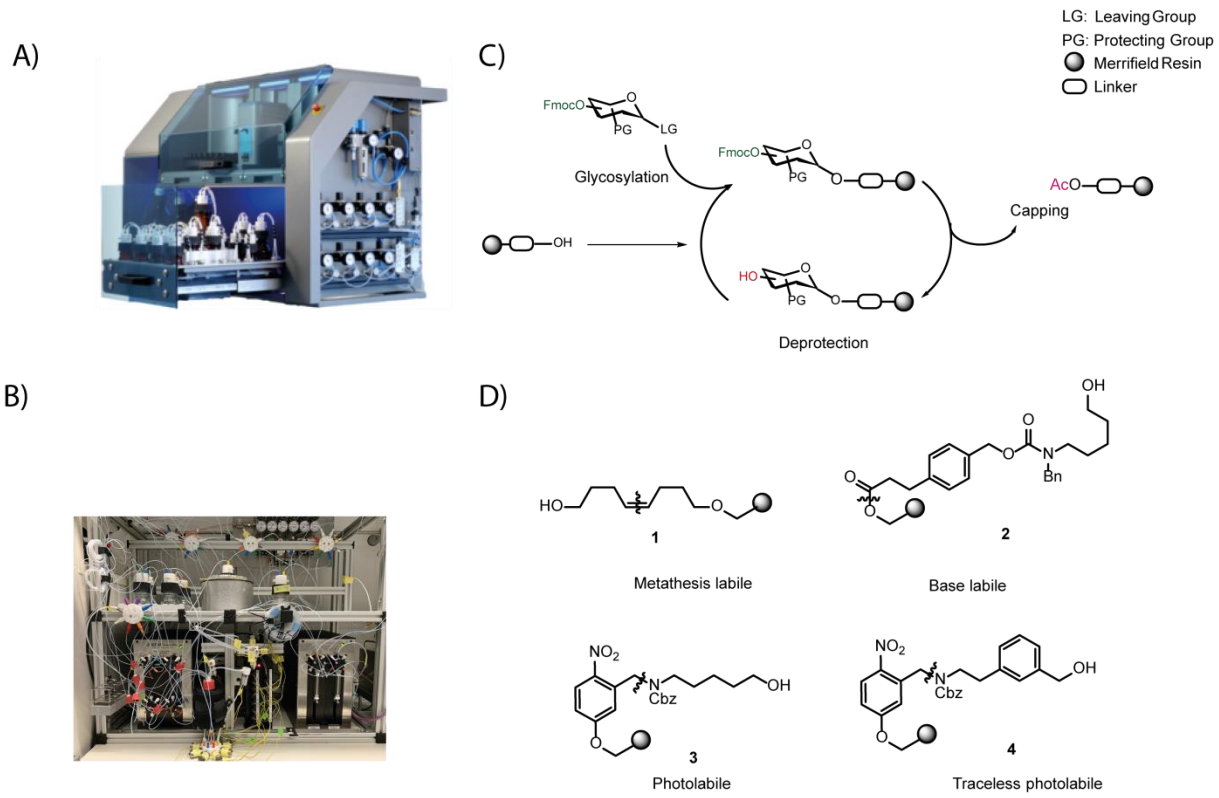

Figure 1.5 A) The commercial Glyconeer 2.1™ AGA synthesizer, B) Home-built AGA synthesizer, C) Overview of the coupling cycle, D) Linkers used for AGA.

To further improve the coupling cycle, a capping step was introduced to block any unreacted acceptor in less than 30 minutes by acetylation using methanesulfonic acid and acetic anhydride.[64] Capping is compatible with all the protecting groups used to date, increases the isolated yield of the desired compound and facilitates the purification of the reaction mixture by reducing the number of side-products. The capping step was tested for the assembly of a polymannoside (50-mer) resulting in a four-fold yield increase (20% yield) while reducing the amount of building block used by 33%.[65] Capping is now incorporated in the standard coupling cycle.

1.4.3. Synthetic Improvements

AGA had been mainly used to synthesize *trans*-glycosidic linkages, where the C-2 participating protecting group ensures stereoselective couplings. Since stereocontrol during *cis*-glycosylations cannot rely on C-2 participation, anomeric mixtures are normally observed. Oligosaccharides containing multiple *cis*-glycosidic linkages can be prepared efficiently by AGA using monosaccharide BBs equipped with acetyl or benzoyl esters as remote participating

protecting groups.[37] Nine biologically important structures containing *cis*-galactosidic and *cis*-glucosidic linkages were assembled (Figure 1.6).

Access to sialylated glycans remains challenging. In particular, glycosylation with *N*-acetyl-neuraminic acid (Neu5Ac) results in low yields and anomeric mixtures due to low reactivity and lack of stereocontrol. The attempt to produce α-(2,6) and α-(2,3) sialylated glycans by AGA using a sialyl-monomer was successful, albeit low yielding.[66] A combination where the glycan backbone is obtained by AGA and further functionalized with sialyltransferase (PmST1) permitted easy access to five (2,3)-sialylated glycans. [67]

Glycosaminoglycans (GAGs) are an important class of negatively charged glycans. Their structures are highly sulfated, representing one of the most challenging targets for carbohydrate chemists. Chondroitin sulfate GAGs with different sulfation patterns were prepared using a glucuronic acid BB and two *N*-acetyl-galactosamine BBs equipped with two temporary protecting groups. The Fmoc group was used for chain elongation and the orthogonal levulinoyl (Lev) esters marked the hydroxyl groups for sulfation. Fully protected chondroitin-6-sulfate and chondroitin-4-sulfate hexasaccharides were synthesized.[60,68] Keratan sulfates (KS) containing β-(1-4) galactose, β-(1-3) *N*-acetyl-galactosamine and different sulfation patterns were obtained following a similar approach. Three different temporary protecting groups were exploited: Nap and Lev esters for subsequent sulfation and Fmoc for chain elongation. The orthogonality of the protecting groups permitted to obtain four differently sulfated KS tetrasaccharides from a common tetrasaccharide precursor.[69]

Most of the previously described advancements were applied for the synthesis of oligosaccharides associated with blood group determinants.[70] Those are tumor-associated carbohydrate antigens (TACAs) and cancer vaccine candidates, also associated with immunodeficiency disorders, atherosclerosis, and Guillain–Barré syndrome. c*is*-Linkage formation, sulfation as well as the use of orthogonal temporary protective groups permitted the fast assembly of biologically relevant glycans including Lewis H-type I (3) and II (4) glycans.

1.4.4. Instrumentation

The commercial Glyconeer 2.1™ has been placed in several laboratories around the world.[56] The combination of this instrument with standardized purifications and quality-control techniques allows easy access to synthetic glycans.[56,71,72] The introduction of a novel

cianopyvaloyl (Piv-CN) protecting group into a rhamnose BB was key to the assembly of 16-mer oligorhamnans on the Glyconeer.[73]

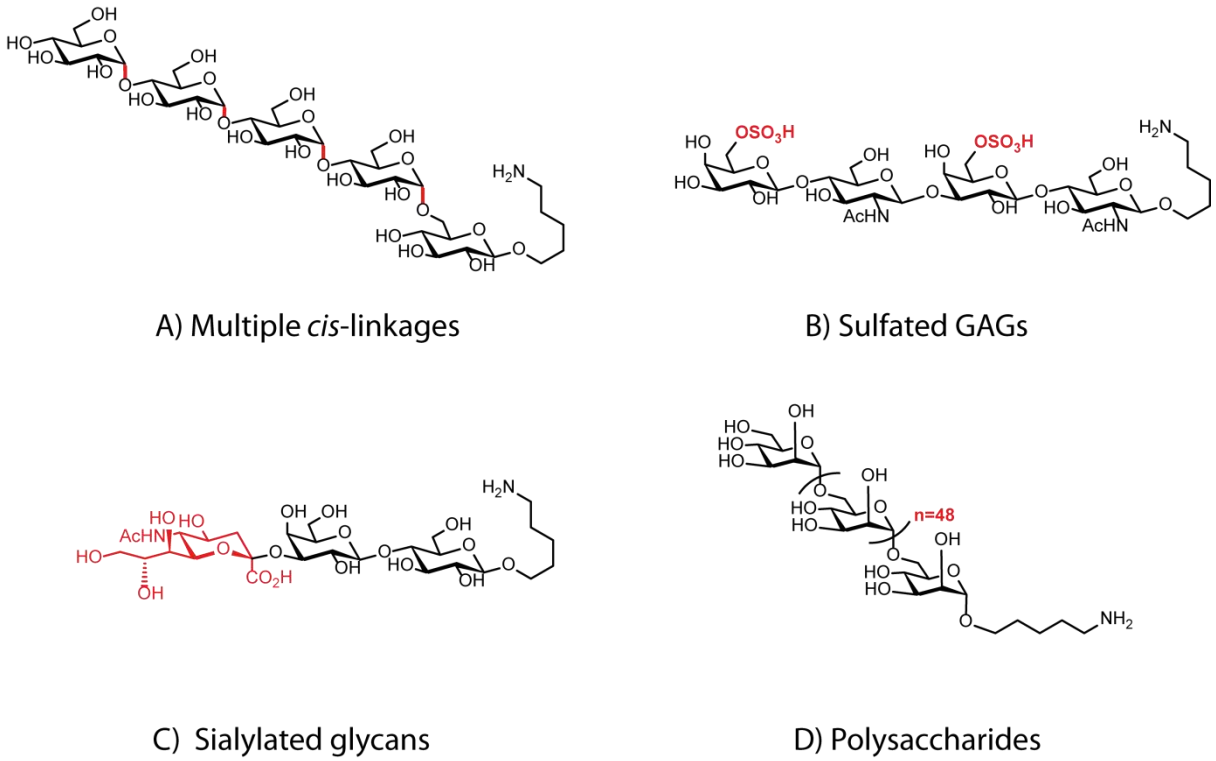

Figure 1.6 Recent AGA milestones include the synthesis of: A) oligosaccharides containing multiple *cis*-glycosidic linkages. B) sulfated GAGs C) sialylated glycans D) polysaccharides.

.

Efforts to develop an inexpensive synthesis instrument employed a modified HPLC.[39,74] A column packed with solid support is used as a reactor. A JandaJel resin functionalized with a base labile linker serves as the glycosyl acceptor. HPLC pumps are used to deliver the glycosyl donor (glucosyl imidate BB, five to ten equivalents) and the deprotection solution. The promotor is delivered through the autosampler. The synthesis is monitored using the integrated UV detector set at 254 nm. This simple set up has been limited to the production of a pentaglucoside so far. Temperature control throughout the synthesis and delivery lines for reagents will be key points to be addressed for further development of this system.

1.5. **Applications of Glycans Assembled by AGA**

1.5.1. Glycan Arrays

Glycan arrays are standard tools for the high throughput analysis of protein-carbohydrate interactions.[75] Antibodies associated with diseases, can be detected in biological samples on glycan microarrays.[75,76] Access to pure glycans for covalent attachment to a surface of the array remains a limiting factor. AGA is the ideal tool to create large collections of related compounds, permitting to study glycans with a medicinal chemistry approach. For example, conjugation-ready linear β-(1,3)- and branched β-(1,3)-β-(1,6)-glucan oligosaccharides were assembled and immobilized on microarrays. Incubation with human sera revealed that most individuals create antibodies that bind to linear glucan, but not to the non-protective branched analogs.[77] In another report, synthetic keratan sulfate analogs with different sulfation patterns obtained with AGA were printed on microarrays. Specific interaction between the disulfated KS tetrasaccharide and the adeno-associated virus AAVrh10 gene-therapy vector was observed.[69] AGA was also used to create glycans for determining the binding epitopes of a large number of plant cell-wall glycan-directed monoclonal antibodies (mAbs) using a microarray.[78-80] This information provided a tool for *in situ* cell wall labeling studies to gain detailed information on cell wall polysaccharides in model organism *Brachypodium distachyon*.[81] The binding specificities for 25 mAbs that recognize galactosylated xyloglucans (XG) structures were determined using the same approach.[82]

1.5.2. Enzyme Substrate Determination

The oligosaccharide fragments of plant glycans assembled by AGA were used to characterize the enzymes involved in biosynthesis. Plant arabinogalactan, glucan and arabinoxylan oligosaccharides were assembled to study the substrate specificity of β(1,4)-endogalactanases,[83] lichenase,[84] and to map the active site of GH10 and GH11 xylanases.[85] These findings have implications for the structural analyses of pectic polysaccharides. These plants oligosaccharides toolbox is currently applied to the characterization of biosynthetic enzymes as well as arabinogalactan- and arabinan-directed antibodies.[86]

1.5.3. Vaccine Development

Glycoconjugates containing synthetic oligosaccharides attached to a carrier protein are attractive candidates as semisynthetic vaccines against infectious diseases. Semisynthetic

oligosaccharides, resembling the capsular polysaccharides from *Streptococcus pneumonia* ST8, assembled with AGA, were combined with the marketed polysaccharide-based pneumococcal vaccine Prevnar13® while retaining the immunogenicity of both components.[15] Synthetic antigens from ST3, prepared by AGA, are tested as vaccine candidates.[87]

1.5.4. Materials Chemistry

The synthesis of 50-mer oligomannosides, the longest polysaccharides assembled from a single monomer, set the stage to use AGA for the investigations of carbohydrates as materials.[64,65] Well-defined oligo- and polysaccharides, resembling natural as well as unnatural structures, are ideal probes for the fundamental study of polysaccharides.[63] Molecular dynamics simulations suggested that different classes of polysaccharides adopt fundamentally different conformations. Single-site substitutions alter such conformations and thus permits tuning the shape and properties (*i.e.* solubility) of such compounds.

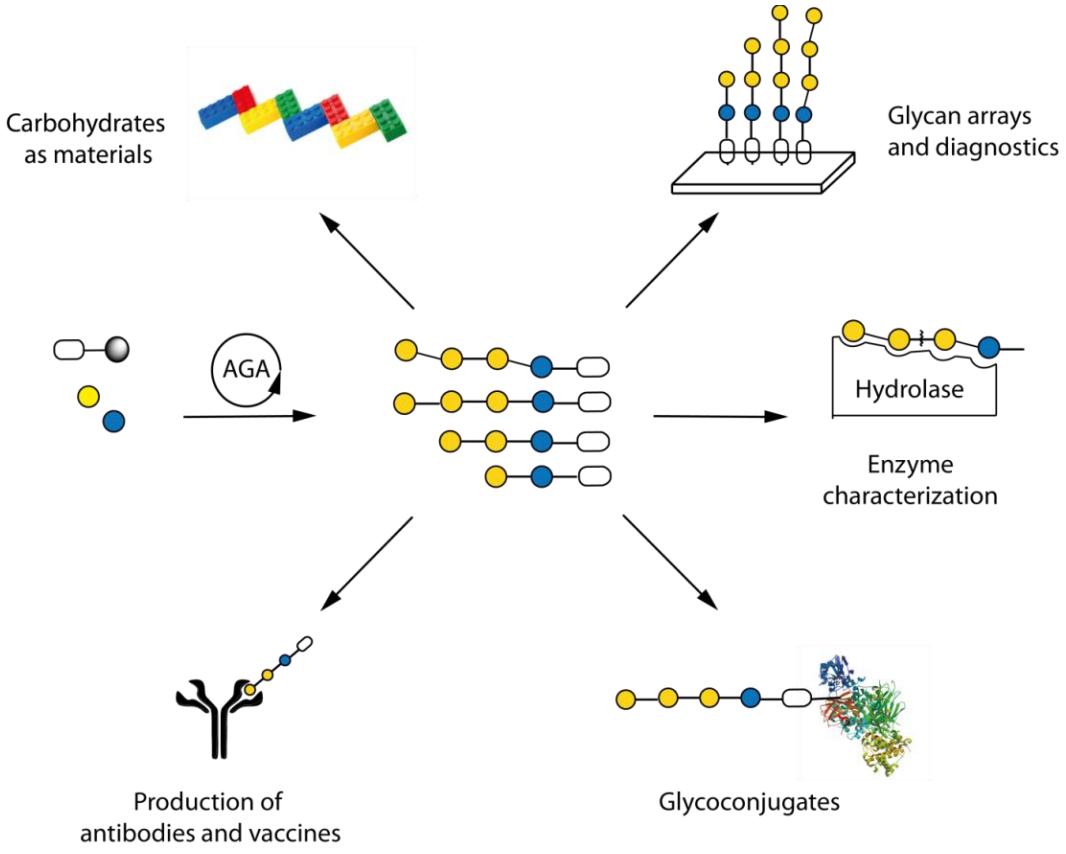

Figure 1.7 Applications of glycans synthesized using AGA.

1.5.5. Perspectives

Over the past two decades, AGA has evolved from humble beginnings to a reliable synthesizer, optimized reaction conditions, and commercially-available building blocks that made the rapid synthesis of complex oligosaccharides a reality.[56,57] Even though challenging *cis*-linkages and structures such as charged polysaccharides are accessible now, some linkages (*e.g.* β-mannose) as well as the stability of sulfates during the deprotection process, remain synthetic bottlenecks. Additionally, as longer polysaccharides can be assembled, new challenges arise, such as the formation of insoluble compounds and/or aggregates after global deprotection. The detailed structural analysis of defined oligo- and polysaccharides will advance the synthesis. Specific substitution aiming to alter the structure and properties of these compounds will be systematically studied using AGA. These achievements, together with improvements in quality control and purification techniques, will have an enormous impact on glycoscience.[71]

With an expanding collection of pure and well-defined glycans, it will be possible to shed more light on new aspects of glycobiology such as carbohydrate-protein interactions as well as to stimulate the development and characterization of new enzymes and antibodies. Diagnostic and vaccine discovery are being enabled by AGA. Multivalent systems, so far limited to simple mono- or disaccharides,[88] can now benefit from AGA to use more complex structures to resemble the biological environment. AGA will grant access to new carbohydrate-based materials for probing fundamental information on polysaccharides. The envisage of unnatural compounds such as DNA and peptide conjugates with tuned properties. With AGA technologies available as for DNA and peptides, we expect new possibilities and applications for carbohydrates.

1.6. **Aim of the Thesis**

The thesis aims to continue the development of a robust and reliable automated platform general for glycan synthesis through improved methodologies to obtain glycan libraries, which provide valuable materials to understand the functions and the structure of glycans.

The first objective was to optimize the synthesis of a collection of arabinomannan (AM), (Chapter 2.1). For this purpose, a collection of AM oligosaccharides from the *Mycobacterium tuberculosis* was synthesized. The introduction of a capping step after each glycosylation and optimized reaction conditions allowed for the assembly of larger oligosaccharides up to 12 units

in a faster and more efficient way. With an optimized methodology and reliable platform, the limits of AGA were pushed towards the longest polysaccharide ever synthesized, the linear 100-mer polysaccharide. After 188 hours and 201 steps the polymannoside was obtained with 99% average yield (Chapter 2.4). Convergent block coupling allowed going even longer, using oligosaccharide fragments (30- and 31-mers) prepared by AGA, a branched 151-mer polysaccharide was obtained, proving AGA as a solid and mature platform to obtain complex molecules. This collection of arabinomannosides were used as standards for the developing of a new analytical technique, namely, direct imaging of single glycan molecules with sub-nanometer resolution using scanning tunneling microscopy (STM). In collaboration with Dr. Xu Wu. Direct visualization of mannosides at subnanometer resolution permitted the differentiation of α-(1,2) and α-(1,6) linkages together with the localization of the branching point at a single-molecule scale. This technique is expected to be useful for the identification of recurrent structural features of glycans with biological importance.

The final objective (chapter 3) was to assemble a collection linear α-(1,6)-mannosides and β-(1,3)-glucans with specific β-(1,6)- and β-(1,4)-linkages. These compounds were used to characterize carbohydrate-degrading enzymes obtained from marine sources. Synthetic α-(1,6)-mannosides permitted the characterization of the putative mannanase GH76A from *Salegentibacter sp*.. In collaboration with Dr. Solanki, a detailed 3D structure of the active site of GH76A was obtained after the co-crystallization of synthetic mannose tetramer with mutant mannanase GH76. Incubation of these synthetic α-(1,6)-mannosides with GH76A generated hydrolyzed glycans, this suggested that the enzyme GH76A functions as an endo α-(1,6)-mannanase.

2. Pushing the limits of AGA

This chapter has been modified in part from the following article:

Pardo-Vargas A., Bharate P., Delbianco M., Seeberger P.H. **Automated Glycan Assembly of Arabinomannan Oligosaccharides from Mycobacterium tuberculosis**. *Beilstein Journal of Organic Chemistry*, **2019,** 15, 2936-2940. DOI: 10.3762/bjoc.15.288

2.1. Abstract

Automated Glycan Assembly (AGA) was employed to prepare the core structure of arabinomannosides (AM) from *M. tuberculosis*, containing α-(1,6)-Man, α-(1,5)-Ara and α-(1,2)-Man linkages. The introduction of a capping step after each glycosylation and further optimized reaction conditions (time and temperature) allowed for the synthesis of a series of oligosaccharides, ranging from hexa- to branched dodecasaccharides. These improvements towards a more robust AGA platform ensure high coupling efficiencies and granted access to a 100-mer polysaccharide. Using a different strategy namely convergent block coupling a set of oligosaccharide fragments prepared by AGA, yielded a multiple-branched 151-mer polymannoside, the largest polysaccharide prepared by any synthetic method to date. This collection of arabinomannosides represents valuable analytical standards for the developing analytical techniques like direct imaging of single glycan molecules with sub-nanometer resolution using scanning tunneling microscopy (STM).

2.2. Optimizing the assembly of Arabinomannan from *M. tuberculosis*

Bacterial infections caused by *Mycobacterium Tuberculosis* (MTB) killed 1.7 million people in 2017. Additionally, more than 10 million new TB cases were reported, with multidrug-resistant tuberculosis accounting for almost 10% of registered cases.[89] The development of novel therapeutic agents and more efficient strategies to detect MTB infections at an early stage is essential, as an early diagnosis would help to prevent most deaths from TB.[89] Arabinomannans (AM), one of the main components of the mycobacterial cell wall,[90] are

composed of α-(1,5), α-(1,3) and β-(1,2) arabinoses and α-(1,6) and α-(1,2) mannosides.[91-93] AM are potential clinical biomarkers for infection[94-98] due to their roles in the interaction with host cells, interference with macrophage activation, and immunosuppression of T cell responses.[99,100] Identification of novel anti-TB agents that specifically target arabinomannans with high sensitivity are required.[101-104] Automated Glycan Assembly (AGA) reduces time and effort to access complex glycans[105] including linear and branched oligoarabinofuranosides α-(1,5) and α-(1,3),[106] and arabinomannose.[107,108]

Here, the optimization of AGA modules is described and exemplified for the synthesis of oligosaccharides **10**-**17** that resemble portions of the *M. tuberculosis* AM core structure (Figure 2.1). Just three building blocks **1**-**3** are required to access all six oligosaccharides ranging from hexa- to dodecasaccharides.

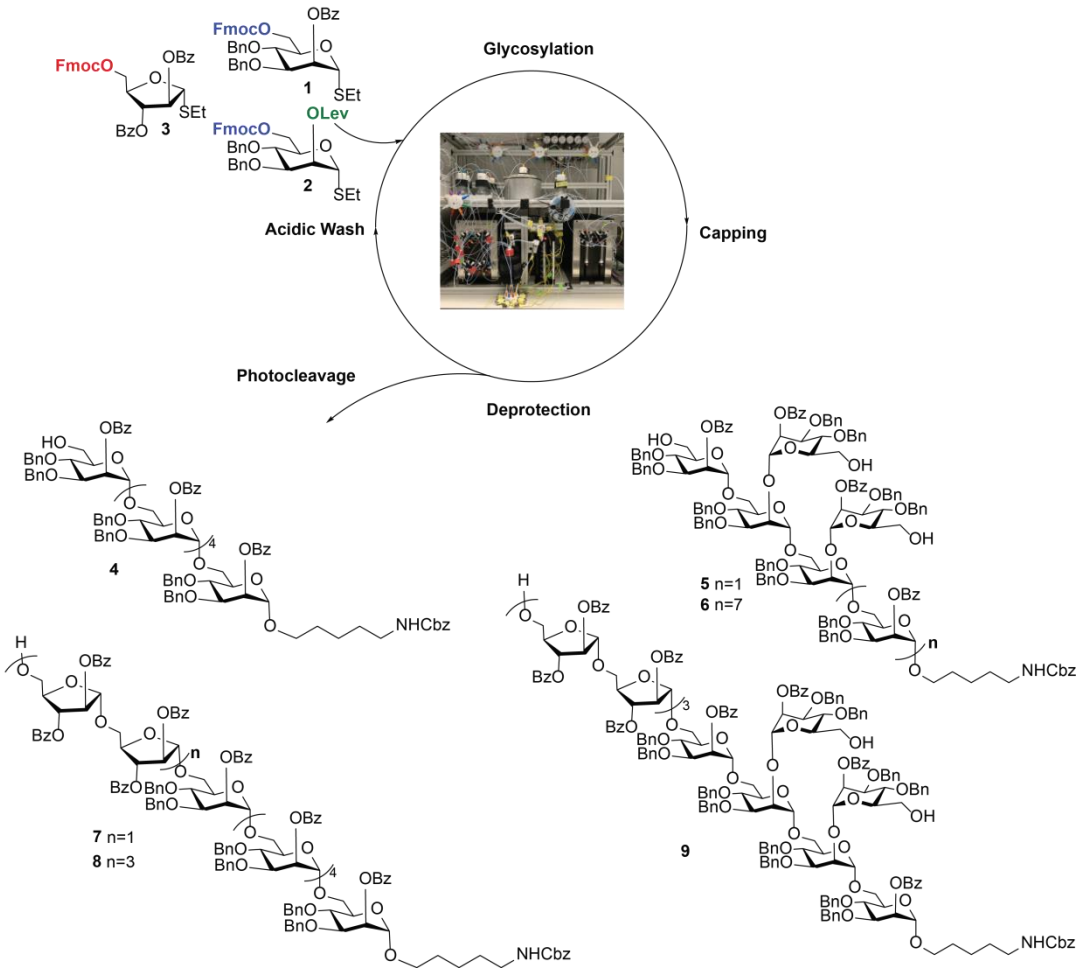

Figure 2.1 Schematic representation of AGA for oligomannanosides and oligoarabino-mannosides using building blocks **1**-**3**.

The automated syntheses of oligomannoside **4-6** and oligoarabinomannosides **7-9** were performed on a home-built automated synthesizer using a Merrifield resin functionalized with a photocleavable linker as solid support.[109] A typical AGA cycle consists of three modules (Procedure A- Figure 2.2). The acidic wash module prepares the resin for the glycosylation by quenching any remaining base from the previous step (20 min). In the glycosylation module, the thioglycoside donor is coupled to the resin upon activation with NIS and TfOH (from -40 °C to -20 °C). Finally, the deprotection module removes the temporary protecting group such as Fmoc/Lev to reveal a free hydroxyl group that allows for further chain elongation in the next cycle. Fmoc and Lev were used as orthogonal temporary protecting groups, whereby Fmoc is cleaved by piperidine (20% solution in DMF) while Lev is removed using hydrazine acetate. Iterative cycles continue until the desired structure is obtained. The oligosaccharide products are cleaved from the solid support using a flow UV-photoreactor, followed by purification and global deprotection.[109]

Linear α-(1,6) hexamannoside **4** was synthesized using six coupling cycles with 6.5 equivalents of mannose BB **1 (**Procedure A) was performed in collaboration with Dr Priya Bharate. No deletion sequences were observed, and the crude product was purified using normal phase HPLC to obtain hexamannoside **4** in 55% yield, based on resin loading.

2.3. **Toward more efficient procedures**

The doubly branched hexamannoside **5** was assembled using BB **1** for α-(1,6) linkages and BB **2** for the α-(1,6) α-(1,2) branching points. First, the linear α-(1,6) trimannose was assembled, followed by deprotection of both Lev and Fmoc to reveal three hydroxyl groups. Three sequential glycosylation cycles, using BB **1**, afforded compound **5** in 37% yield. The chromatographic analysis revealed compound **5** as a major product along with pentamer and tetramer deletion sequences. To improve the glycosylation efficiency, a new glycosylation module, employing higher incubation and reaction temperatures (from -20 °C to 0 °C), was introduced (Procedure B) (Figure 2.2). In addition, a capping step after each glycosylation was introduced to prevent the formation of undesired side-products.[110] These two modifications improved the isolated yield of **5** to 53% with no detectable deletion sequences.

2 Pushing the limits of AGA

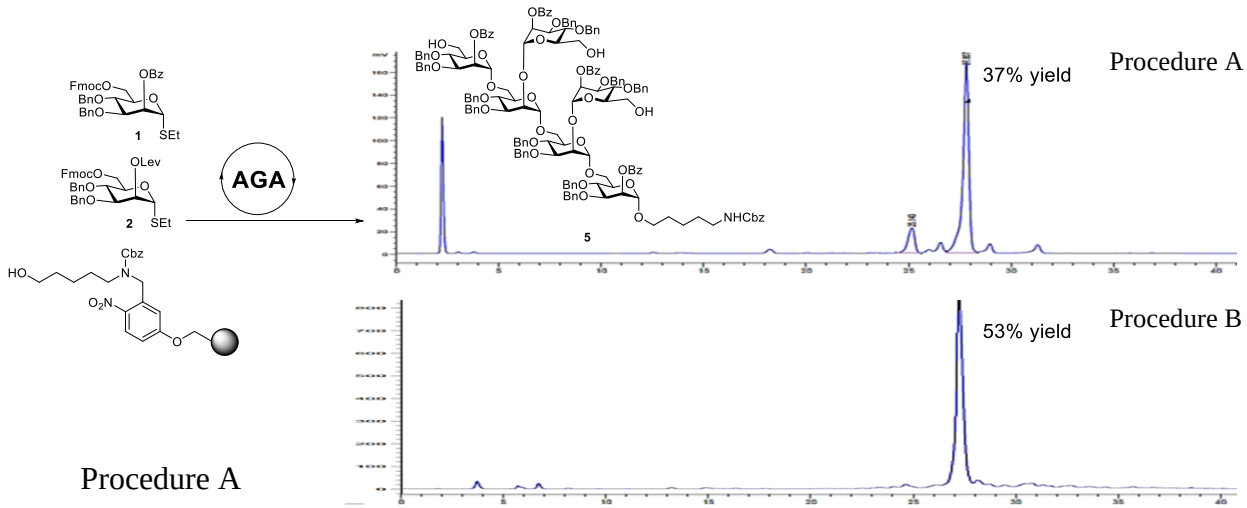

Procedure A

	Module	Conditions
	A: Resin Preparation for Synthesis	
	B: Acidic Wash with TMSOTf Solution **C**: Thioglycoside Glycosylation **E**: Fmoc Deprotection	**BB1** 6.5 eq, -40 °C for 5 min, -20 °C for 30 min
2	**B**: Acidic Wash with TMSOTf Solution **C**: Thioglycoside Glycosylation **E**: Fmoc Deprotection	**BB1** 6.5 eq, -40 °C for 5 min, -20 °C for 30 min
	F: Lev Deprotection **B**: Acidic Wash with TMSOTf Solution **3**x **C**: Thioglycoside Glycosylation **E**: Fmoc Deprotection	**BB1** 13 eq, -40 °C for 5 min, -20 °C for 30 min

Procedure B

	Module	Conditions
	A: Resin Preparation for Synthesis	
	B: Acidic Wash with TMSOTf Solution **C**: Thioglycoside Glycosylation **D:** Capping **E**: Fmoc Deprotection	**BB1** 6.5 eq, -20 °C for 5 min, 0 °C for 20 min
2	**B**: Acidic Wash with TMSOTf Solution **C**: Thioglycoside Glycosylation **D:** Capping **E**: Fmoc Deprotection	**BB2** 6.5 eq, -20 °C for 5 min, 0 °C for 20 min
	E: Lev Deprotection **B**: Acidic Wash with TMSOTf Solution 3x **C**: Thioglycoside Glycosylation **D:** Capping **E**: Fmoc Deprotection	**BB1** 6.5 eq, -20 °C for 5 min, 0 °C for 20 min

Figure 2.2 AGA of arabinomannoside **5** using standard procedure A (37% yield) and optimized procedure B (53% yield). The differences between procedures A and B are underlined.

The inclusion of a capping step in the AGA synthesis cycle (Procedure **B**) was further illustrated for the synthesis of oligosaccharide **6**-**9**. AGA of the branched 12-mer mannoside **6** showed a dramatic improvement, with yields rising from 6% (Procedure A) to 48% (Procedure B). Syntheses of linear octamer-arabinomannanoside **7** and linear 12-mer **8,** was addressed using BB **1** and arabinose BB **3** for the α-(1,5)-Ara linkage. Procedure **A** efficiently provided the linear mannose backbone but resulted only in partial glycosylation of arabinose BB **3**, thus giving the hexamannoside as main product together with multiple side-products missing one or more arabinoses. The desired products **6** and **7** were isolated in only 9% and 7% yield, respectively. In contrast, when procedure **B** was employed, most deletion sequences were absent and **6** and **7** were isolated in 56% and 61% yield respectively.

The advantage of the new procedure became even more apparent for the AGA of dodecamer **9**, which requires all three BBs. While procedure **A** afforded dodecamer **9** only in a 3% yield (Figure 2.3A), procedure B gave **9** as major product (26% yield, Figure 2.3B).

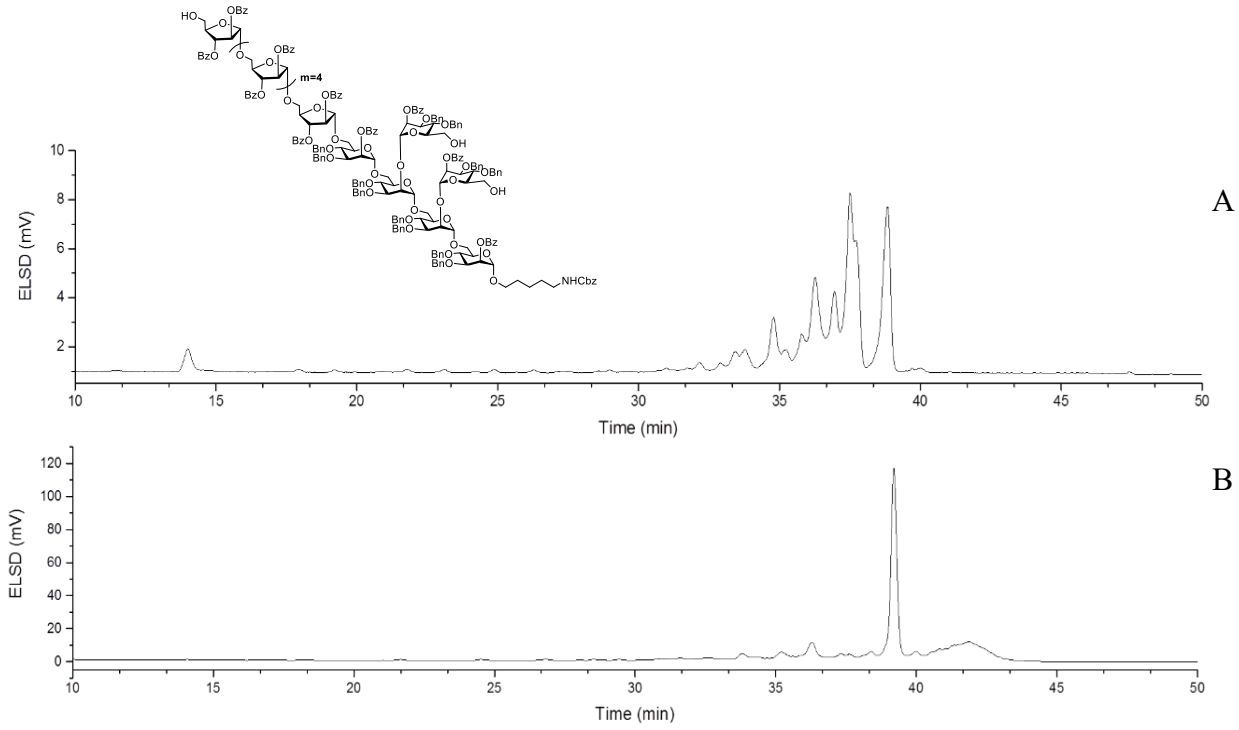

Figure 2.3 ELSD trace of crude-normal phase HPLC of dodecamer **9** obtained with either AGA procedure A or B.

Compound	Procedure A	Procedure B
4	55%	-
5	37%	53%
6	6%	48%
7	9%	56%
8	7%	61%
9	3%	26%

Table 2.1 AGA of arabinomannosides **4-9**. Procedure A modules: i) Acidic wash ii) Glycosylation (from -40 °C to -20 °C) and iii) Fmoc/Lev deprotection. Procedure B modules: i) Acidic wash, ii) Glycosylation (from -20°C to 0 °C) iii) Capping, and iv) Fmoc/Lev deprotection.

The global deprotection of oligosaccharides **4-9** was achieved by removal of the benzoate ester protecting groups using Zemplén methanolysis, followed by Pd/C catalyzed hydrogenolysis of the carboxybenzyl group and the benzyl ethers. Mannosides **4-6** were deprotected and purified using reverse-phase HPLC to obtain fully deprotected mannosides **10-12**. For the arabinomannanosides **7-9**, the acid-labile arabinose chain was cleaved during hydrogenation (Figure 2.4). To overcome this problem, hydrogenolysis with $Pd(OH)_2$ was performed to access the fully deprotected arabinomanosides **13-15**.

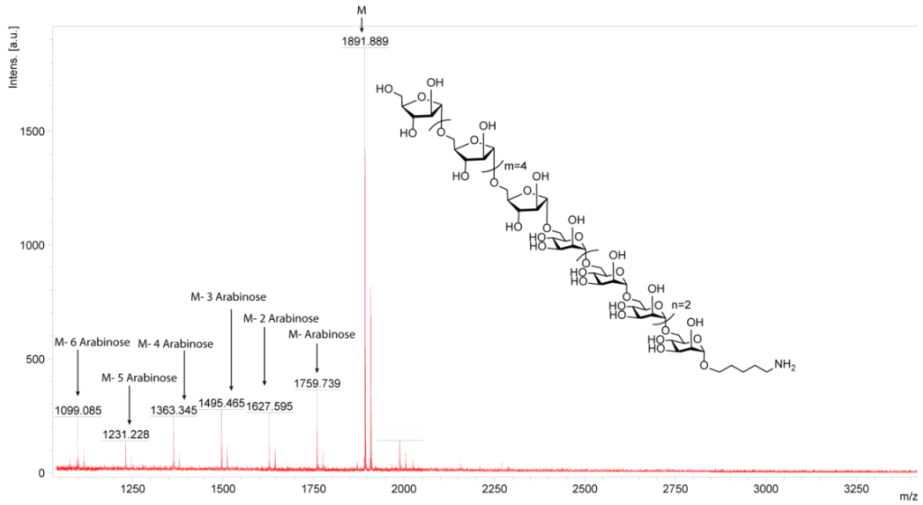

Figure 2.4 MALDI spectra of AM **8** after acidic hydrogenolysis with Pd/C. Partially cleaved arabinose side-products were observed.

Standard post-synthesizer manipulations include photocleavage, global deprotection (methanolysis and hydrogenolysis), and two purifications steps, at the protected and at the deprotected stage. To simplify this sequence, on resin methanolysis and only one purification was attempted and exemplified with the synthesis of the linear pentamannoside **16** and branched **17.** After AGA, the resin was stirred overnight in a basic solution of MeONa in DCM:MeOH, followed by photocleavage of the polymannoside from the resin. Complete deprotection of benzoyl groups was confirmed using MALDI. Afterwards, benzyl ethers were removed by hydrogenolysis with Pd/C followed by RP-HPLC purification. For linear pentamannoside **16** 42% yield was obtained based on resin loading. Likewise, for branched mannoside **17**, this protocol yielded 11%. Both **16** and **17** were obtained in a fast and efficient way avoiding a purification step with comparable yields over the traditional 2 steps purification.

With these optimized conditions, a total of eight AM oligosaccharides containing α-(1,6)-Man, α-(1,5)-Ara and α-(1,2)-Man were synthesized by automated glycan assembly, using three monosaccharide building blocks (Figure 2.5).

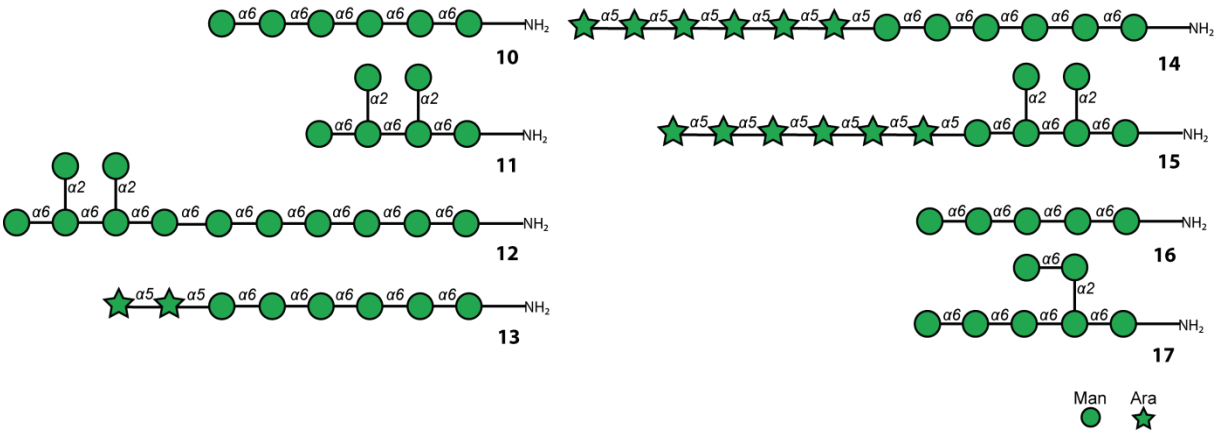

Figure 2.5 Schematic representation of LM and AM oligomers using AGA.

2.4. **Pushing the limits: Towards the total synthesis of polysaccharides**

AGA is a highly efficient platform for the synthesis of long polysaccharides, with an average yield of 98.5% for every coupling step.[110,111] Since efficiency sets the size limit of the molecule that can be prepared without intermediate purification, this work plans to push the limits of AGA towards the longest oligosaccharide ever synthesized by any synthetic method. Polymannosides were chosen to illustrate the concept as they do not form rigid tertiary structures that complicate the assembly of cellulose and chitin oligomers.[113] For AGA the previous limit was reached at 50-mer polysaccharides.[110,111] Using the optimized procedure **B**

(Section 2.3), the synthesis of a 100-mer polymannoside **18**, the largest polysaccharide, was pursued in collaboration with Dr. Joseph Abragam (Figure 2.6).

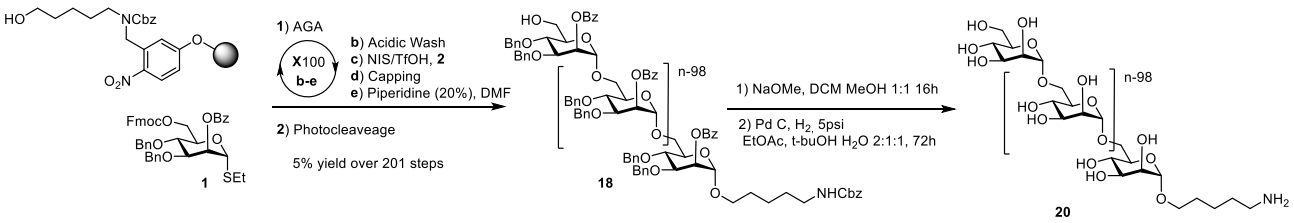

Figure 2.6 AGA of protected 100-mer α-(1,6)-polymannoside **18** followed by photo-cleavage and two steps global deprotection yielded 100-mer α-(1,6)-polymannoside **20.**

Standard Merrifield resin equipped with a photo-cleavable linker and mannose thioglycoside BB **1** was employed on 19 µmol scale using a four-steps cycle (Procedure B). After every twenty or thirty coupling cycles, ten beads of resin were removed from the reaction vessel and the product was cleaved and analyzed by HPLC and MALDI to ascertain synthesis success. At the 40-mer stage, the glycosylation time was doubled from 20 to 40 min to ensure quantitative reactions as failure sequences were increasingly detected in the crude products. At the 70-mer stage, following the reaction progress became extremely challenging since no ionization was observed in MALDI using 2,5-dihydroxybenzoic acid (DHB) as a matrix. A different matrix based on 2′,4′,6′-Trihydroxyacetophenone (THAP) was used to overcome the challenge since it is less prone to fragment glycans. Beyond the 80-mer stage, all glycosylations were allowed to proceed for 60 min to ensure the highest possible yields.

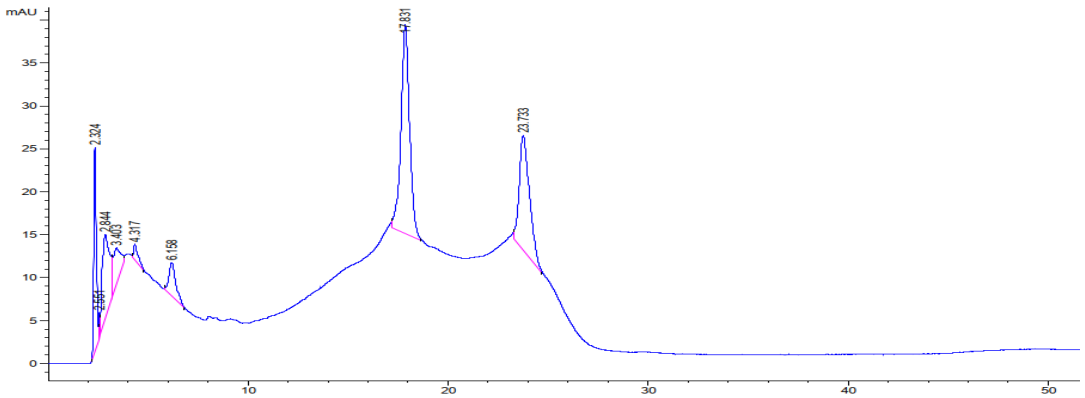

Figure 2.7 Crude HPLC of 100-mer **18** (t_R 17.8 min) and main side-product 100-mer **19** (t_R 23.7 min) lacking three benzyl ether protective groups.

After 188 hours and 100 coupling cycles, 9 g of building block **1** were consumed to obtain 100-mer **18** in a 5% yield **(**Figure 2.7) after photo-cleavage and HPLC purification. As main side-product, compound **19** was identified as a 100-mer missing three benzyl ether protective groups, lost during photochemical release from the resin. To avoid this side reaction, the photocleavage setup was revisited. The mercury lamp with a 280 nm filter used to photocleave the resin was replaced by a 365 nm UV lamp. However, after 30 min of irradiation time, the amount of the side-product **19** increased. For future experiments deprotection of long polysaccharides, it is recommended to reduce the irradiation time.

Cleavage of all ester protective groups by treatment with sodium methoxide, followed by palladium-catalyzed hydrogenation under pressure for 72 h to release all benzyl ether protective groups yielded the 100-mer polymannoside **20.** The compound was purified with reversed phase HPLC. 100-mer polymannoside **20** was characterized by ^{1}H-and ^{13}C-NMR as well as MALDI analysis. To assure that **19** was, in fact, the 100-mer missing three benzyl groups, the same two steps deprotection used for **18** were performed**.** MALDI, NMR and chromatographic data unequivocally identify **20** as the product of deprotection of **19.**

AGA of **20** the largest polysaccharide assembled to date illustrates the efficiency, and reliability of this platform. AGA maintained for 188 hours an average yield of 98.5% per step after 200 synthetic steps. To demonstrate that AGA is not only a reliable but also flexible platform, a branched and longer structure will be synthesized using a block coupling strategy.

2.5. **Convergent [31+30+30+30+30] block coupling**

Block couplings of polysaccharides prepared by AGA could give raise to even larger and more complex polysaccharides. Two polysaccharide blocks, a linear 30-mer α-(1,6) polymannoside **23** and branched 31-mer polymannoside **24,** unified in a 31+30+30+30+30 coupling, will create branched 151-mer **25** (Figure 2.8).

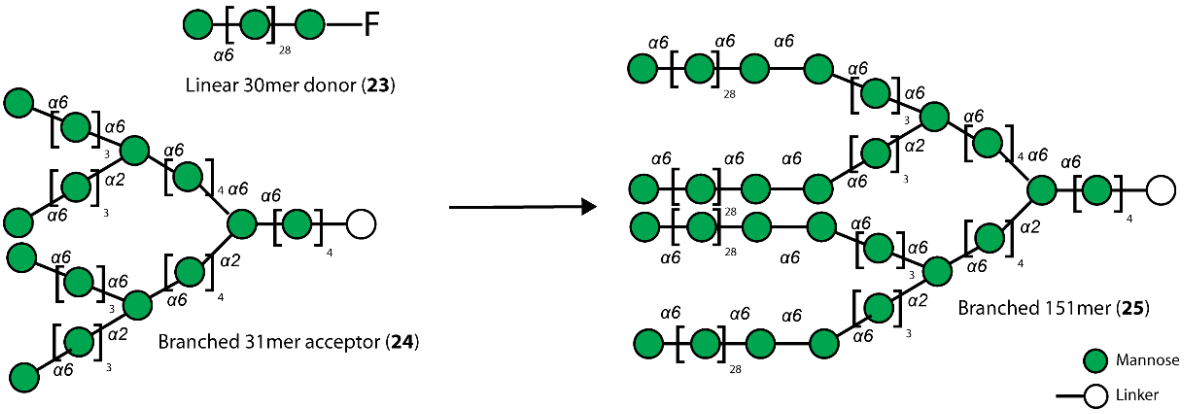

Figure 2.8 Schematic representation of convergent [31+30+30+30+30] block coupling for synthesis branched 151-mer.

To synthesize the fluoride donor **23,** a recently developed traceless photocleavable linker **21** based on the *o*-nitrobenzyl scaffold was used (Figure 2.9).[114] This linker, upon photo-cleavage, reveals an oligosaccharide with a free reducing end that can be further functionalized to obtain a glycosyl donor or deprotected to obtain fully natural glycans.

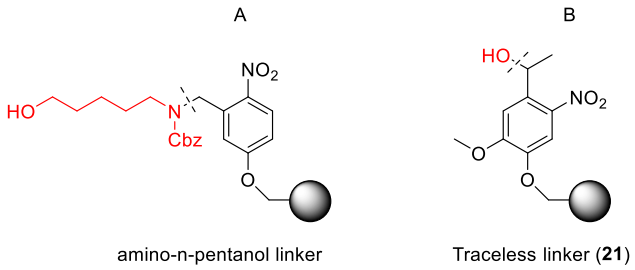

Figure 2.9 Photocleavable linkers attached to a Merrifield resin **A.,** After photocleavage standard resin reveals a Cbz protected amino-n-pentanol linker (in red) **B,** Photocleavage of **21** will reveal the product with a free reducing end.

After thirty AGA cycles with BB **1** the partially protected 30-mer **22** was obtained in 30% yield**.** Synthesis of the donor was performed by Dr. Abragam fluoride donor **23** in 90% yield by treatment of **22** with deoxo-fluor. (Figure 2.10)

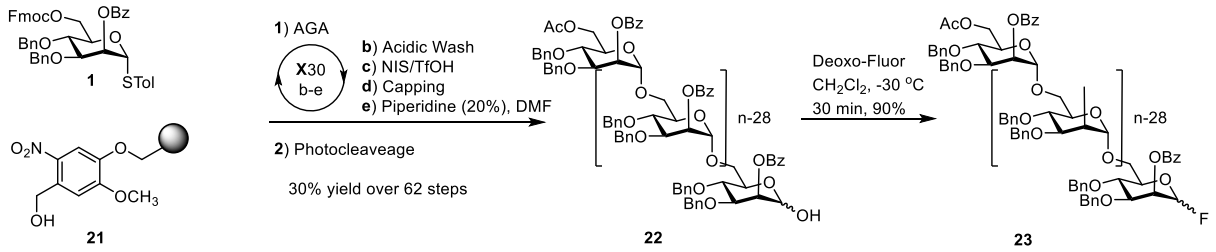

Figure 2.10 AGA of 30-mer glycosylating agents **23** by AGA.

Branched 31-mer polymannoside **24** (Figure 2.11) that will serve as acceptor in the subsequent block coupling was prepared by AGA using α-(1,6) mannose BB **1** and mannose BB **2** for the branching positions. Merrifield resin equipped with standard amine linker at the reducing end was used to prepare 31-mer **24**. After incorporating four times mannose thioglycoside BB **1** (6.5 eq), branching BB **2** followed. The first two parallel couplings with BB **1** required ten equivalents to glycosylate the secondary C2-hydroxyl group and install an α-(1,2) linkage. After the next three parallel glycosylations with BB **1**, this process was repeated following incorporation of two further branching points with BB **2**, in order to rapidly grow 31-mer polymannoside. Photo-cleavage and subsequent purification yielded 30 mg of 31-mer polymannoside acceptor **24** (Figure 2.11).

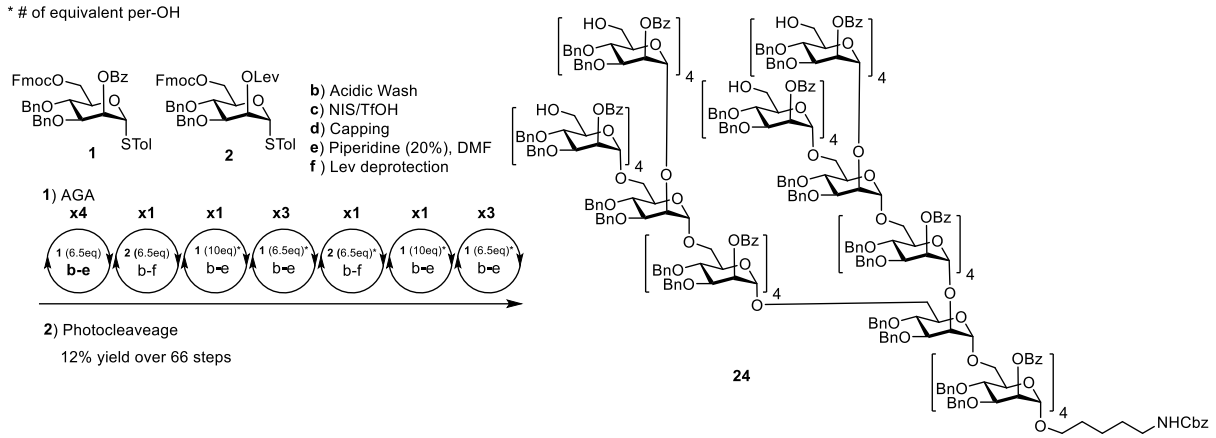

Figure 2.11 AGA of 31-mer polymannoside acceptor **24**.

Dr. Abragam optimized the block coupling conditions to connect four units of 30-mer glycosyl fluoride **23** and 31-mer acceptor **24.** Six equivalents of **23** in the presence of a silver perchlorate as a promotor. These activation conditions completed the glycosylation without the formation of significant amounts of side-products in just 30 minutes affording the desired 151-mer **25** in a 78% yield.

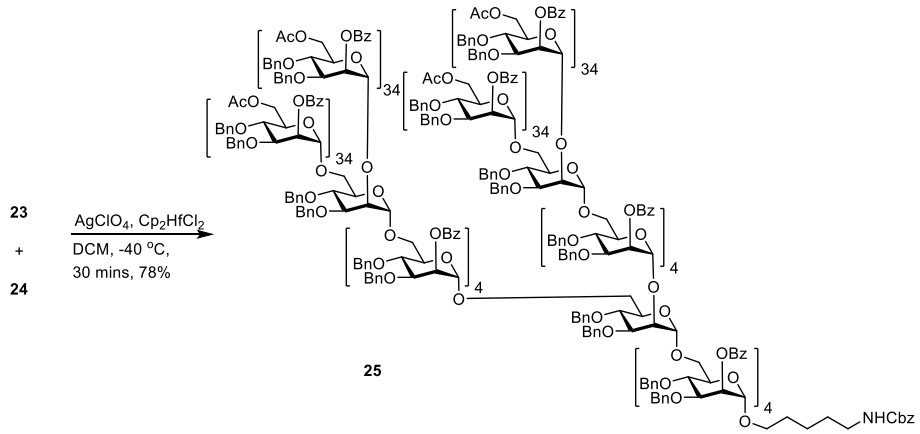

Figure 2.12 30-mer donor **23** and branched 31-mer acceptor **24** yielded 78% of fully protected 151-mer **25.**

Purification of **25** was challenging since the products diffuses throughout the elution run (Figure 2.12). This could be ascribed to the size of **25** that is in fact bigger than the pore size of the diol column employed (300 Å). However, after three purifications by normal-phase HPLC, the desired 151-mer product **25** was separated from the 121-mer side-product and isolated in a 78% yield.

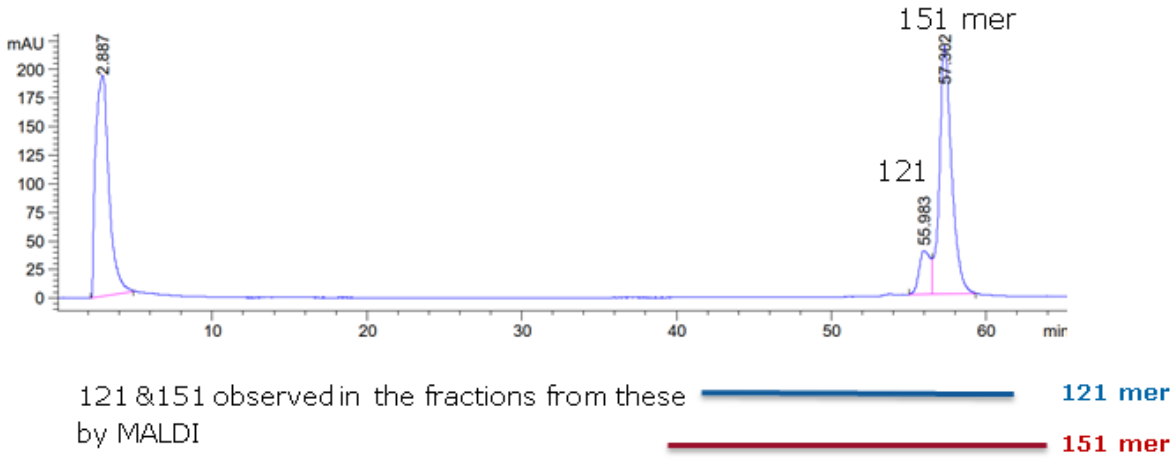

Figure 2.12 HPLC trace of **25** after one NP purification. Two more sequential HPLC run were needed to obtain pure 151-mer. Both compounds diffused throughout the elution run.

To remove 302 benzyl ethers protective groups, 144 benzoate and four acetate esters as well as one Cbz amine protective group, fully protected 151-mer **25** was treated with sodium methoxide for 16 h to cleave all 148 ester groups, followed by hydrogenation in the presence

of palladium on carbon under hydrogen pressure for 60 h to cleave all benzyl ethers and the Cbz group.

Standard purification methods including C-18 RP column and Hypercarb column resulted in mixtures of **26** with side-products of incomplete deprotection. Size exclusion chromatography using a TSKgel G3000 PWXL column with water as eluent, furnished fully deprotected 151-mer **26** in 41% yield. Analysis by ^{1}H-, and ^{13}C-NMR as well as MALDI-mass spectrometry unequivocally ascertained the synthesis of branched 151-mer **26** as the largest synthetic polysaccharide to date (Figure 2.13).

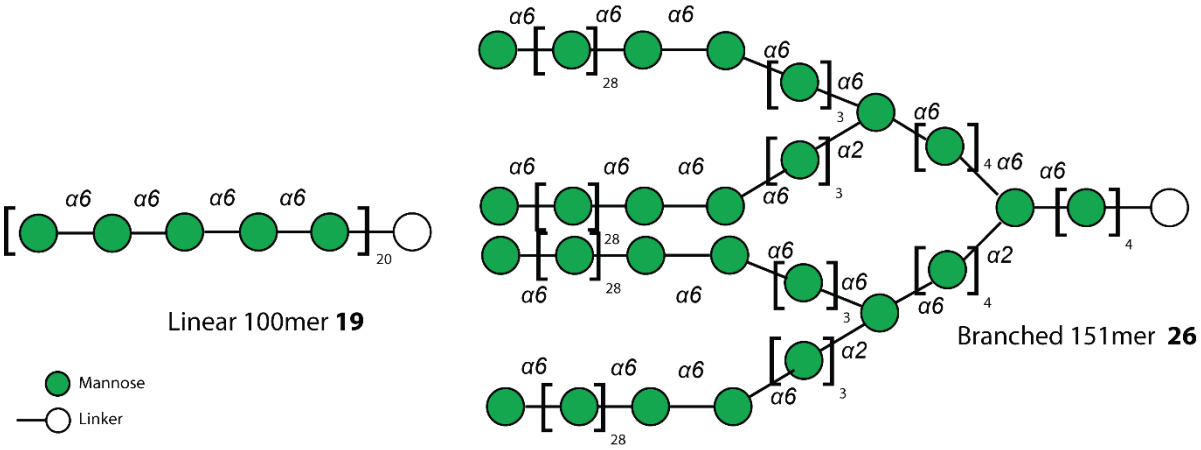

Figure 2.13 Linear 100-mer **19** and branched 151-mer **26**.

2.6. **Perspectives of AGA as source of materials for structural analysis**

AGA offers a fast and efficient platform to obtain oligo- and polysaccharides with defined substitution patterns to systematically study the structure of glycans. These collections of related compounds offer the perfect substrate for the development of new structure sensitive methods. Traditional analytical methods like NMR analysis of long polysaccharides are complex, and so far, the detailed structural analysis of glycans has been ignored. Nonetheless, new analytical methods have been developed using oligosaccharides produced by AGA as standards to obtain detailed structural information, for instance, ion mobility- mass spectrometry (IM-MS)[117] have permitted to unambiguously identify regio- and stereoisomers. Other analytical techniques like cryo-IR[118] spectroscopy coupled to mass selectors give fingerprints of intact glycans and their fragment ions may eventually enable the reliable identification of any given glycan.[118,119] AGA offered analytical standards to exploit the full

potential of these new emerging analytical techniques. Here, it is presented a new method for structural analysis by direct imaging of single glycan molecules with sub-nanometer resolution using scanning tunneling microscopy (STM) and oligosaccharides produced by AGA as reference compounds.

2.6.1. Single Glycan Imaging

In collaboration with the Max Planck Institute for Solid State Research, we developed a method to directly visualize single glycan molecules through the combination of ion beam deposition and scanning tunneling microscopy (STM) in ultra-high vacuum (UHV), Glycan samples are prepared via electrospray ion beam deposition (ES-IBD).A molecular ion beam of intact, non-volatile glycans (Figure 2.14a)is purified by a mass-to-charge ratio (m/z), filter, and monitored by time-of-flight mass spectrometry before its gentle deposition onto the atomically clean Cu(100) surface in UHV.[120,121] Only a minute amount of sample, in the range of microgram, is needed for a series of experiments (by Dr Xu Wu).

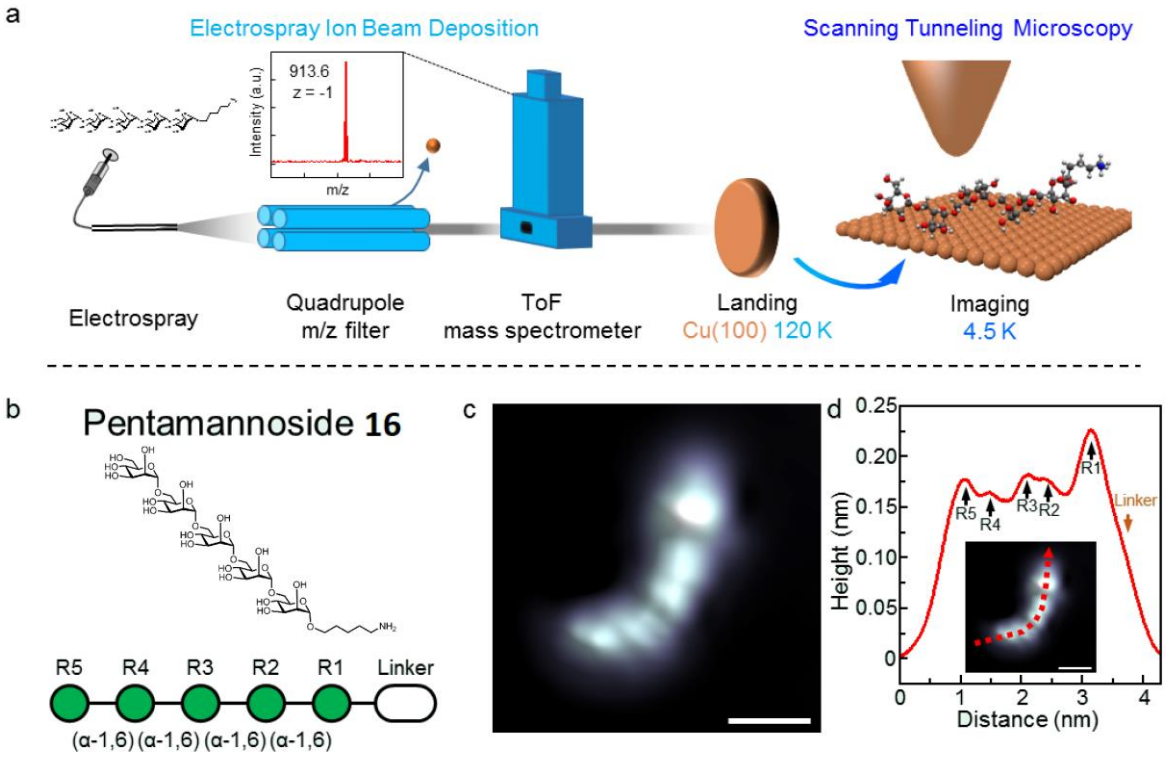

Figure 2.14 STM image of the linear mannoside **16 a**, Schematic workflow of glycan transfer, purification and deposition via ES-IBD combined with mass selection and single glycan STM imaging in UHV. **c,** STM image of α-(1,6) pentamannoside **16** showing a protrusion for every monosaccharide unit and a low-intensity protrusion for the linker. The scale bar is 1 nm.

Pure oligosaccharides with defined sequence and connectivity were prepared by AGA[122] as mentioned in section 2.3 and deposited on the surface as negatively charged glycans by ES-IBD. Single-molecule deposition is obtained by suppressing molecular surface diffusion that leads to agglomeration by maintaining the sample in ultra-high vacuum at 120 ºK during deposition and transfer, and at 4 ºK for imaging. Single molecule preparation allows for detailed structural inspection and comparison of different oligosaccharide sequences.

α-(1,6) Pentamannoside **16** containing an alkylamino linker group at the reducing end, was used for initial imaging experiments. Single monosaccharide subunits are resolved as five protrusions (Figure 2.14d). The heights of each monosaccharide vary between 0.15 and 0.25 nm, often clearly separated from each other by local minima (see the red line profile in Figure 2.14d). The distance between monosaccharides is 0.51 ± 0.08 nm (peak to peak). The alkylamino linker is seen as a low height feature at one end of the molecule, permitting to identify the glycan reducing end. Shape, size and spacing of the subunits is consistent with recent findings of STM imaging of disaccharides.[123]

To explore whether isomers with different connectivity can be distinguished, two branched hexamannosides, hexamannoside **11** (Figure 2.15 a) containing two α-(1,2) branching points at residues R2 and R3, and hexamannoside **17** (Figure 2.15 d) containing only one α-(1,2) branching point at R2 were deposited on the Cu surface and directly imaged. Representative STM images reveal structures where branching is clearly visible (Figure2.15). The STM image of **11** shows two side chains branching out at nearly a 90° angle to the opposite sides of the linear backbone. Three interunit distances of 0.49 ± 0.06 nm are assigned to the α-(1,6) linkage, in agreement with the observation for the linear pentamannoside **16**. The α-(1,2) linkages appear significantly longer (0.62 ± 0.04 nm). The subsequent, unambiguous assignment of the complete molecule **11** reveals a bend in the α-(1,6) connected backbone. The interunit distance does not represent the exact distances of the glycosidic linkage,[123] however, as the distances measured were reproduced for several molecules, it is a reliable parameter to distinguish between α-(1,2) and α-(1,6) linkages.

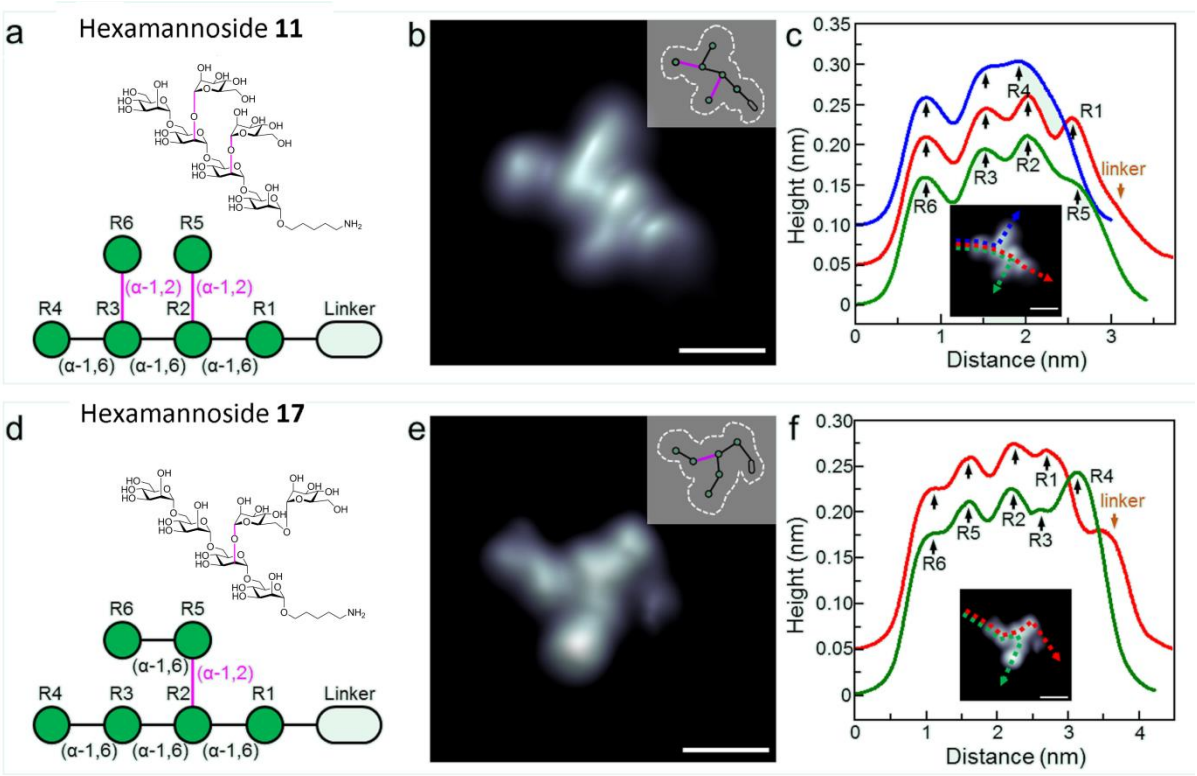

Figure 2.15 STM image of branched hexamanosides **a, 11** and **d, 17. b, e,** Typical STM image of the branched hexamannosides **11** and **17** with schematic diagrams of the conformations on the top right corner. The scale bar is 1 nm. **c, f,** Line profile of the molecules showing peaks for every monosaccharide unit. The different colored line profiles have an offset of 0.05 nm. The inset shows the direction of the line profile.

The features observed in the STM image of hexamannoside **17** are a result of the greater flexibility of this oligosaccharide. The conformational freedom of the longer side branch often impedes the direct distinction of the branching point due to 3D folding. The representative STM image of **17** (Figure 2.15e) shows a molecule sufficiently spread to allow for the direct identification of the branching point. The amino linker identifies residue R1 and thereby the position of the branching point related to the overall structure. The increased distance of the α-(1,2) linked branch allows for the unambiguous assignment of oligosaccharide **17**.

The direct visualization of single glycans at subnanometer resolution opens up new avenues for glycan characterization. Single glycans can be imaged and their structure can be unambiguously determined. Loss of information due to conformational averaging over time is prevented by cryogenic conditions. The tandem approach of preparative mass spectrometry with scanning probe microscopy is expected to be useful for the identification of recurrent structural features of glycans that are of biological importance.

2.7. **Conclusions**

AGA is a technology in constant development. Improvements in hardware, modules and conditions over the last two decades made AGA a robust technology. Shorter cycles, the introduction of a capping step after each glycosylation, and optimized reaction conditions increased the efficiency of every coupling steps and permitted the synthesis of AM oligosaccharides containing α-(1,6)-Man, α-(1,5)-Ara and α-(1,2)-Man, using three monosaccharide building blocks. AGA of the 100mer, the largest polysaccharide assembled to date illustrated the efficiency and reliability of this platform since AGA was consistent over 201 synthetic steps with an average yield of 98.5% per step. AGA is still in constantly developing, and now is more flexible since the introduction of new traceless linker to synthesize polysaccharide donors that allowed the assembly of the biggest synthetic polysaccharide to date a 151 polymannoside.

AGA offers a fast and efficient platform to obtain oligo- and polysaccharides with defined substitution patterns to systematically study the structure of glycans. Direct visualization of single glycans of mannosides at sub-nanometer resolution using STM permitted the differentiation of α-(1,2) and α-(1,6) linkages together with the localization of the branching point at a single-molecule scale. This opens up new avenues for glycan characterization. Single glycans can be imaged and their structure can be unambiguously determined. The tandem approach of preparative mass spectrometry with scanning probe microscopy is expected to be useful for the identification of recurrent structural features of glycans that are of biological importance.

Experimental section

2.8. General Materials and Methods

All chemicals used were reagent grade and used as supplied unless otherwise noted. All building blocks used were purchased from *GlycoUniverse*, Germany. Automated syntheses were performed on a home-built synthesizer developed at the Max Planck Institute of Colloids and Interfaces.[108] Merrifield resin LL (100-200 mesh, Novabiochem^{TM}) was modified and used as solid support.[105] Analytical thin-layer chromatography (TLC) was performed on Merck silica gel 60 F254 plates (0.25 mm). Compounds were visualized by UV irradiation or dipping the plate in a p-anisaldehyde (PAA) solution. Flash column chromatography was carried out by using forced flow of the indicated solvent on Fluka Kieselgel 60 M (0.04 – 0.063 mm). Analysis and purification by normal and reverse phase HPLC was performed using an Agilent 1200 series. Products were lyophilized using a Christ Alpha 2-4 LD plus freeze dryer. ^{1}H, ^{13}C and HSQC NMR spectra were recorded on a Varian 400-MR (400 MHz), Varian 600-MR (600 MHz), or Bruker Biospin AVANCE700 (700 MHz) spectrometer. Spectra were recorded in $CDCl_3$ by using the solvent residual peak chemical shift as the internal standard ($CDCl_3$: 7.26 ppm ^{1}H, 77.0 ppm ^{13}C) or in D_2O using the solvent as the internal standard in ^{1}H NMR (D_2O: 4.79 ppm ^{1}H) and a D6-acetone spike as the internal standard in ^{13}C NMR (acetone in D_2O: 30.89 ppm ^{13}C) unless otherwise stated. High resolution mass spectra were obtained using a 6210 ESI-TOF mass spectrometer (Agilent) and a MALDI-TOF Autoflex^{TM} (Bruker). MALDI and ESI mass spectra were run on IonSpec Ultima instruments.

Solvents used for dissolving building block and preparing the activator, TMSOTf and capping solutions were taken from an anhydrous solvent system (jcmeyer-solvent systems). Other solvents used were HPLC grade. The building blocks were co-evaporated three times with toluene and dried 2 h under high vacuum before use. Activator, deprotection, acidic wash, capping and building block solutions were freshly prepared and kept under argon during the automation run. All yields of products obtained by AGA were calculated based on resin loading. Resin loading was determined by performing one glycosylation (Module C) with ten equivalents of building block followed by DBU promoted Fmoc-cleavage and determination of dibenzofulvene production by measuring its UV absorbance.

2.9. Preparation of stock solution.

- **Building block:** building block was dissolved in 1 mL dichloromethane (DCM).
- **Activator solution:** 1.56 g of recrystallized NIS was dissolved in 60 mL of a 2:1 mixture of anhydrous DCM and anhydrous dioxane. Then triflic acid (67 µL) was added. The solution is kept at 0 °C for the duration of the automation run.
- **Fmoc deprotection solution:** A solution of 20% piperidine in dimethylformamide (DMF) (v/v) was prepared.
- **TMSOTf solution:** Trimethylsilyl trifluoromethanesulfonate (TMSOTf) (0.9 mL) was added to DCM (90 mL).
- **Capping solution:** A solution of 10% acetic anhydride (Ac_2O) and 2% methanesulfunic acid (MsOH) in anhydrous DCM (v/v) was prepared.
- **Lev deprotection solution**: Hydrazine Acetate (550 mg) was dissolved in a solution of 4:1:0.25 Pyridine:AcOH:H_2O (40 mL).

2.10. Modules for automated synthesis

2.10.1. Module A: Resin Preparation for Synthesis (20 min)

All automated syntheses were performed on 19 µmol scale. Resin was placed in the reaction vessel and swollen in DCM for 20 min at room temperature prior to synthesis. During this time, all reagent lines required for the synthesis were washed and primed. Before the first glycosylation, the resin was washed with the DMF, tetrahydrofuran (THF), and DCM (three times each with 2 mL for 25 s). This step is conducted as the first step for every synthesis.

2.10.2. Module B: Acidic Wash with TMSOTf Solution (20 min)

The resin was swollen in 2 mL DCM and the temperature of the reaction vessel was adjusted to -20 °C. Upon reaching the temperature, TMSOTf solution (1 mL) was added drop wise to the reaction vessel. After bubbling for 3 min, the acidic solution was drained and the resin was washed with 2 mL DCM for 25 s.

2.10.3. Module C: Thioglycoside Glycosylation (20-60 min)

The building block solution (0.150 mmol of BB in 1 mL of DCM per glycosylation) was delivered to the reaction vessel. After the set temperature (T1) was reached, the reaction was started by drop wise addition of the activator solution (1.0 mL, excess). The glycosylation was performed by increasing the temperature to T2 for 20-60 min (depending on oligosaccharide length). After completion of the reaction, the solution is drained and the resin was washed with DCM, DCM:dioxane (1:2, 3 mL for 20 s) and DCM (twice, each with 2 mL for 25 s). The temperature of the reaction vessel is increased to 25 °C for the next module.

2.10.4. Module D: Capping (30 min)

The resin was washed with DMF (twice with 2 mL for 25 s) and the temperature of the reaction vessel was adjusted to 25 °C. Pyridine solution 2 mL (10% in DMF) was delivered into the reaction vessel. After 1 min, the reaction solution was drained, and the resin washed with DCM (three times with 3 mL for 25 s). The capping solution 4 mL was delivered into the reaction vessel. After 20 min, the reaction solution was drained, and the resin washed with DCM (three times with 3 mL for 25 s).

2.10.5. Module E: Fmoc Deprotection (14 min)

The resin was washed with DMF (three times with 2 mL for 25 s) and the temperature of the reaction vessel was adjusted to 25 °C. Fmoc deprotection solution (2 mL) was delivered into the reaction vessel. After 5 min, the reaction solution was drained, and the resin washed with DMF (three times with 3 mL for 25 s) and DCM (five times each with 2 mL for 25 s). The temperature of the reaction vessel is decreased to -20 °C for the next module.

2.10.6. Module F: Lev deprotection (ca. 100 min)

The resin was washed with DMF (3×30 sec) and 1.3 mL DCM added to the reaction vessel. Solution **F** (0.8 mL) was added to the reaction vessel, and the temperature was adjusted to 25 °C. After 30 min, the reaction solution was drained, and the entire cycle was repeated twice more. After Lev deprotection was complete, the resin was washed with DMF, THF and DCM.

2.11. Post-synthesizer Manipulations

2.11.1. Cleavage from Solid Support

After automated synthesis, the oligosaccharides were cleaved from the solid support using a continuous-flow photo reactor. The Vapourtec E-Series UV-150 Photoreactor Flow Chemistry System with mercury lamp was employed. The resin, suspended in CH_2Cl_2, was loaded into a plastic syringe. The suspension was pumped using a syringe pump (PHD2000, Harvard Aparatus) at 1 mL/min through a 10 mL reactor, constructed of 1/8 inch o.d. FEP tubing. The temperature of the photoreactor was maintained at 20 °C.[108]

For selected cleavages, the mercury lamp was replaced by a LED 365 nm UV lamp.

2.11.2. Oligosaccharide deprotection

Module G: Methanolysis

The protected oligosaccharide was dissolved in MeOH:DCM (1.5 mL,1:1). NaOMe in MeOH (0.1 mL of 0.5M solution) was added to the solution and stirred at room temperature. After 12 h, the solution was neutralized with Amberlite IR-120 (H^+ form) resin, filtered and concentrated *in vacuo.* The crude compound was used for hydrogenolysis without further purification.

Module H: Hydrogenolysis with Pd/C

The crude compound obtained from *Module G* was dissolved in 2 mL of DCM:*t*BuOH:H_2O (1:0.5:0.5) and Pd/C (10%) was added. The reaction was stirred in H_2 bomb with 60 psi pressure for 16 hours. The reaction was filtered, washed with DCM, *t*BuOH and H_2O. The filtrates were concentrated *in vacuo.*

Module I: Hydrogenolysis with $Pd(OH)_2/C$

The crude compound obtained from *Module G* was dissolved in 2 mL of EA:*t*BuOH:H_2O (1:0.5:0.5) and $Pd(OH)_2/C$ was added. The reaction was stirred in H_2 bomb with 60 psi pressure for 16 hours. The reaction was filtered, washed with EA, *t*BuOH and H_2O. The filtrates were concentrated *in vacuo.*

2.11.3. Purification

Solvent was evaporated in vacuo and the crude products were dissolved in 1:1 mixture of hexane and ethyl acetate and analyzed using analytical HPLC (DAD1F, 280 nm). Pure compounds were afforded by preparative HPLC (Agilent 1200 Series spectrometer).

Method A: (YMC-Diol-300 column, 150 x 4.6 mm) flow rate of 1.0 mL / min with Hex – 20% EtOAc as eluent [isocratic 20% EtOAc (5 min), linear gradient to 55% EtOAc (45 min), linear gradient to 100% EtOAc (5 min)].

Method B: (YMC-Diol-300 column, 150 x 20 mm) flow rate of 15 mL / min with Hex – 20% EtOAc as eluent [isocratic 20% EtOAc (5 min), linear gradient to 55% EtOAc (45 min), linear gradient to 100% EtOAc (5 min)].

Method C: (Synergi Hydro RP18 column, 250 x 4.6 mm) flow rate of 1.0 mL / min with H2O (0.1% formic acid) as eluents [isocratic (5 min), linear gradient to 10% ACN (30 min), linear gradient to 100% ACN (5 min)].

Method D: (Synergi Hydro RP18 column, 250 x 10 mm) flow rate of 4.0 mL / min with H_2O (0.1% formic acid) as eluents [isocratic (5 min), linear gradient to 10% ACN (30 min), linear gradient to 100% ACN (5 min)].

Method E: (YMC-Diol-300 column, 150 x 4.6 mm) flow rate of 1.0 mL / min with Hex – 35% EtOAc as eluents [isocratic 35% EtOAc (5 min), linear gradient to 60% EtOAc (5 min), linear gradient to 60% EtOAc (30 min), linear gradient to 100% EtOAc (5 min)].

Method F: (YMC-Diol-300 column, 150 x 20 mm) flow rate of 15 mL / min with Hex – 35% EtOAc as eluents [isocratic 35% EtOAc (5 min), linear gradient to 60% EtOAc (75 min), linear gradient to 100% EtOAc (10 min)].

Method G: (YMC-Diol-300 column, 150 x 4.6 mm) flow rate of 1.0 mL / min with Hex – 40% EtOAc as eluents [isocratic 40% EtOAc (5 min), linear gradient to 70% EtOAc (5 min), linear gradient to 70% EtOAc (30 min), linear gradient to 100% EtOAc (5 min)].

Method H: (YMC-Diol-300 column, 150 x 20 mm) flow rate of 15 mL / min with Hex – 40% EtOAc as eluents [isocratic 40% EtOAc (5 min), linear gradient to 70% EtOAc (75 min), linear gradient to 100% EtOAc (10 min)].

Method I: (TSKgel G 3000 PWXL column, 7.8 mm ID x 30 cm) flow rate of 0.4 mL / min with water as eluent.

Method J: (YMC-Diol-300 column, 150 x 4.6 mm) flow rate of 1.0 mL / min with Hex – 50% EtOAc as eluents [isocratic 50% EtOAc (5 min), linear gradient to 75% EtOAc (5 min), linear gradient to 75% EtOAc (30 min), linear gradient to 100% EtOAc (5 min)].

Method K: (YMC-Diol-300 column, 150 x 20 mm) flow rate of 15 mL / min with Hex – 50% EtOAc as eluents [isocratic 50% EtOAc (5 min), linear gradient to 75% EtOAc (75 min), linear gradient to 100% EtOAc (10 min)].

Method J: (Hypercarb column, 150 x 4.6 mm) flow rate of 0.7 mL / min with H_2O (0.1% formic acid) as eluents [isocratic (5 min), linear gradient to 30% ACN (30 min), linear gradient to 100% ACN (5 min)].

Method K: (Hypercarb column, 150 x 10 mm) flow rate of 1.3 mL / min with H_2O (0.1% formic acid) as eluents [isocratic (5 min), linear gradient to 30% ACN (30 min), linear gradient to 100% ACN (5 min)].

Method L: (Synergi Hydro RP18 column, 250 x 4.6 mm) flow rate of 1.0 mL / min with H_2O (0.1% formic acid) as eluents [isocratic (5 min), linear gradient to 30% ACN (30 min), linear gradient to 100% ACN (5 min)].

Method M: (Synergi Hydro RP18 column, 250 x 10 mm) flow rate of 4.0 mL / min with H_2O (0.1% formic acid) as eluents [isocratic (5 min), linear gradient to 30% ACN (30 min), linear gradient to 100% ACN (5 min)].

2.12. AGA synthesis

2.12.1. Synthesis of α-(1,6) linear hexamannoside (4)

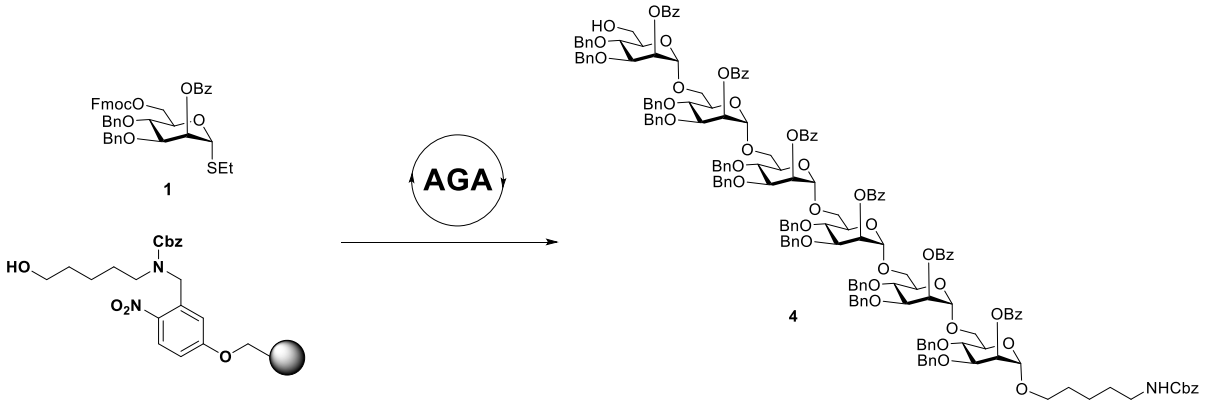

Procedure A

	Module	Conditions
	A: Resin Preparation for Synthesis	
6	B: Acidic Wash with TMSOTf Solution C: Thioglycoside Glycosylation E: Fmoc Deprotection	BB1 6.5 eq, -40 °C for 5 min, -20 °C for 30 min

Cleavage from the solid support as described in *Post-synthesizer manipulations*, followed by purification using preparative HPLC (Method B) afforded the fully protected hexasaccharide **4** (20 mg, 55%).

Crude NP-HPLC of hexasaccharide **4** (ELSD trace, Method A, t_R = 25.3 min)

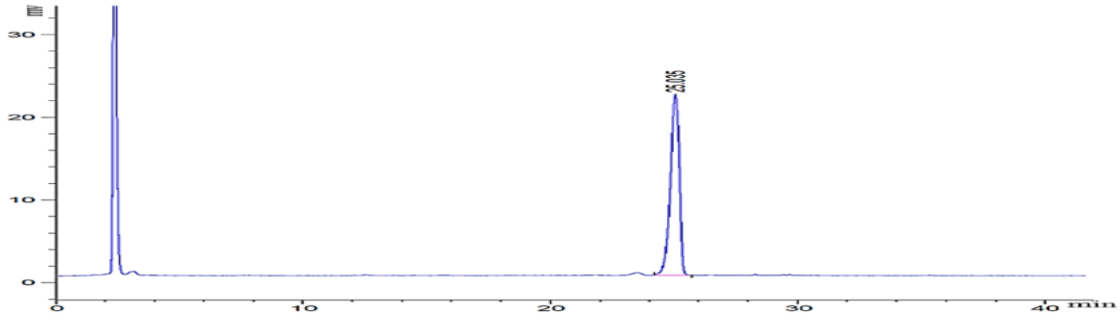

^{1}H NMR (400 MHz, $CDCl_3$) δ 8.24 – 8.09 (m, 12H), 7.64 (s, 1H), 7.56 – 7.46 (m, 17H), 7.38 – 7.30 (m, 12H), 7.29 – 7.11 (m, 56H), 5.85 (d, *J* = 9.0 Hz, 4H), 5.80 (s, 1H), 5.67 (s, 1H), 5.14 (s, 1H), 5.12 – 5.03 (m, 6H), 4.95 – 4.74 (m, 12H), 4.61 (dd, *J* = 15.6, 11.1 Hz, 2H), 4.52

– 4.41 (m, 7H), 4.37 (d, *J* = 12.4 Hz, 2H), 4.14 – 3.86 (m, 13H), 3.84 – 3.59 (m, 11H), 3.58 – 3.52 (m, 2H), 3.47 (dd, *J* = 16.9, 9.7 Hz, 4H), 3.22 – 3.16 (m, 2H), 1.64 – 1.56 (m, 2H), 1.55 – 1.47 (m, 2H), 1.41 – 1.33 (m, 2H); m/z (HRMS+) 2937.160 $[M + Na]^+$ ($C_{175}H_{175}NO_{39}Na$ requires 2937.163).Proton signals are in agreement with previous reports by Delbianco *et al.*[63]

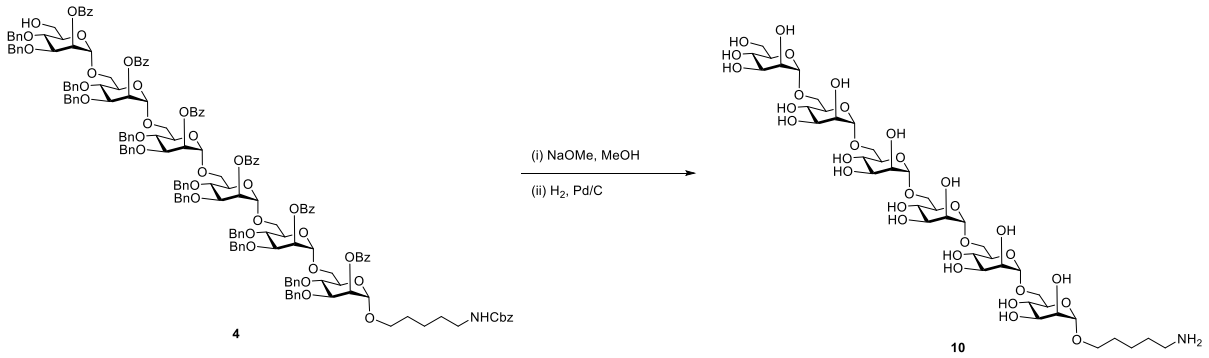

Deprotection of **4** (as described in Module G and H), followed by purification using preparative HPLC (Method L, t_R = 22.2 min) afforded compound **10** (3.9 mg, 52%).

RP-HPLC of purified hexasaccharide **10** (ELSD trace, Method J, t_R = 22.2 min)

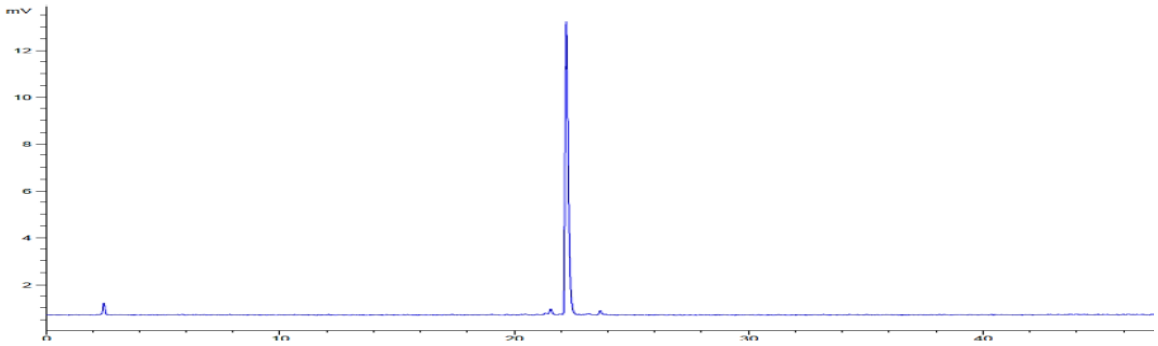

Analytical data for **10**.^{1}H NMR (400 MHz, D_2O) δ 4.89 – 4.85 (m, 5H), 4.83 (s, 1H), 3.98 – 3.95 (m, 5H), 3.94 – 3.88 (m, 7H), 3.85 (s, 1H), 3.84 – 3.82 (m, 5H), 3.80 – 3.77 (m, 5H), 3.76 – 3.71 (m, 8H), 3.71 (d, *J* = 2.3 Hz, 2H), 3.69 – 3.60 (m, 4H), 3.57 – 3.51 (m, 1H), 2.98 (t, *J* = 7.6 Hz, 2H), 1.71 – 1.61 (m, 4H), 1.50 – 1.37 (m, 2H); ^{13}C NMR (100 MHz, D_2O) δ 99.89, 99.42, 99.30, 72.73, 70.92, 70.84, 70.80, 70.78, 70.72, 70.69, 70.55, 70.07, 69.98, 69.94, 67.63, 66.75, 66.61, 66.56, 65.61, 65.58, 65.53, 60.94, 39.38, 28.04, 26.57, 22.53; m/z (HRMS+) 1076.424 $[M + H]^+$ ($C_{41}H_{73}NO_{31}$ requires 1076.423). Proton and Carbon signals are in concordance as previously reported by Delbianco *et al.*[63]

2.12.2. Synthesis of α-(1,6) linear α-(1,2) branched hexamannoside (5)

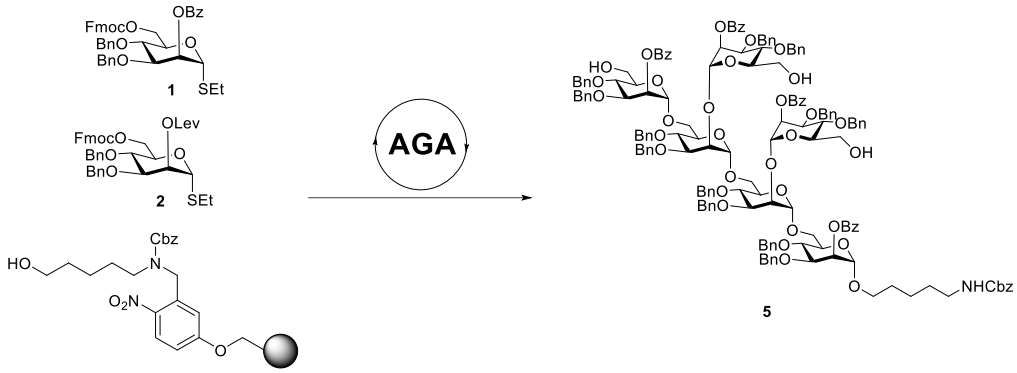

Procedure A

	Module	Conditions
	A: Resin Preparation for Synthesis	
	B: Acidic Wash with TMSOTf Solution C: Thioglycoside Glycosylation E: Fmoc Deprotection	BB1 6.5 eq, -40 °C for 5 min, -20 °C for 30 min
2	B: Acidic Wash with TMSOTf Solution C: Thioglycoside Glycosylation E: Fmoc Deprotection	BB1 6.5 eq, -40 °C for 5 min, -20 °C for 30 min
	F: Lev Deprotection B: Acidic Wash with TMSOTf Solution 3x C: Thioglycoside Glycosylation E: Fmoc Deprotection	BB1 13 eq, -40 °C for 5 min, -20 °C for 30 min

Procedure B

	Module	Conditions
	A: Resin Preparation for Synthesis	
	B: Acidic Wash with TMSOTf Solution C: Thioglycoside Glycosylation D: Capping E: Fmoc Deprotection	BB1 6.5 eq, -20 °C for 5 min, 0 °C for 20 min
2	B: Acidic Wash with TMSOTf Solution C: Thioglycoside Glycosylation D: Capping E: Fmoc Deprotection	BB2 6.5 eq, -20 °C for 5 min, 0 °C for 20 min
	F: Lev Deprotection B: Acidic Wash with TMSOTf Solution 3x C: Thioglycoside Glycosylation D: Capping E: Fmoc Deprotection	BB1 6.5 eq, -20 °C for 5 min, 0 °C for 20 min

Cleavage from the solid support as described in *Post-synthesizer manipulations* followed by purification using a preparative HPLC (Method B), to provide the fully protected branched hexasaccharide **5**. For procedure **A:** 12.5 mg, 4.62 μmol, 37%, based on resin loading. For procedure **B:** 18.0 mg, 6.65 μmol, 53%, based on resin loading.

Crude NP-HPLC of hexasaccharide **5.** A) Procedure **A** . B) Procedure **B** (ELSD trace, Method A, t_R = 28.5 min)

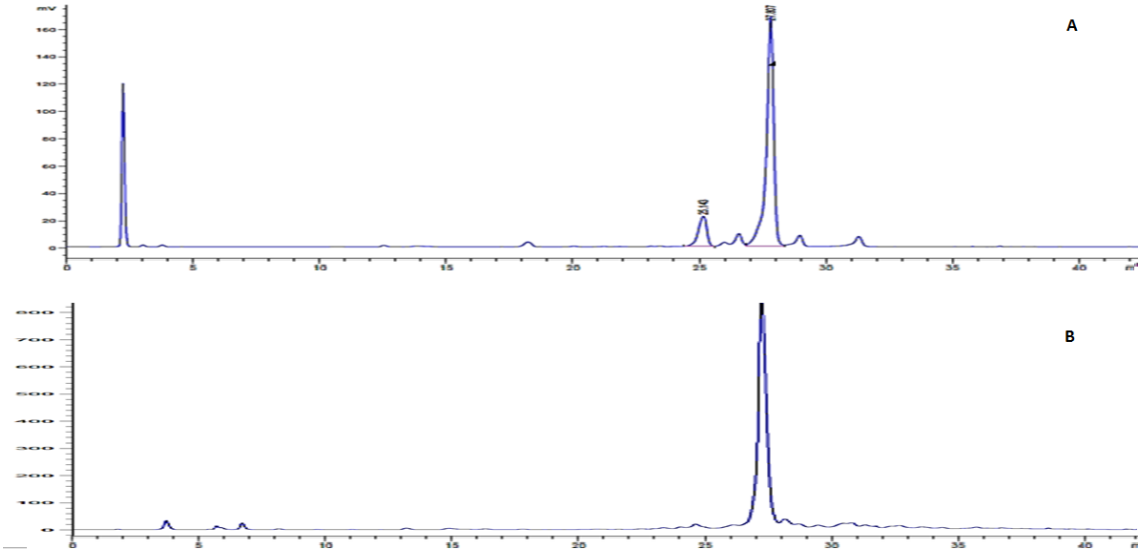

^{1}H NMR (400 MHz, $CDCl_3$) δ 8.08 – 7.87 (m, 9H), 7.55 – 7.45 (m, 4H), 7.41 – 7.30 (m, 8H), 7.27 – 6.92 (m, 65H), 5.83 – 5.78 (m, 1H), 5.61 (t, *J* = 2.4 Hz, 1H), 5.54 (t, *J* = 2.3 Hz, 1H), 5.45 – 5.40 (m, 1H), 5.24 (s, 1H), 5.11 (s, 1H), 5.03 – 4.97 (m, 3H), 4.84 – 4.82 (m, 3H), 4.79 – 4.67 (m, 7H), 4.62 – 4.26 (m, 14H), 4.17 – 4.08 (m, 2H), 4.02 – 3.90 (m, 6H), 3.87 – 3.75 (m, 9H), 3.72 – 3.48 (m, 14H), 3.44 – 3.26 (m, 5H), 3.11 – 3.02 (m, 2H), 1.48 – 1.38 (m, 4H), 1.26 (d, *J* = 9.1 Hz, 2H); ^{13}C NMR (100 MHz, $CDCl_3$) δ 165.98, 165.52, 165.43, 165.38, 156.51, 138.66, 138.53, 138.49, 138.29, 138.21, 138.10, 138.05, 137.90, 137.81, 137.66, 137.14, 136.79, 136.76, 133.52, 133.43, 133.27, 133.22, 130.26, 130.05, 129.99, 129.90, 129.78, 129.34, 128.63, 128.55, 128.43, 128.35, 128.28, 128.17, 128.14, 128.02, 127.97, 127.88, 127.81, 127.77, 127.71, 127.56, 127.47, 127.34, 100.24, 99.87, 99.28, 98.87, 97.64, 97.55, 79.24, 79.11, 78.97, 78.61, 78.50, 75.33, 75.21, 75.12, 74.93, 74.58, 74.42, 74.10, 73.99, 73.40, 72.78, 72.49, 71.91, 71.81, 71.75, 71.38, 71.24, 71.06, 70.49, 69.63, 69.57, 69.23, 68.81, 67.84, 66.69, 66.02, 65.87, 62.59, 62.27, 61.94, 41.05, 29.87, 29.14, 23.54; m/z (HRMS+) 2708.198 $[M + H]^+$ ($C_{161}H_{168}NO_{37}$ requires 2708.136).

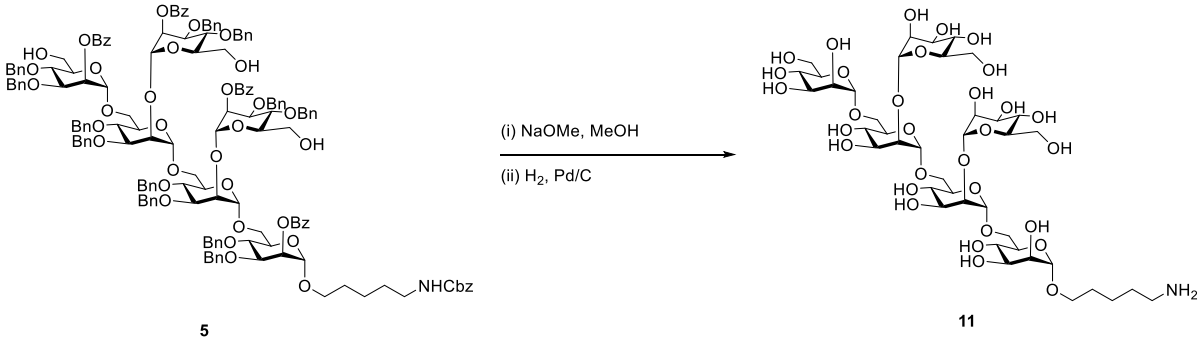

5 11

Deprotection of **5** as described in Module G and H, followed by purification using preparative HPLC (Method L) afforded compound **11** (3.1 mg, 2.88 µmol, 62% over two steps).^{1}H NMR (600 MHz, D_2O) δ 5.15 (s, 1H), 5.14 (s, 1H), 5.07 (s, 1H), 5.05 (s, 1H), 4.95 (s, 1H), 4.87 (s, 1H), 4.12 – 3.54 (m, 38H), 3.02 (t, J = 7.7 Hz, 2H), 1.74 – 1.65 (m, 4H), 1.52 – 1.41 (m, 2H); ^{13}C NMR (150 MHz, D_2O) δ 102.24 , 99.22, 99.11, 98.88, 78.72, 73.24, 73.17, 72.73, 71.17, 71.08, 70.83, 70.57, 70.38, 69.93, 67.55, 66.64, 66.61, 66.58, 66.50, 66.42, 65.78, 65.58, 65.11, 60.99, 60.96, 60.86, 39.29, 27.95, 26.49, 22.43; m/z (HRMS+) 1076.425 $[M + H]^+$ ($C_{41}H_{73}NO_{31}$ requires 1076.423).

RP-HPLC of purified hexasaccharide **11** (ELSD trace, Method J, t_R = 21.3 min)

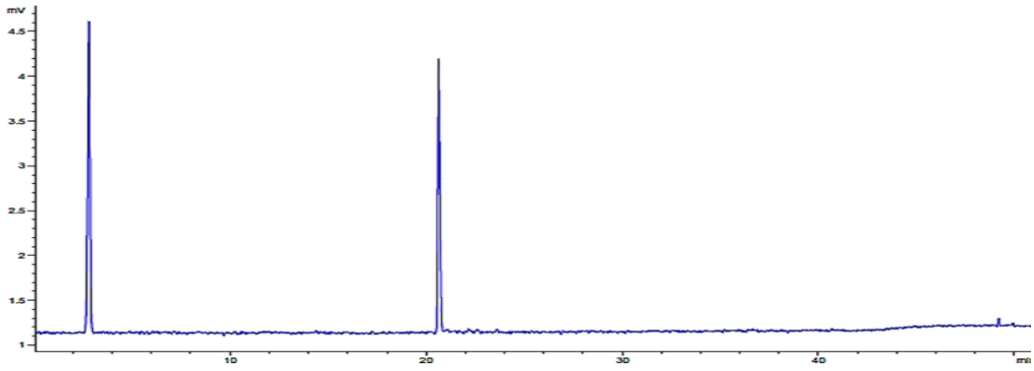

2.12.3. Synthesis of α-(1,6) linear α-(1,2) branched dodecamannoside (6)

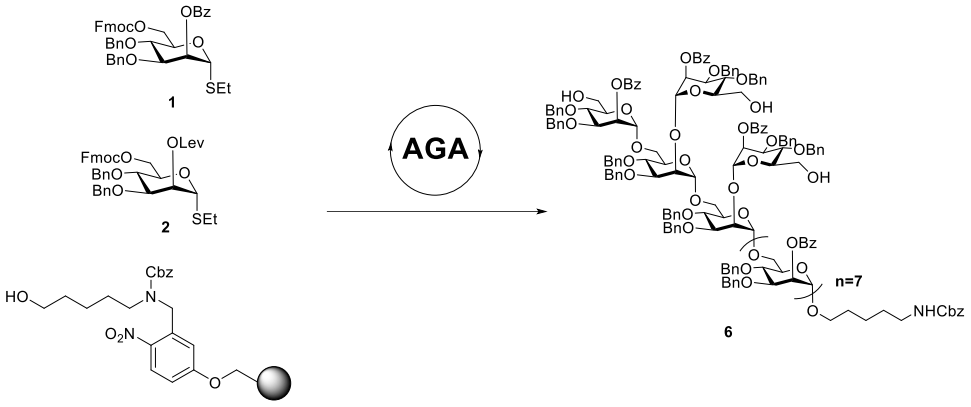

Procedure A:

	Module	Conditions
	A: Resin Preparation for Synthesis	
7	B: Acidic Wash with TMSOTf Solution C: Thioglycoside Glycosylation E: Fmoc Deprotection	BB1 6.5 eq, -40 °C for 5 min, -20 °C for 30 min
2	B: Acidic Wash with TMSOTf Solution C: Thioglycoside Glycosylation E: Fmoc Deprotection	BB2 6.5 eq, -40 °C for 5 min, -20 °C for 30 min
	F: Lev Deprotection B: Acidic Wash with TMSOTf Solution 3x C: Thioglycoside Glycosylation E: Fmoc Deprotection	BB1 13 eq, -40 °C for 5 min, -20 °C for 30 min

Procedure B:

	Module	Conditions
	A: Resin Preparation for Synthesis	
7	B: Acidic Wash with TMSOTf Solution C: Thioglycoside Glycosylation D: Capping E: Fmoc Deprotection	BB1 6.5 eq, -20 °C for 5 min, 0 °C for 20 min
2	B: Acidic Wash with TMSOTf Solution C: Thioglycoside Glycosylation D: Capping E: Fmoc Deprotection	BB2 6.5 eq, -20 °C for 5 min, 0 °C for 20 min
	E: Lev Deprotection B: Acidic Wash with TMSOTf Solution 3x C: Thioglycoside Glycosylation D: Capping E: Fmoc Deprotection	BB1 6.5 eq, -20 °C for 5 min, 0 °C for 20 min

Cleavage from the solid support as described in *Post-synthesizer manipulations* followed by purification using a preparative HPLC (Method B), to provide the fully protected branched dodecasaccharide **6.** For procedure **A,** 2.2 mg, 0.75 µmol, 6%, based on resin loading. For procedure **B,** 30 mg, 6.05 µmol, 48%, based on resin loading.

Crude NP-HPLC of dodecasaccharide **6** A) Procedure **A**. B) Procedure **B** (ELSD trace, Method A, t_R = 31.3 min)

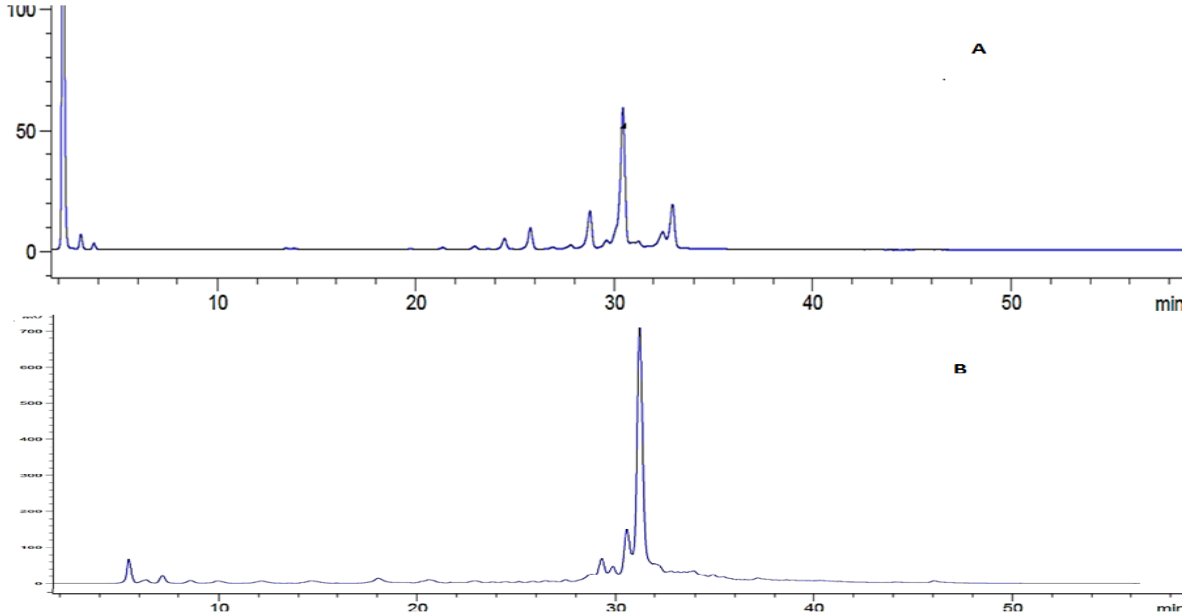

^{1}H NMR (600 MHz, $CDCl_3$) δ 8.18 – 8.14 (m, 8H), 8.11 – 8.08 (m, 2H), 8.06 – 8.00 (m, 6H), 7.96 (d, *J* = 7.7 Hz, 2H), 7.56(t, *J* = 7.5 Hz, 1H), 7.54 – 7.34 (m, 25H), 7.33 – 7.00 (m, 116H), 5.88 (s, 1H), 5.82 – 5.78 (m, 4H), 5.72 (s, 1H), 5.67 (s, 1H), 5.64 – 5.60 (m, 2H), 5.30 (s, 1H), 5.12 (s, 1H), 5.09 – 5.01 (m, 8H), 4.93 (s, 1H), 4.90 – 4.74 (m, 20H), 4.67 (dd, *J* = 10.9, 6.7 Hz, 2H), 4.63 – 4.29 (m, 25H), 4.27 (s, 1H), 4.22 (dd, *J* = 9.0, 3.1 Hz, 1H), 4.12 –3.98 (m, 11H), 3.95 – 3.30 (m, 45H), 3.16 (s, 2H), 1.50 – 1.45 (m, 4H), 1.35 – 1.32 (m, 2H); ^{13}C NMR (152 MHz, $CDCl_3$) δ 165.99, 165.76, 165.73, 165.67, 165.53, 165.44, 165.39, 165.31, 156.52, 138.75, 138.61, 138.57, 138.49, 138.38, 138.31, 138.25, 138.08, 138.00, 137.91, 137.79, 137.73, 137.69, 137.63, 137.57, 136.83, 133.44, 133.21, 130.14, 130.06, 130.00, 129.90, 129.81, 128.78, 128.71, 128.62, 128.62, 128.47, 128.40, 128.31, 128.17, 128.11, 127.88, 127.81, 127.77, 127.56, 127.50, 127.39, 127.26, 127.11, 100.32, 99.57, 99.33, 99.04, 98.70, 98.65, 98.55, 98.43, 98.27, 98.01, 97.71, 78.73, 78.44, 78.37, 78.31, 78.24, 75.32, 75.19, 75.12, 74.34, 74.05, 73.95, 73.90, 73.59, 71.97, 71.86, 71.78, 71.68, 71.55, 71.47, 71.44, 71.38, 71.24, 71.20, 71.10, 71.01, 70.96, 70.87, 69.22, 68.89, 68.81, 68.71, 68.59, 68.54, 67.91, 66.69, 66.25,

65.95, 65.88, 41.10, 29.86, 29.19, 23.58. m/z (HRMS+) 2716.056 $[2M + Na]^{++}$ ($C_{323}H_{323}NO_{73}Na$ requires 2716.074).

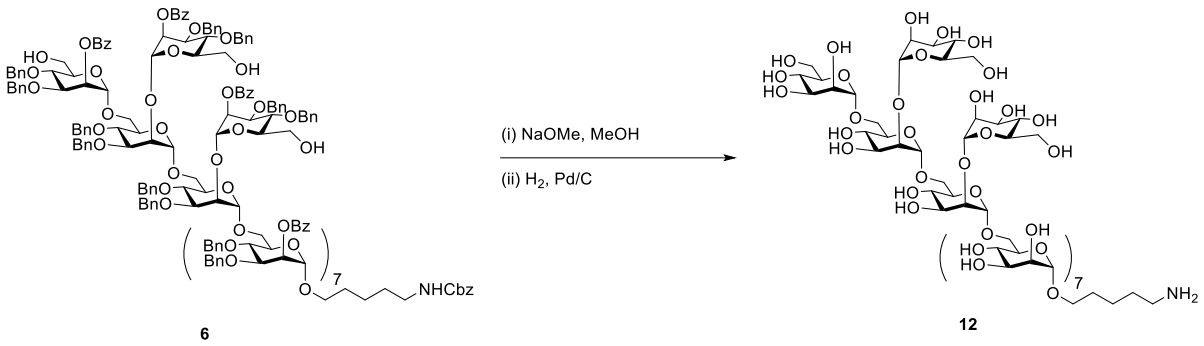

6 12

Deprotection of **6** as described in Modules G and H, followed by purification using preparative HPLC (Method L) afforded compound **12.** (2.3 mg, 1.21 µmol, 20% over two steps).^{1}H NMR (700 MHz, D_2O) δ 5.17 (s, 1H), 5.15 (s, 1H), 5.08 – 5.06 (m, 2H), 4.96 (s, 1H), 4.92 (d, J = 6.1 Hz, 5H), 4.89 (s, 1H), 4.13 – 4.10 (m, 2H), 4.06 (s, 2H), 4.02 (d, J = 4.6 Hz, 8H), 4.00 – 3.95 (m, 8H), 3.94 – 3.91 (m, 3H), 3.91 – 3.82 (m, 19H), 3.81 – 3.74 (m, 20H), 3.73 – 3.66 (m, 5H), 3.60 (d, J = 10.1, 6.1 Hz, 1H), 3.03 (t, J = 7.6 Hz, 2H), 1.75 – 1.67 (m, 4H), 1.53 – 1.42 (m, 2H); 13C NMR (175 MHz, D2O) δ 102.29, 102.20, 99.87, 99.42, 99.40, 99.33, 99.28, 98.16, 98.07, 80.47, 78.79, 78.71, 76.13, 73.46, 73.26, 73.21, 72.78, 72.37, 71.20, 71.11, 70.99, 70.90, 70.88, 70.81, 70.77, 70.66, 70.61, 70.59, 70.42, 70.19, 70.04, 69.98, 69.96, 69.79, 69.03, 67.61, 67.24, 66.81, 66.69, 66.63, 66.56, 66.54, 66.47, 65.63, 65.54, 65.47, 65.16, 61.18, 61.05, 61.00, 60.91, 39.37, 28.03, 26.65, 24.46, 23.23, 22.53. m/z (HRMS+) 1886.677 $[M + H]^{+}$ ($C_{71}H_{123}NO_{56}$ requires 1886.688).

RP-HPLC of purified dodecasaccharide **12** (ELSD trace, Method J, t_R = 24.2 min)

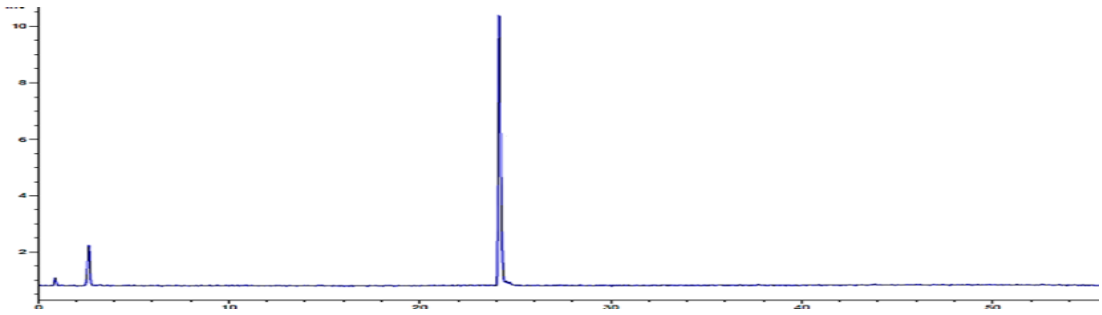

2.12.4. Synthesis of α-(1,6) linear α-(1,2) branched octaarabinomannoside (7)

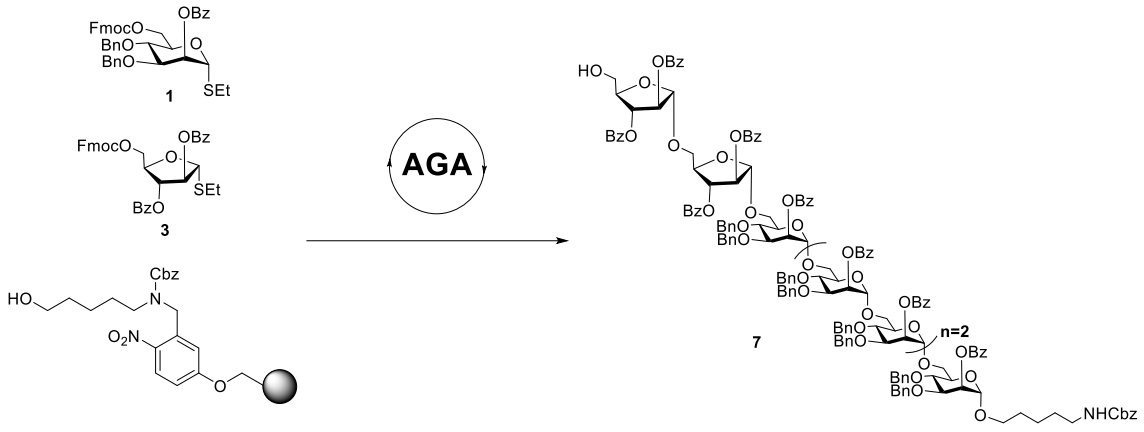

Procedure A

	Module	Conditions
	A: Resin Preparation for Synthesis	
6	B: Acidic Wash with TMSOTf Solution C: Thioglycoside Glycosylation E: Fmoc Deprotection	BB1 6.5 eq, -40 °C for 5 min, -20 °C for 30 min
2	B: Acidic Wash with TMSOTf Solution C: Thioglycoside Glycosylation E: Fmoc Deprotection	BB3 13 eq, -40 °C for 5 min, -20 °C for 30 min

Procedure B

	Module	Conditions
	A: Resin Preparation for Synthesis	
6	B: Acidic Wash with TMSOTf Solution C: Thioglycoside Glycosylation D: Capping E: Fmoc Deprotection	BB1 6.5 eq, -20 °C for 5 min, 0 °C for 20 min
2	B: Acidic Wash with TMSOTf Solution C: Thioglycoside Glycosylation D: Capping E: Fmoc Deprotection	BB3 6.5 eq, -20 °C for 5 min, 0 °C for 20 min

Cleavage from the solid support as described in *Post-synthesizer manipulation* followed by purification using a preparative HPLC (Method B), to provide the fully protected linear octasaccharide **7.** For procedure **A** 4 mg, 1.10 µmol, 9%, based on resin loading. For procedure **B** 25 mg, 6.8 µmol, 56%, based on resin loading.

Crude NP-HPLC of octasaccharide **7** A) Procedure **A**. B) Procedure **B** (ELSD trace, Method A, t_R = 28.6 min)

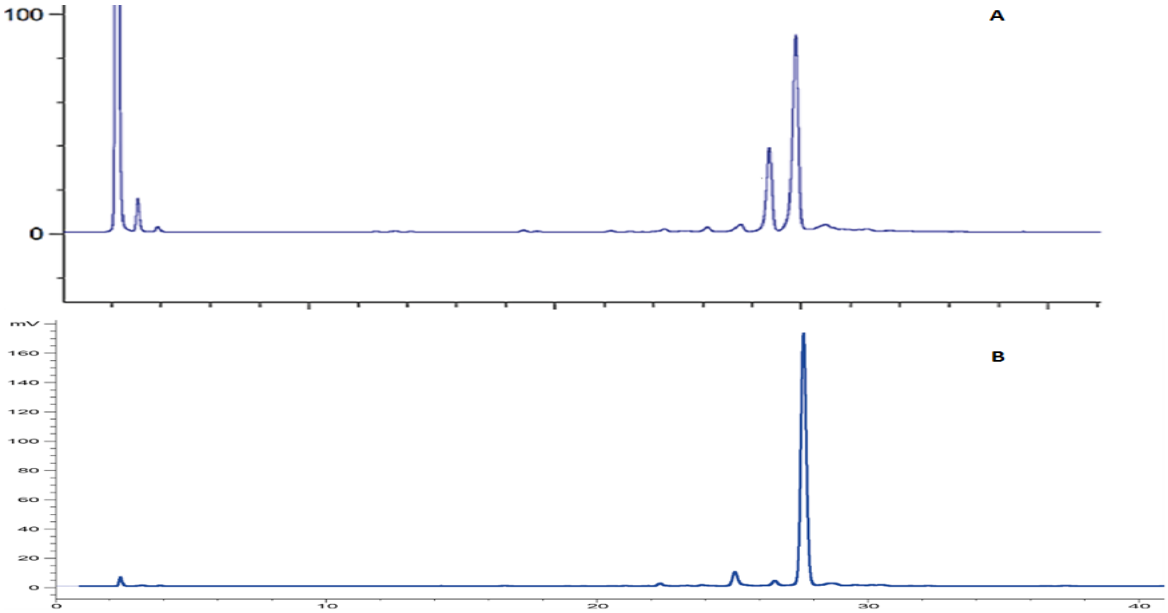

^{1}H NMR (400 MHz, $CDCl_3$) δ 8.19 – 8.09 (m, 12H), 8.06 – 8.01 (m, 4H), 7.83 – 7.76 (m, 4H), 7.62 – 7.56 (m, 1H), 7.53 – 7.06 (m, 90H), 6.98 – 6.89 (m, 4H), 5.88 – 5.74 (m, 6H), 5.62 (dd, *J* = 3.3, 1.9 Hz, 1H), 5.56 (dd, *J* = 7.9, 2.8 Hz, 2H), 5.42 (s, 1H), 5.37 – 5.30 (m, 2H), 5.10 – 5.01 (m, 6H), 4.90 – 4.76 (m, 12H), 4.66 (d, *J* = 11.4 Hz, 1H), 4.54 (d, *J* = 11.0 Hz, 1H), 4.48 – 4.31 (m, 12H), 4.26 – 4.18 (m, 1H), 4.13 (d, *J* = 3.6 Hz, 1H), 4.09 – 3.99 (m, 8H), 3.99 – 3.90 (m, 7H), 3.90 – 3.81 (m, 4H), 3.79 – 3.71 (m, 6H), 3.67 (d, *J* = 8.6 Hz, 3H), 3.58 (t, *J* = 10.4 Hz, 3H), 3.51 – 3.35 (m, 5H), 3.19 – 3.11 (m, 2H), 1.52 – 1.42 (m, 4H), 1.36 – 1.32 (m, 2H); ^{13}C NMR (150 MHz, $CDCl_3$) δ 165.95, 165.81, 165.57, 165.47, 165.29, 165.02, 138.54, 138.51, 138.47, 138.45, 138.40, 138.22, 137.91, 137.60, 137.55, 137.49, 137.26, 133.49, 133.46, 133.42, 133.25, 133.21, 133.16, 133.13, 133.06, 129.96, 129.91, 129.82, 129.73, 129.68, 129.59, 129.14, 128.90, 128.59, 128.50, 128.44, 128.38, 128.29, 128.24, 128.17, 128.15, 128.12, 127.99, 127.63, 127.59, 127.37, 127.30, 127.21, 127.07, 127.04, 126.97, 105.99, 105.78, 98.45, 98.44, 98.09, 97.83, 83.50, 83.22, 81.55, 81.44, 78.55, 78.17, 77.97, 75.13, 75.01, 74.97, 74.18, 73.99, 73.87, 73.79, 73.73, 73.68, 71.77, 71.60, 71.54, 71.38, 71.30, 71.25,

71.20, 71.15, 70.97, 70.87, 70.70, 70.04, 69.03, 68.53, 68.41, 68.36, 68.07, 67.76, 67.73, 66.51, 66.08, 65.81, 65.79, 65.75, 65.64, 65.53, 62.19, 40.92, 29.74, 29.00, 23.39; m/z (HRMS+) 3617.345 $[M + Na]^+$ ($C_{213}H_{207}NO_{51}Na$ requires 3617.352).

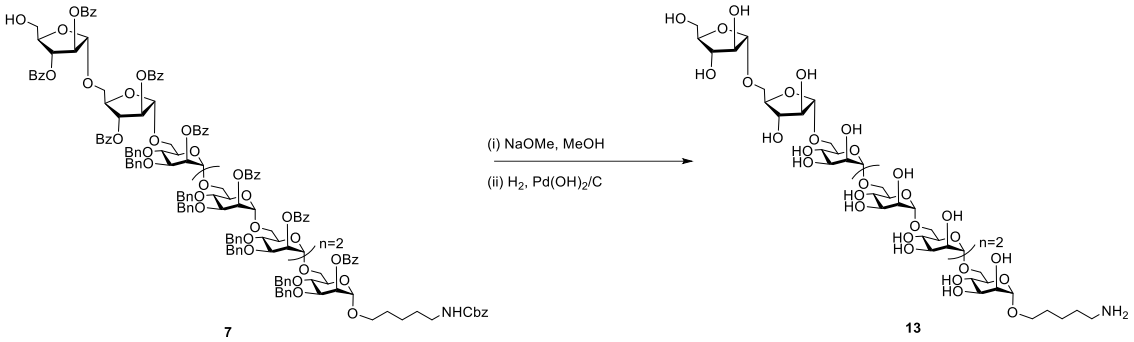

Deprotection of **7** as described in Module G and I, followed by purification using preparative HPLC (Method L) afforded compound **13**. (1.8 mg, 1.34 µmol, 26% over two steps).^{1}H NMR (700 MHz, D_2O) δ 5.13 (s, 1H), 5.11 (s, 1H), 4.94 – 4.91 (m, 5H), 4.89 (s, 1H), 4.25 (s, 1H), 4.16 (d, J = 6.7 Hz, 2H), 4.13 (s, 1H), 4.04 (s, 1H), 4.01 (s, 5H), 3.97 (q, J = 11.5, 9.6 Hz, 8H), 3.93 – 3.72 (m, 28H), 3.68 (dd, J = 11.8, 4.5 Hz, 1H), 3.62 – 3.57 (m, 1H), 3.02 (t, J = 7.7 Hz, 3H), 1.74 – 1.67 (m, 3H), 1.53 – 1.43 (m, 2H); ^{13}C NMR (151 MHz, d_2o) δ 107.32, 107.18, 99.82, 99.35, 99.31, 99.26, 83.88, 82.03, 80.83, 80.76, 76.59, 76.44, 70.90, 70.85, 70.76, 70.62, 70.49, 69.99, 69.91, 69.86, 67.56, 66.68, 66.57, 66.52, 65.44, 61.10, 39.30, 27.96, 26.51, 22.47. m/z (HRMS+) 1340.501. $[M + H]^+$ ($C_{51}H_{89}NO_{39}$ requires 1340.508).

RP-HPLC of purified hexasaccharide **13** (ELSD trace, Method J, t_R = 25.5 min)

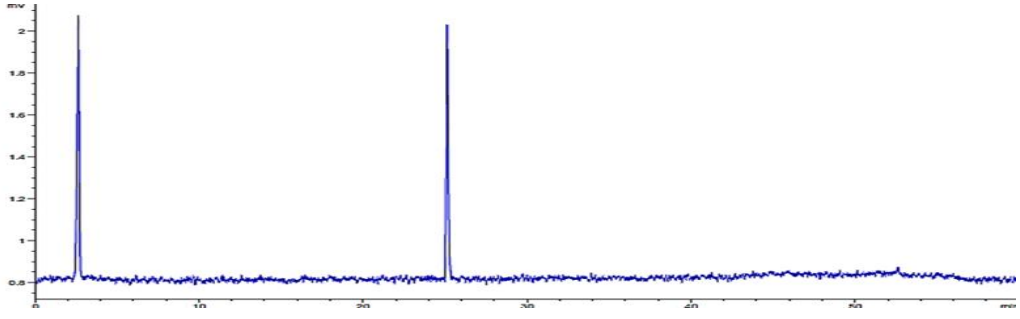

2.12.5. Synthesis of α-(1,6) α-(1,5) linear dodecaarabinomannoside (8)

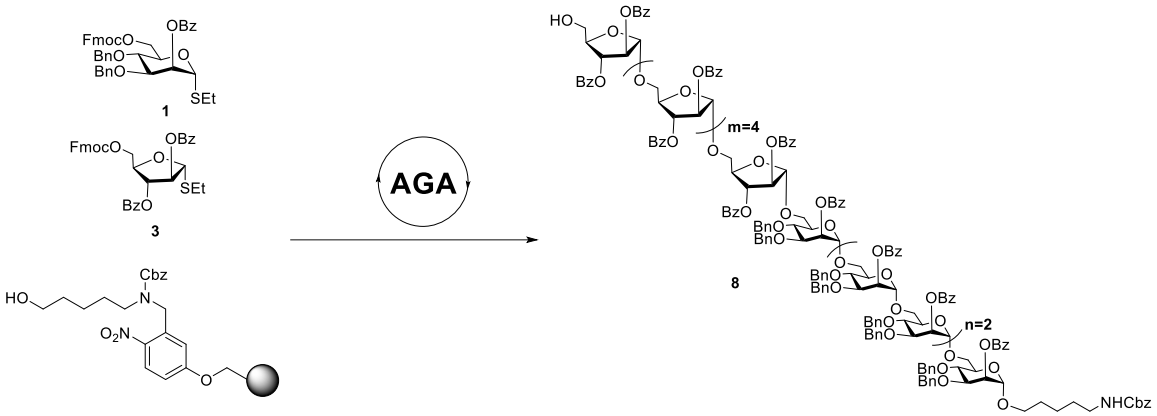

Procedure A:

	Module	Conditions
	A: Resin Preparation for Synthesis	
6	B: Acidic Wash with TMSOTf Solution C: Thioglycoside Glycosylation E: Fmoc Deprotection	BB1 6.5 eq, -40 °C for 5 min, -20 °C for 30 min
6	B: Acidic Wash with TMSOTf Solution C: Thioglycoside Glycosylation E: Fmoc Deprotection	BB3 13eq, -40 °C for 5 min, -20 °C for 30 min

Procedure B:

	Module	Conditions
	A: Resin Preparation for Synthesis	
6	B: Acidic Wash with TMSOTf Solution C: Thioglycoside Glycosylation D: Capping E: Fmoc Deprotection	BB1 6.5 eq, -20 °C for 5 min, 0 °C for 20 min
6	B: Acidic Wash with TMSOTf Solution C: Thioglycoside Glycosylation D: Capping E: Fmoc Deprotection	BB3 6.5 eq, -20 °C for 5 min, 0 °C for 20 min

Cleavage from the solid support as described in *Post-synthesizer manipulations* followed by purification using a preparative HPLC (Method B), to provide the fully protected linear dodecasaccharide **8.** For procedure **A:** 4 mg, 0.80 μmol, 7%, based on resin loading. For Procedure **B:** 38 mg, 7.38 μmol, 61%, based on resin loading.

Crude NP-HPLC of dodecasaccharide **8** . A) Procedure **A**. B) Procedure **B** (ELSD trace, Method A t_R = 36.5 min)

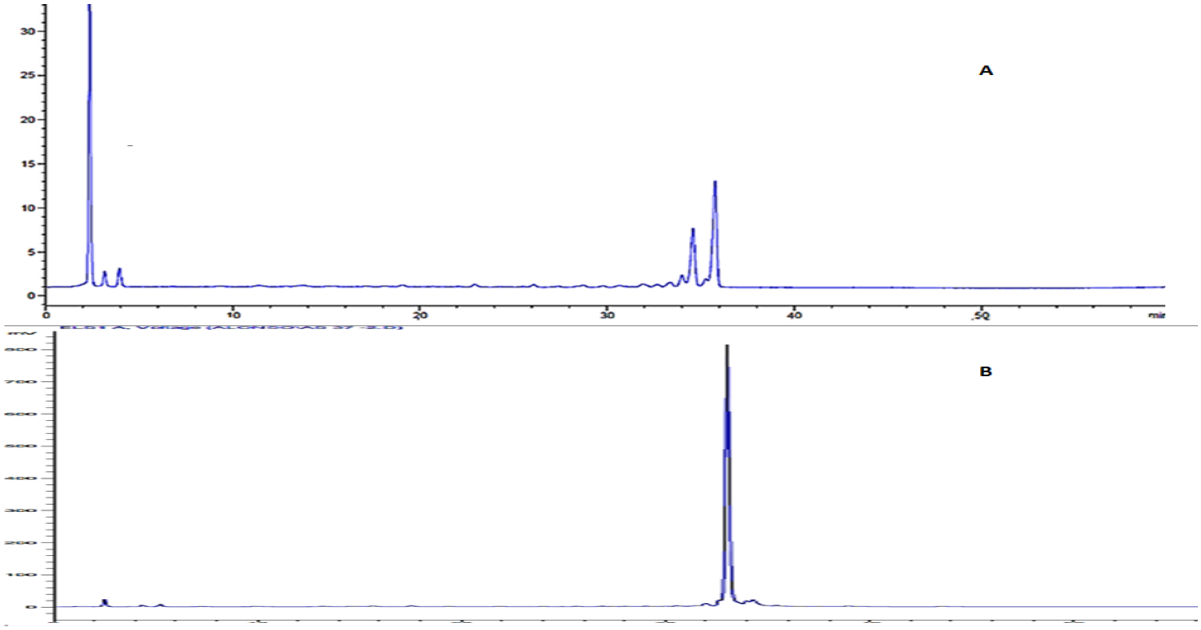

^{1}H NMR (600 MHz, $CDCl_3$) δ 8.17 – 7.99 (m, 24H), 7.90 – 7.75 (m, 12H), 7.61 – 7.05 (m, 115H), 6.98 – 6.88 (m, 4H), 5.86 – 5.74 (m, 6H), 5.64 – 5.54 (m, 11H), 5.41 – 5.34 (m, 6H), 5.31 (s, 1H), 5.15 – 4.99 (m, 7H), 4.89 – 4.74 (m, 11H), 4.67 (d, *J* = 11.4 Hz, 1H), 4.58 – 4.51 (m, 3H), 4.48 – 4.21 (m, 10H), 4.15 – 3.37 (m, 50H), 3.20 – 3.11 (m, 2H); ^{13}C NMR (100 MHz, $CDCl_3$) δ 165.76, 165.66, 165.60, 165.22, 138.64, 138.59, 137.79, 137.68, 133.64, 133.54, 133.44, 133.21, 130.15, 129.96, 129.89, 129.76, 129.26, 129.15, 128.78, 128.63, 128.47, 128.35, 127.82, 127.77, 127.37, 127.24, 127.12, 106.01, 98.64, 98.28, 83.76, 83.48, 82.19, 81.65, 81.59, 75.32, 75.20, 71.48, 71.08, 69.22, 68.61, 66.72, 66.25, 65.97, 29.86, 29.19; m/z (HRMS+) 4979.837 $[M + Na]^+$ ($C_{161}H_{168}NO_{37}Na$ requires 4979.738).

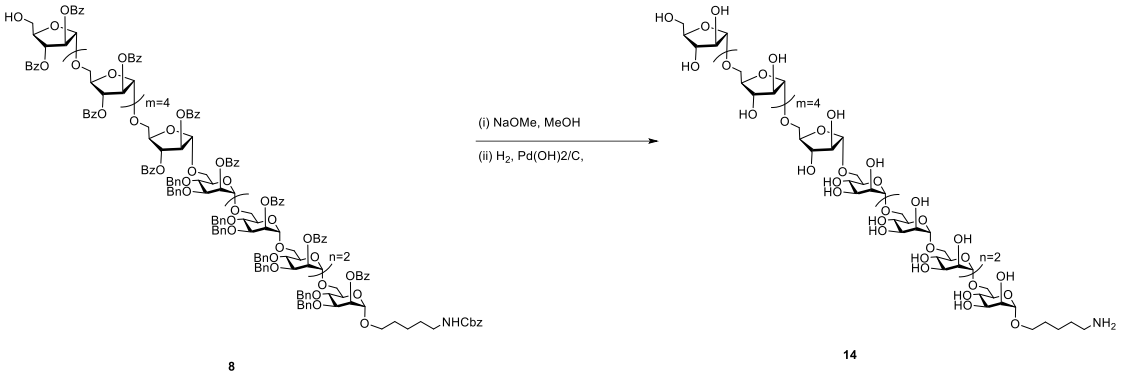

Deprotection of **8** as described in Modules G and I, followed by purification using preparative HPLC (Method L) afforded compound **14** (3.6 mg, 1.90 µmol, 25% over two steps)^{1}H NMR (700 MHz, D_2O) δ 5.13 – 5.12 (m, 6H), 4.94 – 4.91 (m, 5H), 4.89 (s, 1H), 4.26 – 4.22 (m, 5H), 4.17 – 4.15 (m, 6H), 4.13 – 4.12 (m, 1H), 4.06 – 3.94 (m, 17H), 3.94 – 3.72 (m, 37H), 3.67 (dd, J = 11.6, 4.3 Hz, 1H), 3.61 – 3.58 (m, 1H), 3.02 (t, J = 7.7 Hz, 2H), 1.74 – 1.66 (m, 4H), 1.53 – 1.43 (m, 2H); ^{13}C NMR (176 MHz, D_2O) δ 107.48, 107.37, 107.25, 99.87, 99.39, 99.35, 99.30, 99.27, 83.92, 82.31, 82.30, 82.06, 80.87, 80.80, 80.78, 76.68, 76.63, 76.47, 70.94, 70.90, 70.88, 70.81, 70.78, 70.76, 70.69, 70.65, 70.53, 70.03, 69.96, 69.90, 67.59, 66.83, 66.72, 66.60, 66.56, 66.54, 66.52, 66.29, 65.63, 65.52, 65.47, 61.13, 46.68, 39.33, 28.01, 26.54, 22.51. m/z (HRMS+) 1868.680 $[M + H]^+$ ($C_{71}H_{121}NO_{55}$ requires 1868.677).

RP-HPLC of purified dodecasaccharide **14** (ELSD trace, Method J, t_R = 29.6 min)

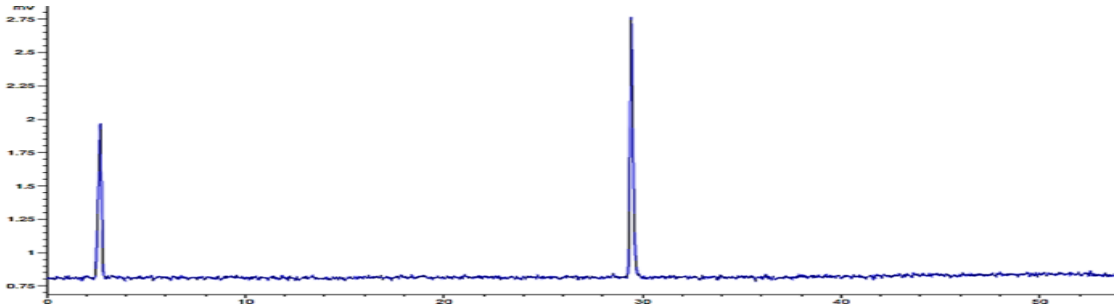

2.12.6. Synthesis of α-(1,6) α-(1,2) α-(1,5) dodecaarabinomannoside (9)

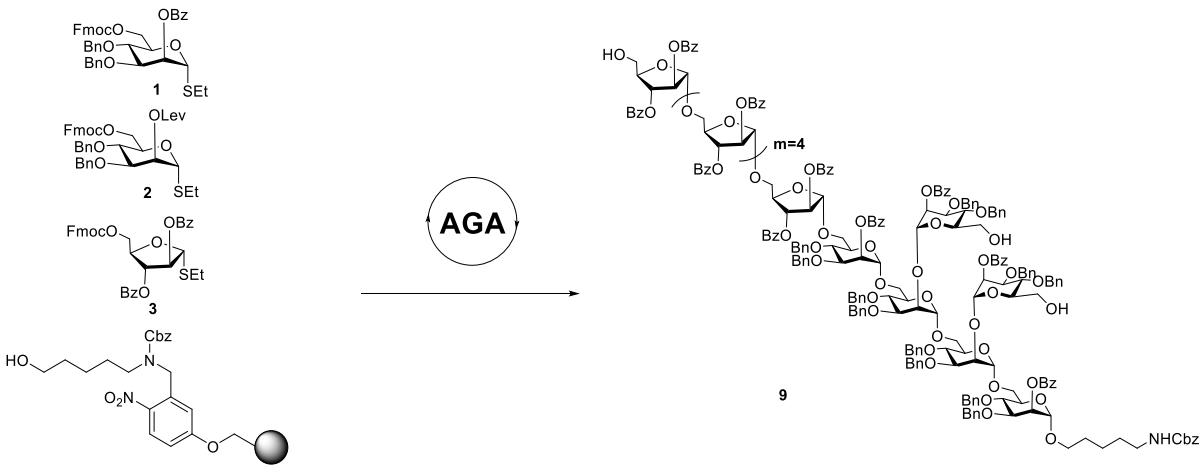

Procedure A:

	Module	Conditions
	A: Resin Preparation for Synthesis	
	B: Acidic Wash with TMSOTf Solution C: Thioglycoside Glycosylation E: Fmoc Deprotection	BB1 6.5 eq, -40 °C for 5 min, -20 °C for 30 min
2	B: Acidic Wash with TMSOTf Solution C: Thioglycoside Glycosylation E: Fmoc Deprotection	BB2 6.5 eq, -40 °C for 5 min, -20 °C for 30 min
	B: Acidic Wash with TMSOTf Solution C: Thioglycoside Glycosylation E: Fmoc Deprotection	BB1 6.5 eq, -40 °C for 5 min, -20 °C for 30 min
6	B: Acidic Wash with TMSOTf Solution C: Thioglycoside Glycosylation E: Fmoc Deprotection	BB3 13 eq, -40 °C for 5 min, -20 °C for 30 min
	F: Lev Deprotection B: Acidic Wash with TMSOTf Solution 2x C: Thioglycoside Glycosylation E: Fmoc Deprotection	BB1 13 eq, -40 °C for 5 min, -20 °C for 30 min

Procedure B:

	Module	Conditions
	A: Resin Preparation for Synthesis	
	B: Acidic Wash with TMSOTf Solution C: Thioglycoside Glycosylation D: Capping E: Fmoc Deprotection	BB1 6.5 eq, -20 °C for 5 min, 0 °C for 20 min
2	B: Acidic Wash with TMSOTf Solution C: Thioglycoside Glycosylation D: Capping E: Fmoc Deprotection	BB2 6.5 eq, -20 °C for 5 min, 0 °C for 20 min
	B: Acidic Wash with TMSOTf Solution C: Thioglycoside Glycosylation D: Capping E: Fmoc Deprotection	BB1 6.5 eq, -20 °C for 5 min, 0 °C for 20 min
6	B: Acidic Wash with TMSOTf Solution C: Thioglycoside Glycosylation D: Capping E: Fmoc Deprotection	BB3 6.5 eq, -20 °C for 5 min, 0 °C for 20 min
	F: Lev Deprotection B: Acidic Wash with TMSOTf Solution 2x C: Thioglycoside Glycosylation D: Capping E: Fmoc Deprotection	BB1 6.5 eq, -20 °C for 5 min, 0 °C for 20 min

Cleavage from the solid support as described in *Post-synthesizer manipulations* followed by purification using a preparative HPLC (Method B, t_R = 38.8 min), to provide the fully protected branched dodecasaccharide **9.** For procedure **A:** 2 mg, 0.411 μmol, 3%, based on resin loading. For procedure **B:** 16 mg, 3.22 μmol, 26%, based on resin loading.

Crude NP-HPLC of dodecasaccharide **9 .** A) Procedure **A**. B) Procedure **B** (ELSD trace, Method A, t_R = 38.8 min)

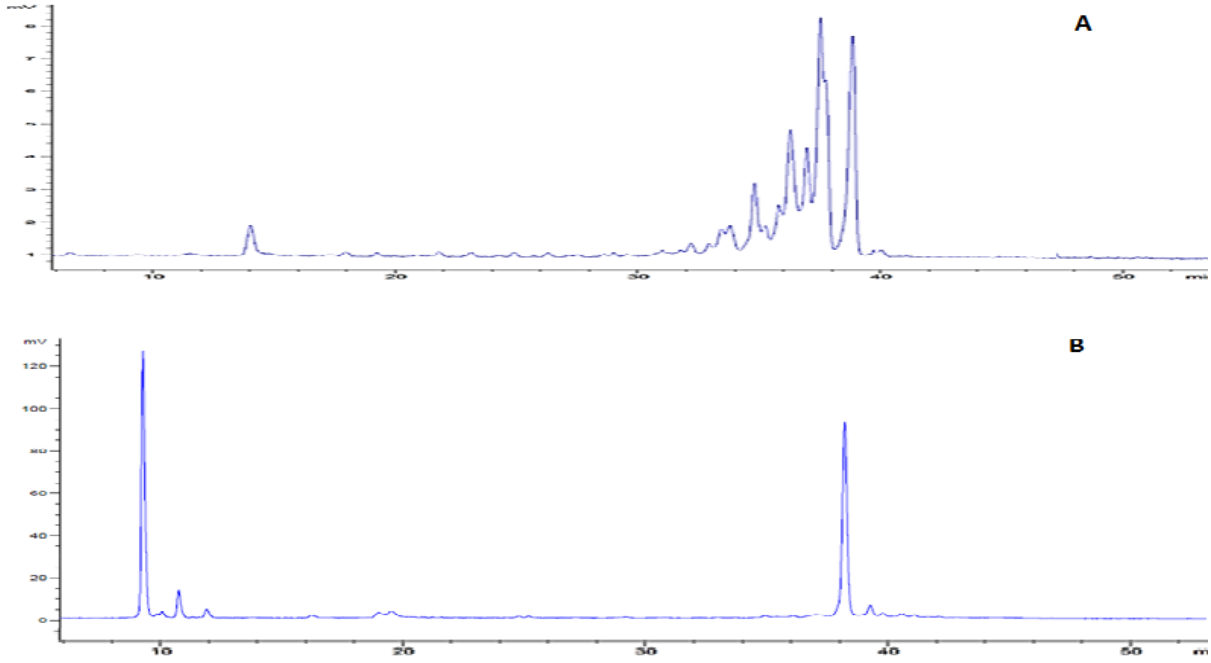

^{1}H NMR (600 MHz, Chloroform-*d*) δ 8.15 – 8.07 (m, 3H), 8.05 – 7.98 (m, 25H), 7.96 – 7.92 (m, 2H), 7.87 (dd, *J* = 8.2, 1.4 Hz, 4H), 7.83 (ddd, *J* = 8.3, 6.8, 1.4 Hz, 12H), 7.76 (dt, *J* = 8.4, 1.7 Hz, 7H), 5.88 (d, *J* = 2.4 Hz, 1H), 5.75 (s, 1H), 5.69 – 5.64 (m, 1H), 5.64 – 5.54 (m, 19H), 5.16 (d, *J* = 1.7 Hz, 1H), 5.06 (d, *J* = 5.7 Hz, 6H), 4.97 (d, *J* = 1.9 Hz, 1H), 4.92 – 4.33 (m, 57H), 4.27 – 3.59 (m, 61H), 3.57 – 3.31 (m, 8H), 3.13 (q, *J* = 6.8 Hz, 4H), 1.56 – 1.50 (m, 4H), 1.46 (t, *J* = 7.5 Hz, 2H), 1.34 – 1.28 (m, 2H).^{13}C NMR (151 MHz, cdcl$_3$) δ 166.02, 165.58, 165.55, 165.52, 165.42, 165.33, 165.06, 165.02, 138.62, 138.37, 138.07, 137.99, 137.91, 137.79, 136.64, 133.45, 133.35, 133.29, 133.24, 133.09, 133.06, 133.01, 129.87, 129.82, 129.78, 129.70, 129.67, 129.61, 129.58, 129.18, 129.10, 129.00, 128.92, 128.63, 128.54, 128.47, 128.45, 128.43, 128.36, 128.36, 128.25, 128.24, 128.22, 128.19, 128.17, 128.14, 128.11, 128.07, 128.04, 127.99, 127.99 127.94, 127.83, 127.74, 127.71, 127.69, 127.59, 127.49, 127.41, 127.32, 127.26, 127.14, 126.90, 106.00, 105.83, 105.80, 99.34, 97.52, 83.58, 83.29, 82.02, 81.91, 81.63, 81.53, 81.46, 78.37, 77.96, 77.65, 75.13, 74.92, 74.83, 74.05, 73.26, 71.79, 71.66, 71.59, 71.26, 71.16, 70.65, 66.51, 66.08, 65.79, 65.72, 65.61, 62.45, 62.28, 40.91, 29.72, 28.97, 23.39. m/z (HRMS+) 2397.338 $[2M + Na]^{++}$ ($C_{275}H_{263}NO_{73}Na$ requires 2397.337).

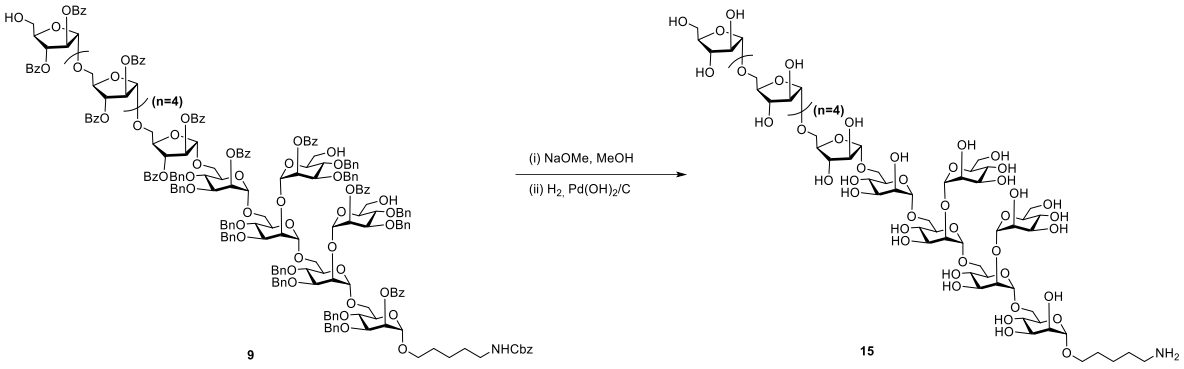

Deprotection of **9** as described in Modules G and I, followed by purification using preparative HPLC (Method L) afforded compound **15** (1.0 mg, 0.53 µmol, 17% over two steps)^{1}H NMR (700 MHz, D_2O) δ 5.17 (s, 1H), 5.15 (s, 1H), 5.12 (s, 6H), 5.07 (s, 1H), 5.06 (s, 1H), 4.95 (s, 1H), 4.88 (s, 1H), 4.27 (s, 5H), 4.17 (d, J = 10.3 Hz, 6H), 4.11 (s, 3H), 4.07 – 3.94 (m, 15H), 3.94 – 3.90 (m, 7H), 3.86 – 3.81 (m, 15H), 3.80 – 3.66 (m, 16H), 3.61 – 3.57 (m, 1H), 3.03 (t, J = 7.6 Hz, 2H), 1.74 – 1.68 (m, 4H), 1.52 – 1.44 (m, 2H); 13C NMR (176 MHz, D_2O) δ 107.5, 107.4, 102.3, 99.9, 99.6, 98.2, 84.0, 82.3, 82.1, 80.9, 80.8, 80.8, 78.8, 76.7, 76.7, 76.7, 76.5, 73.3, 73.2, 71.2, 70.9, 70.9, 70.8, 70.5, 70.5, 70.1, 70.0, 70.0, 67.6, 66.9, 66.9, 66.8, 66.7, 66.7, 66.7, 66.5, 66.5, 66.3, 65.9 61.2, 61.1, 61.0, 43.8, 39.4, 28.0, 26.6, 22.5. m/z (HRMS+) 1868.669 $[M + H]^+$ ($C_{71}H_{121}NO_{55}$ requires 1868.677).

RP-HPLC of purified dodecasaccharide **15** (ELSD trace, Method K, t_R = 28.5 min)

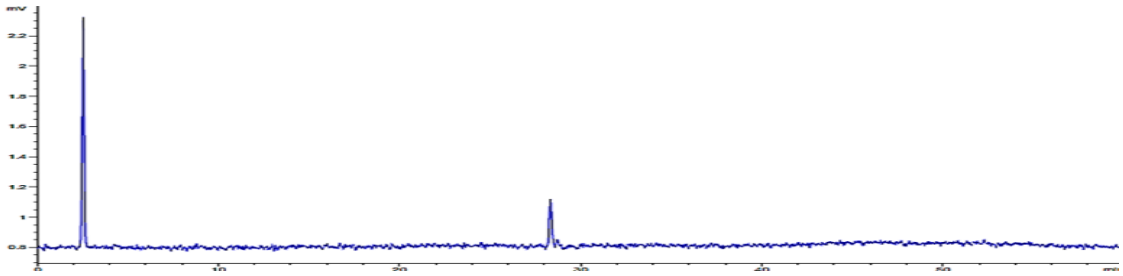

2.12.7. Synthesis of α-(1,6) linear pentamannoside (16)

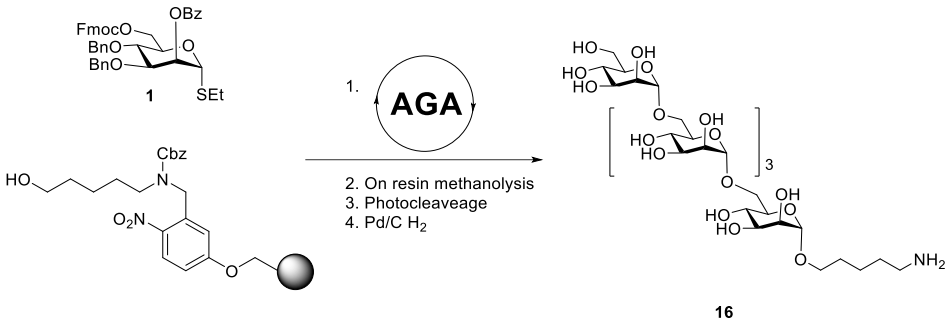

Procedure B:

	Module	Conditions
	A: Resin Preparation for Synthesis	
5	B: Acidic Wash with TMSOTf Solution C: Thioglycoside Glycosylation D: Capping E: Fmoc Deprotection	BB1 6.5 eq, -20 °C for 5 min, 0 °C for 30 min

After checking the outcome of the reaction with MALDI (Module G1), methanolysis on resin was performed (Module H1). Cleavage from the solid support (Module G) and hydrogenolysis (Module I) followed by purification using preparative HPLC (Method K) afforded compound **16** (4.8 mg, 42% based on resin loading).

Analytical data for **16**: ^{1}H NMR (400 MHz, D_2O) δ 4.73 (s, 1H), 4.71 (s, 1H), 4.67 (s, 1H), 3.80 (m, 2H), 3.78 – 3.71 (m, 10H), 3.71 – 3.49 (m, 15H), 2.82 (t, *J* = 7.7 Hz, 2H), 1.56 – 1.43 (m, 4H), 1.27 (h, *J* = 6.5, 6.0 Hz, 2H). ^{13}C NMR (101 MHz, D_2O) δ 99.76, 99.28, 99.13, 72.58, 70.77, 70.63, 70.53, 70.39, 69.83, 67.49, 66.60, 66.43, 65.38, 60.79, 39.23, 27.91, 26.46, 22.42. m/z (HRMS+) 914.3621 $[M + H]^+$ ($C_{35}H_{64}NO_{26}$ requires 914.3711).

RP-HPLC of 16 (ELSD trace, Method J, t_R = 23.2 min)

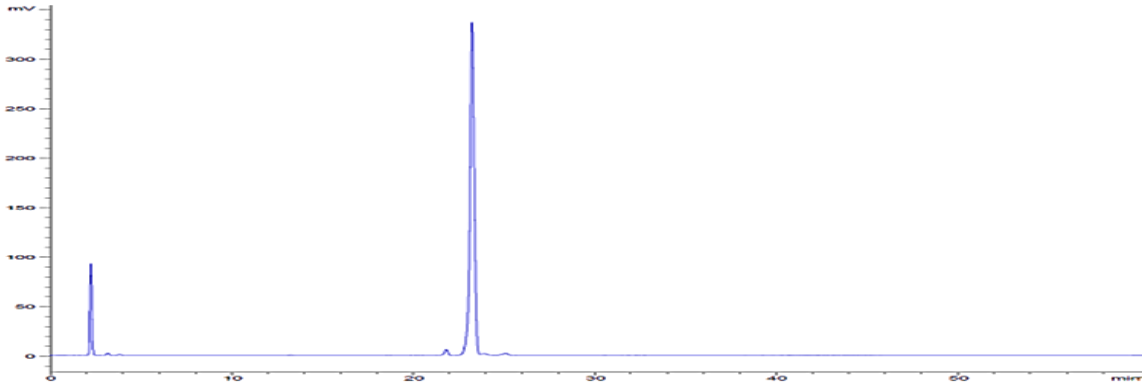

2.12.8. Synthesis of α-(1,6) α-(1,2) branched hexamannoside (17)

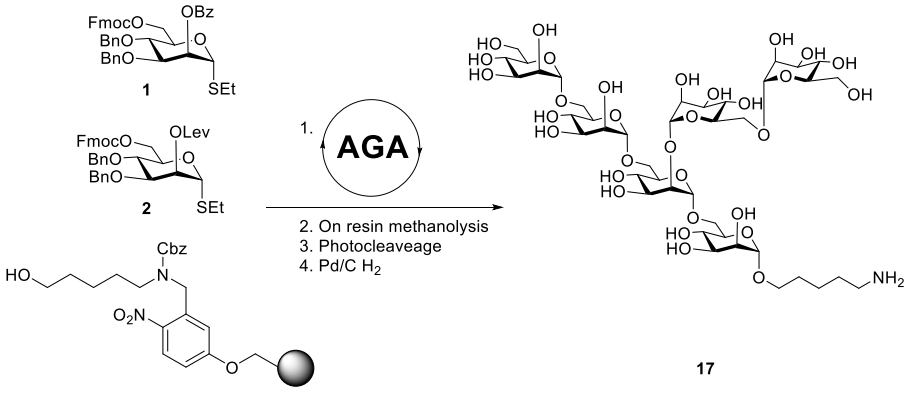

Procedure B:

	Module	Conditions
	A: Resin Preparation for Synthesis	
	B: Acidic Wash with TMSOTf Solution C: Thioglycoside Glycosylation D: Capping E: Fmoc Deprotection	BB1 6.5 eq, -20 °C for 5 min, 0 °C for 20min
	B: Acidic Wash with TMSOTf Solution C: Thioglycoside Glycosylation D: Capping E: Fmoc Deprotection F: Lev Deprotection	BB2 6.5 eq, -20 °C for 5 min, 0 °C for 20min
2	B: Acidic Wash with TMSOTf Solution C: 2* Thioglycoside Glycosylation D: Capping E: Fmoc Deprotection	BB1 6.5 eq, -20 °C for 5 min, 0 °C for 20min

After checking the outcome of the reaction with MALDI (Module G1), methanolysis on resin was performed (Module H1). Cleavage from the solid support (Module G) and hydrogenolysis (Module I) followed by purification using preparative HPLC (Method K) afforded compound **17** (1.0 mg, 11% based on resin loading).

RP-HPLC of 17 (ELSD trace, Method J, t_R = 21.2 min)

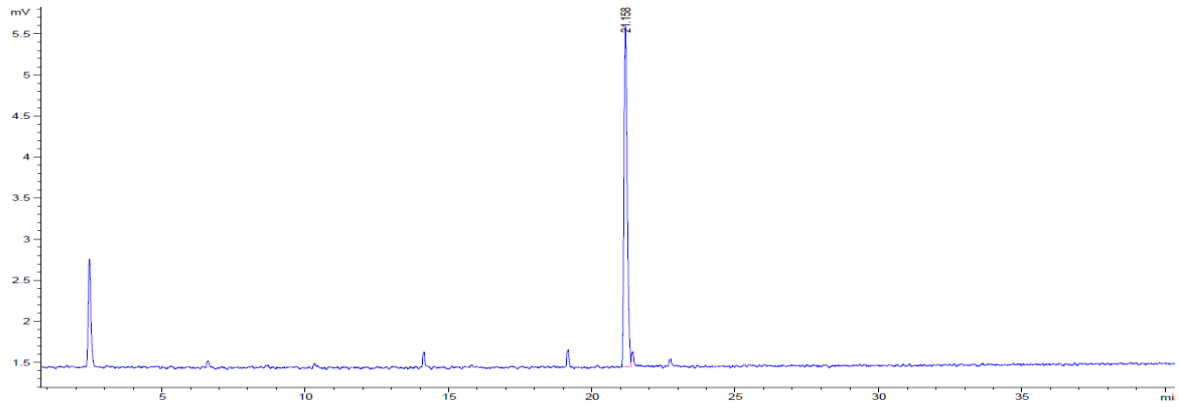

Analytical data for **17**: ^{1}H NMR (700 MHz, D_2O) δ 5.14 (s, 1H), 5.04 (s, 1H), 4.98 (s, 1H), 4.95 (s, 2H), 4.90 (s, 1H), 4.11 (s, 1H), 4.06 – 4.02 (m, 1H), 4.04 – 3.99 (m, 5H), 3.99 – 3.91 (m, 6H), 3.90 – 3.82 (m, 8H), 3.79 (dt, J = 21.7, 8.6 Hz, 10H), 3.74 (d, J = 9.9 Hz, 1H), 3.72 – 3.66 (m, 3H), 3.60 (d, J = 9.3 Hz, 1H), 3.04 (t, J = 7.7 Hz, 2H), 1.73 (m, 4H), 1.49 (tq, J = 14.8, 7.1 Hz, 2H). 13C NMR (176 MHz, D_2O) δ 102.30, 99.93, 99.45, 99.45, 99.19, 97.86, 72.74, 71.33, 71.19, 71.11, 70.94, 70.94, 70.76, 70.61, 70.53, 70.45, 70.04, 70.02, 67.65, 66.82, 66.77, 66.65, 66.56, 66.52, 65.68, 60.97, 39.42, 28.04, 26.61, 22.53. m/z (HRMS+) 1076.428 $[M + H]^+$ ($C_{41}H_{74}NO_{31}$ requires 1076.424).

2.12.9. Synthesis of 100-mer polymannoside (18)

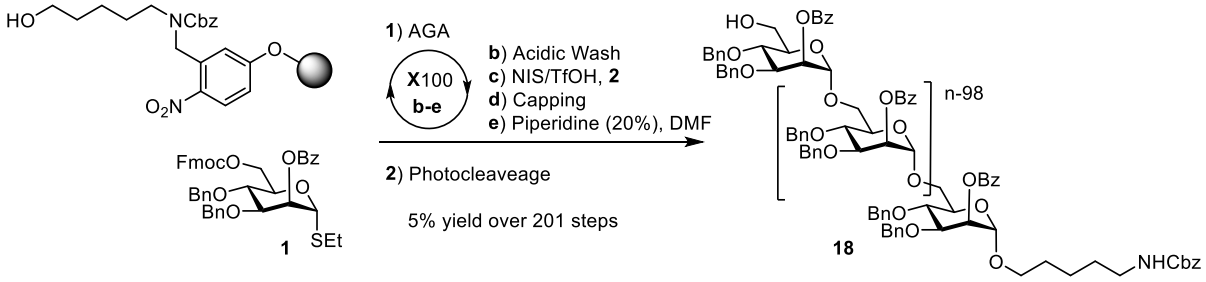

Cycles	Module	Conditions
	A: Resin Preparation for Synthesis	
40	B: Acidic Wash with TMSOTf Solution C: Thioglycoside Glycosylation D: Capping E: Fmoc Deprotection	BB1 (5 equiv)-20 °C for 5 min, 0 °C for 20 min
40	B: Acidic Wash with TMSOTf Solution C: Thioglycoside Glycosylation D: Capping E: Fmoc Deprotection	BB1 (6 equiv)-20 °C for 5 min, 0 °C for 40 min
20	B: Acidic Wash with TMSOTf Solution C: Thioglycoside Glycosylation D: Capping E: Fmoc Deprotection	BB1 (6.5 equiv)-20 °C for 5 min, 0 °C for 60 min

The product was cleaved from the solid support as described in the post-synthesizer manipulations followed by purification using normal phase preparative HPLC with a YMC diol column.(Method K) Linear gradient: Hex – 50% EtOAc as eluents [isocratic 50% EtOAc (5 min), linear gradient to 50% EtOAc (5 min), linear gradient to 75% EtOAc (30 min), linear gradient to 100% EtOAc (5 min)] 100-mer **18**, **19** eluted at 17.63, 24.42 minutes respectively.

HPLC of crude 100-mer **18** (UV 280 nm trace, Method J, t_R = 17.6min)

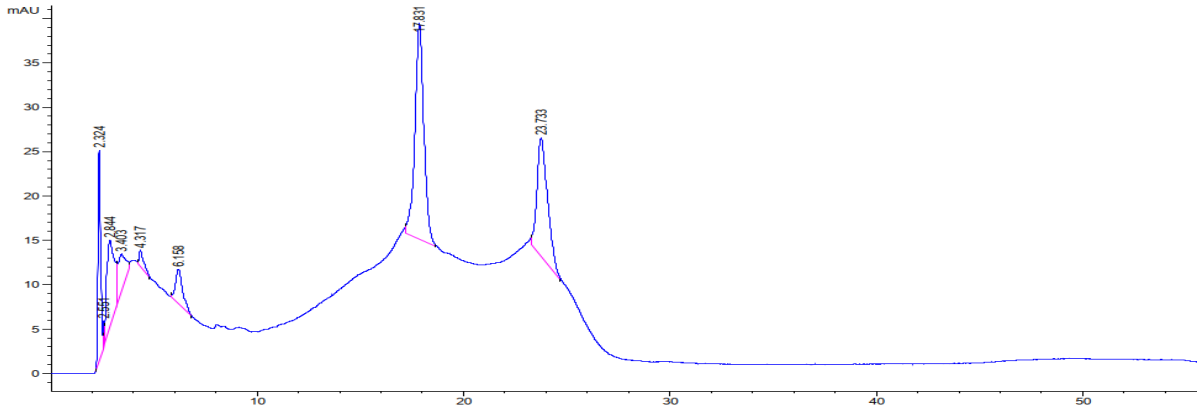

HPLC of purified 100-mer **18** (UV 280 nm trace, Method J, t_R = 17.6 min)

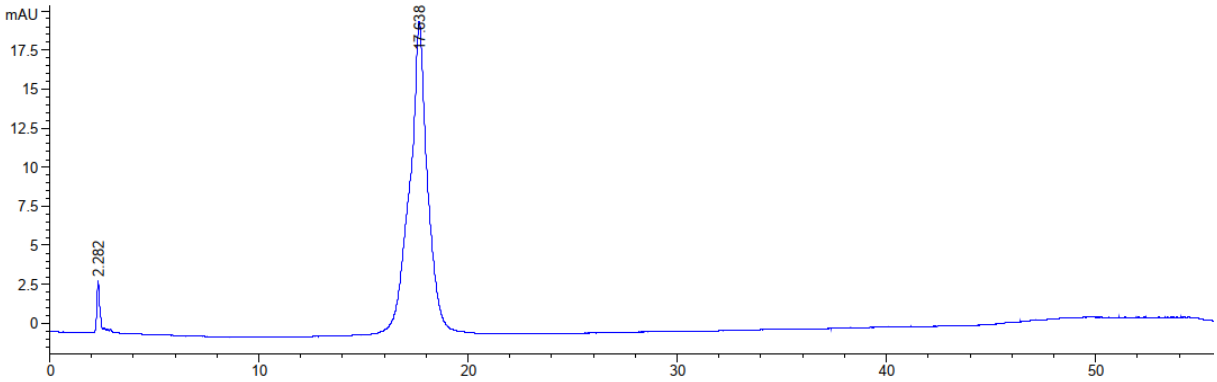

Analytical data for 100-mer polymannose **18**: Yield 5% over 201 steps. ^{1}H NMR (700 MHz, Chloroform-*d*) δ 8.16 (d, *J* = 7.3 Hz, 200H), 7.48 (dt, *J* = 13.6, 7.2 Hz, 250H), 7.21 – 6.99 (m, 1060H), 5.83 (s, 100H), 5.03 (s, 100H), 4.86 (d, *J* = 11.5 Hz, 100H), 4.78 (d, *J* = 10.8 Hz, 100H), 4.40 (d, *J* = 10.8 Hz, 100H), 4.31 (d, *J* = 11.7 Hz, 100H), 4.04 – 3.98 (m, 100H), 3.96 (t, *J* = 9.5 Hz, 100H), 3.70 (d, *J* = 10.6 Hz, 100H), 3.56 (d, *J* = 9.5 Hz, 1H), 3.40 (d, *J* = 11.0 Hz, 100H), 3.16 – 3.15 (m, 2H), 1.58 – 1.53 (m, 2H), 1.49 (m, 2H), 1.36 – 1.32 (m, 2H); ^{13}C NMR (176 MHz, Chloroform-*d*) δ 165.54, 138.49, 137.52, 133.32, 130.02, 129.87, 128.66, 128.37, 128.34, 128.14, 127.69, 127.30, 127.01, 98.56, 78.21, 75.00, 73.72, 71.30, 70.90, 68.39, 65.73, 29.12; m/z (MALTI-TOF) 44888.4201 $[M + Na]^+$ ($C_{2713}H_{2619}NO_{603}Na$ requires 44877.4201).

MALDI-TOF of protected 100-mer (**18**)

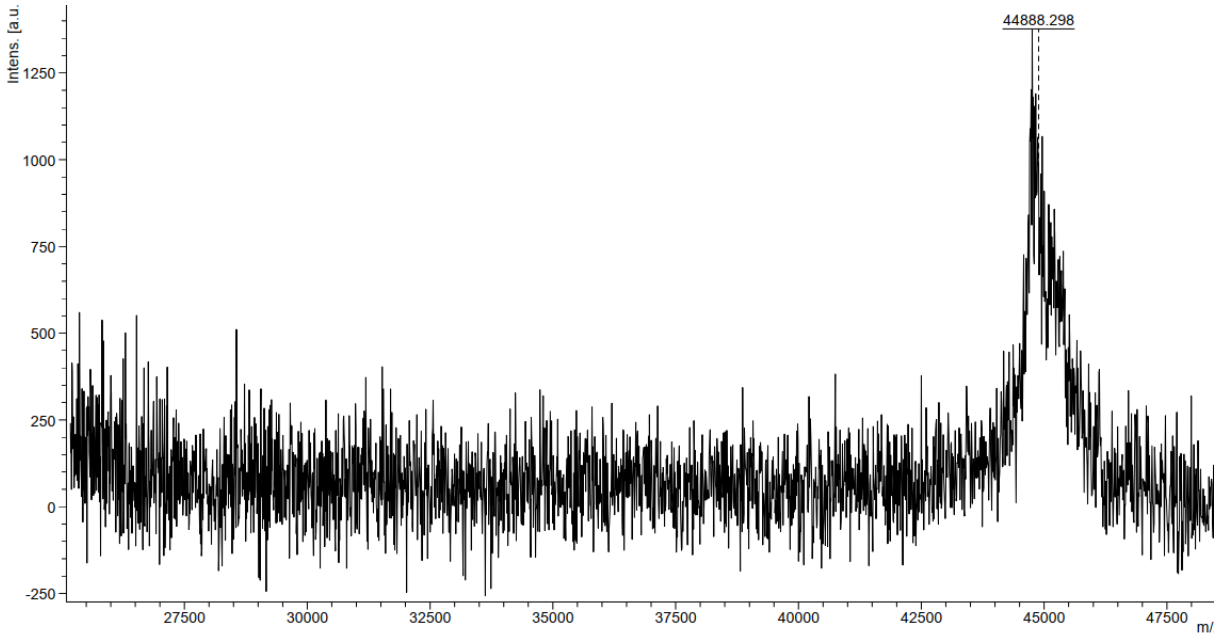

HPLC of purified 100-mer-with 3 benzyl groups cleaved **19** (UV 280 nm trace, Method J, t_R = 17.6 min)

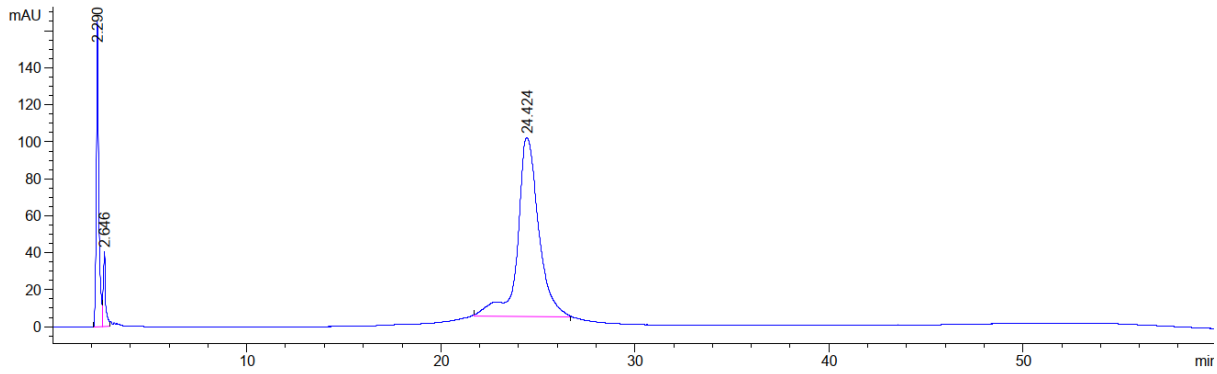

Analytical data for 100-mer polymannose **19**: Yield 3% over 201 steps. ^{1}H NMR (600 MHz, Chloroform-*d*) δ 8.18 – 8.13 (m, 200H), 7.52 – 7.44 (m, 250H), 7.19 – 7.05 (m, 1045H), 5.82 (s, 100H), 5.03 (d, *J* = 1.7 Hz, 100H), 4.86 (d, *J* = 11.6 Hz, 100H), 4.77 (d, *J* = 10.8 Hz, 100H), 4.40 (d, *J* = 10.8 Hz, 100H), 4.31 (d, *J* = 11.7 Hz, 100H), 4.03 – 3.93 (m, 200H), 3.70 (d, *J* = 10.8 Hz, 100H), 3.56 (d, *J* = 9.6 Hz, 100H), 3.40 (q, *J* = 9.5 Hz, 100H); ^{13}C NMR (151 MHz, Chloroform-*d*) δ 165.68, 138.62, 137.64, 133.46, 130.14, 130.00, 128.79, 128.51, 128.48, 128.28, 127.83, 127.43, 127.14, 98.69, 78.34, 75.13, 73.84, 71.43, 71.02, 68.52, 65.85; m/z (MALTI-TOF) 44607.2793 $[M + Na]^+$ ($C_{2692}H_{2601}NO_{603}Na$ requires 44597.5710).

MALDI-TOF of protected 100-mer with 3 benzyl groups cleaved (**19**)

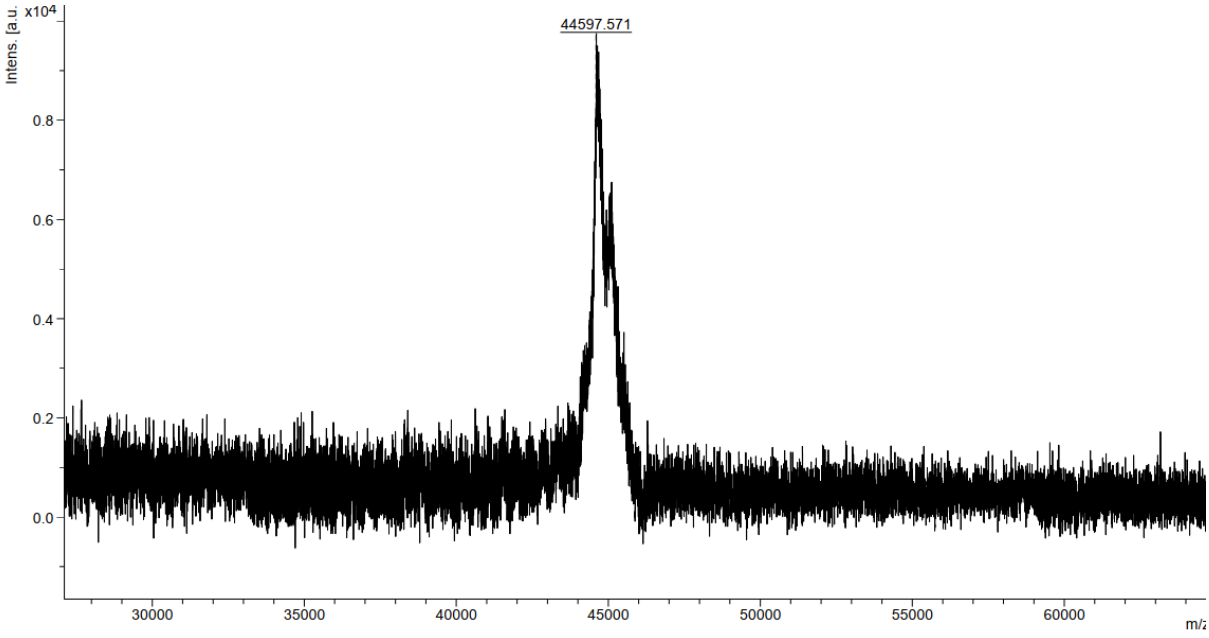

Deprotection of 100-mer polymannoside:

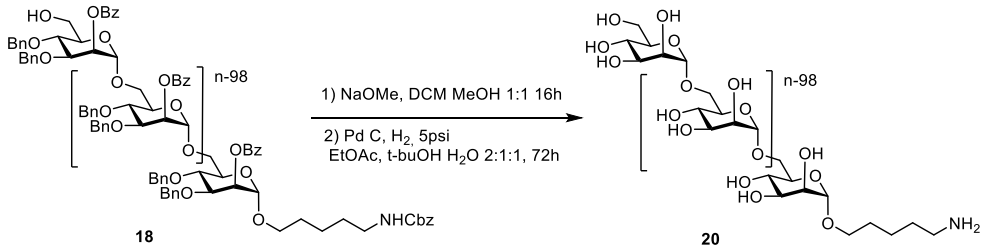

Methanolysis (Module G**).** To a solution of protected oligosaccharide **18** in methanol:CH_2Cl_2 (1:1), was added sodium methoxide in methanol (0.5 M, pH 13) and stirred at room temperature for 16 h, neutralized with Amberlite ion exchange (H+) resin, filtered and concentrated in vacuo and carried forward directly into hydrogenolysis without purification.

Hydrogenolysis (Module H). The product of Zemplén methanolysis was dissolved in EtOAc:*t*-BuOH:H_2O (2:1:1) and transferred to cylindrical vials. Pd-C (10%) (100 weight %) was added and the reaction mixture was stirred under autoclave with hydrogen 5 psi pressure for 72 h. The reaction mixture were filtered through Celite and washed with methanol and water. The filtrates were concentrated in vacuo and purified on Synergy column (Method D) and lyophilized to give a pure compound **20.**

Analytical data for **20**: ^{1}H NMR (700 MHz, D_2O) δ 4.85 (s, 100H), 3.94 (s, 100H), 3.89 (dd, *J* = 11.4, 5.5 Hz, 100H), 3.84 – 3.76 (m, 200H), 3.73 (d, *J* = 11.1 Hz, 100H), 3.67 (t, *J* = 9.8 Hz, 100H), 3.61 (d, *J* = 10.1 Hz, 2H), 2.95 (d, *J* = 9.6 Hz, 2H), 2.80 (d, *J* = 1.7 Hz, 2H), 1.70 – 1.55 (m, 4H); ^{13}C NMR (176 MHz, Deuterium Oxide) δ 171.06, 99.39, 70.88, 70.74, 70.03, 66.65, 65.57 ; m/z (MALTI-TOF) 16433.884 $[M+Na]^+$ ($C_{605}H_{1013}NO_{501}Na$ requires 16331.37).

RP-HPLC of deprotected 100-mer **20** (ELSD trace, Method C, t_R = 14.9 min)

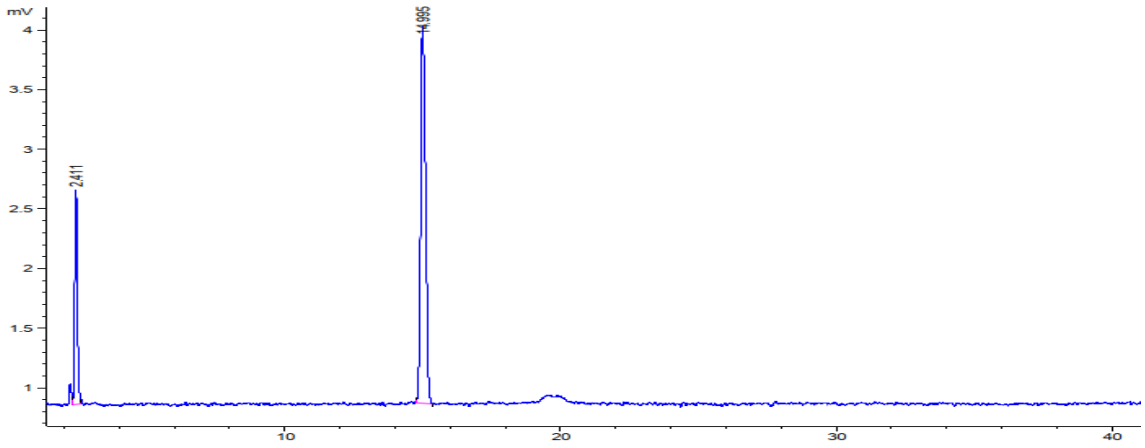

2.13. **Synthesis of 151-mer polymannoside by block coupling**

2.13.1. 30-mer Donor Synthesis (22)

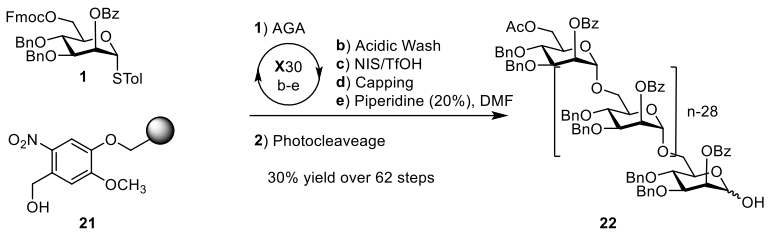

	Module	Conditions
	A: Resin Preparation for Synthesis	
30	B: Acidic Wash with TMSOTf Solution C: Thioglycoside Glycosylation D: Capping E: Fmoc Deprotection	BB1 (5 equiv)-20 °C for 5 min, 0 °C for 20 min
	2x D: Capping	

The product was cleaved from the solid support as described in the post-synthesizer manipulations followed by purification using normal phase preparative HPLC with a YMC diol column. (Method F) Linear gradient: Hex – 35% EtOAc as eluents [isocratic 35% EtOAc (5 min), linear gradient to 35% EtOAc (5 min), linear gradient to 60% EtOAc (30 min), linear gradient to 100% EtOAc (5 min)] 30-mer **22** eluted at 27.43 minutes.

HPLC of 30-mer **22** (UV 280 nm trace, Method E, t_R = 27.4min)

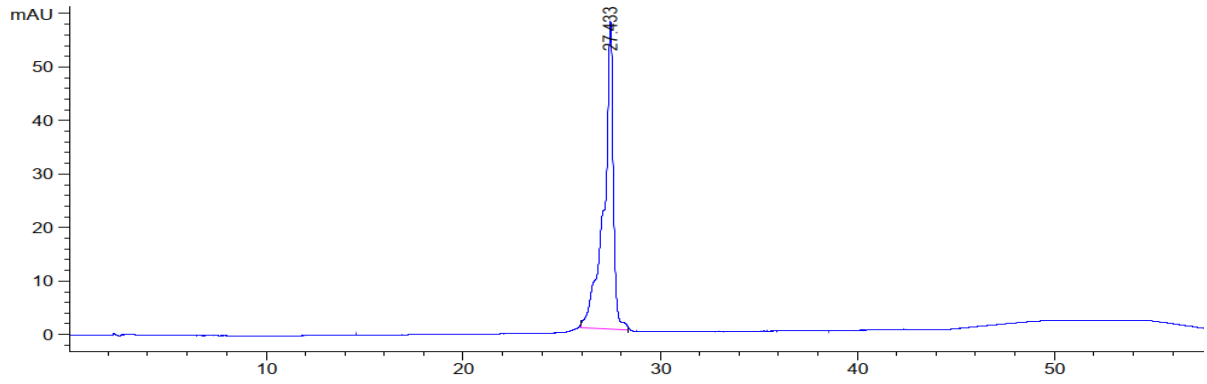

MALDI-TOF spectrum of 30-mer, 1-OH (**22**)

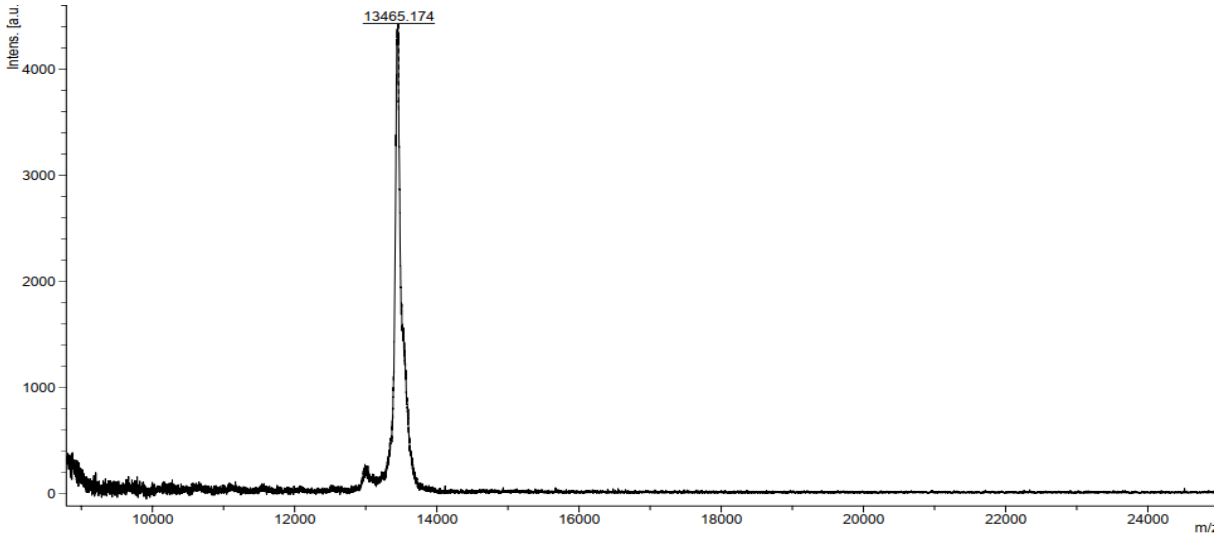

Analytical data for **22**: ^{1}H NMR (400 MHz, Chloroform-*d*) δ 8.23 – 8.15 (m, 60H), 7.52 (d, *J* = 7.0 Hz, 120H), 7.24 – 7.03 (m, 360H), 5.87 (t, *J* = 2.3 Hz, 30H), 5.06 (s, 30H), 4.89 (d, *J* = 11.4 Hz, 30H), 4.81 (d, *J* = 10.7 Hz, 30H), 4.43 (d, *J* = 10.7 Hz, 30H), 4.32 (d, *J* = 11.7 Hz, 30H), 4.08 – 3.93 (m, 90H), 3.71 (d, *J* = 10.2 Hz, 30H), 3.57 (d, *J* = 9.3 Hz, 30H), 3.40 (d, *J* = 11.2 Hz, 30H), 2.20 (s, OAc, 3H); ^{13}C NMR (101 MHz, Chloroform-*d*) δ 165.54, 138.48, 137.45, 133.39, 129.96, 129.89, 128.68, 128.44, 128.38, 128.15, 127.74, 127.30, 126.95, 98.52, 78.21, 77.26, 74.99, 73.64, 71.29, 70.81, 68.30, 65.65, 20.78; m/z (MALTI-TOF) 13465.174 $[M + Na]^+$ ($C_{812}H_{784}O_{182}Na$ requires 13468.199).

2.13.2. Synthesis of 30-mer glycosyl fluoride donor (23)

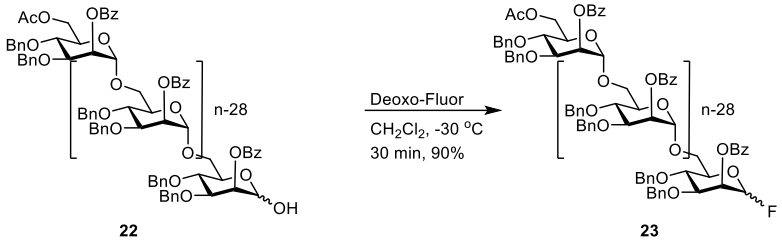

22 23

To a solution of compound **22** (94 mg, 72.8 μmol) in CH_2Cl_2 (2 mL) was added a solution of Deoxo-Fluor (110 μL, 150 μmol) at -30 °C. The reaction was stirred for 30 minutes. The reaction was quenched with 2 mL of $NaHCO_3$. The organic phase was extracted with aqueous citric acid, dried over $MgSO_4$, filtered, concentrated and purified by preparative HPLC (Method F)to provide compound **23** (85 mg, 90% yield).

HPLC of 30-mer **23** (ELSD trace, Method E, t_R = 22.1 min)

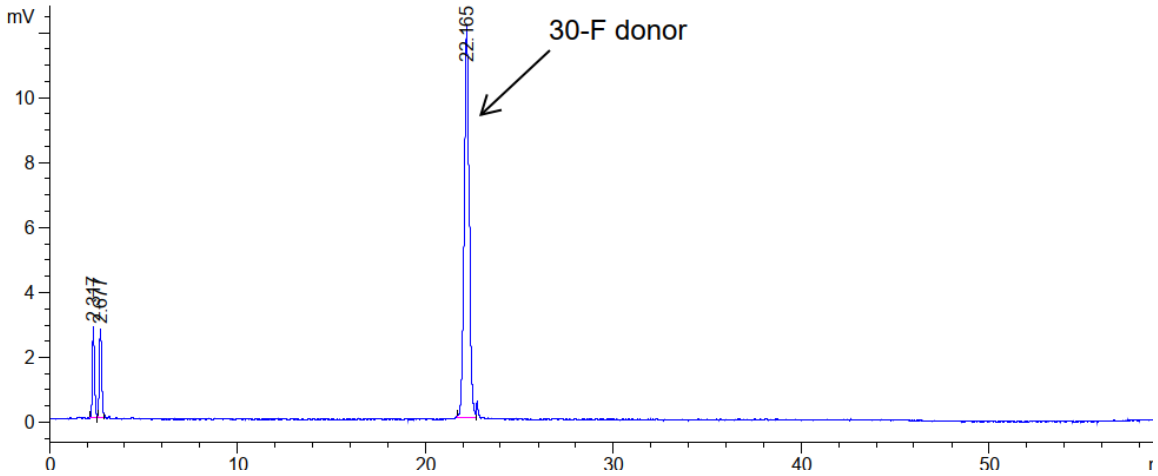

Analytical data for **23**: ^{1}H NMR (700 MHz, Chloroform-*d*) δ 8.21 – 8.17 (m, 60H), 7.51 (qd, *J* = 8.0, 4.2 Hz, 90H), 7.21 – 7.08 (m, 300H), 5.85 (t, *J* = 2.4 Hz, 30H), 5.06 (d, *J* = 1.9 Hz, 30H), 4.89 (d, *J* = 11.5 Hz, 30H), 4.80 (d, *J* = 11.0 Hz, 30H), 4.43 (d, *J* = 11.0 Hz, 30H), 4.35 (dd, *J* = 11.6, 3.4 Hz, 30H), 4.03 (dd, *J* = 9.2, 3.2 Hz, 30H), 4.01 – 3.96 (m, 30H), 3.74 (d, *J* = 11.1 Hz, 30H), 3.61 – 3.57 (m, 30H), 3.45 (dd, *J* = 10.4, 7.7 Hz, 30H), 2.20 (s, OAc, 3H); ^{13}C NMR (101 MHz, Chloroform-*d*) δ 165.54, 138.47, 137.44, 133.39, 129.94, 129.89, 128.68, 128.44, 128.38, 128.14, 127.74, 127.29, 126.94, 98.51, 78.21, 77.26, 76.09, 74.99, 73.63, 71.29, 70.80, 68.29, 65.64, 31.02, 18.59; m/z (MALTI-TOF) 13448.270 $[M + H]^+$ ($C_{812}H_{783}FO_{181}$ requires 13447.2049).

2.13.3. Automated synthesis of branched acceptor (24)

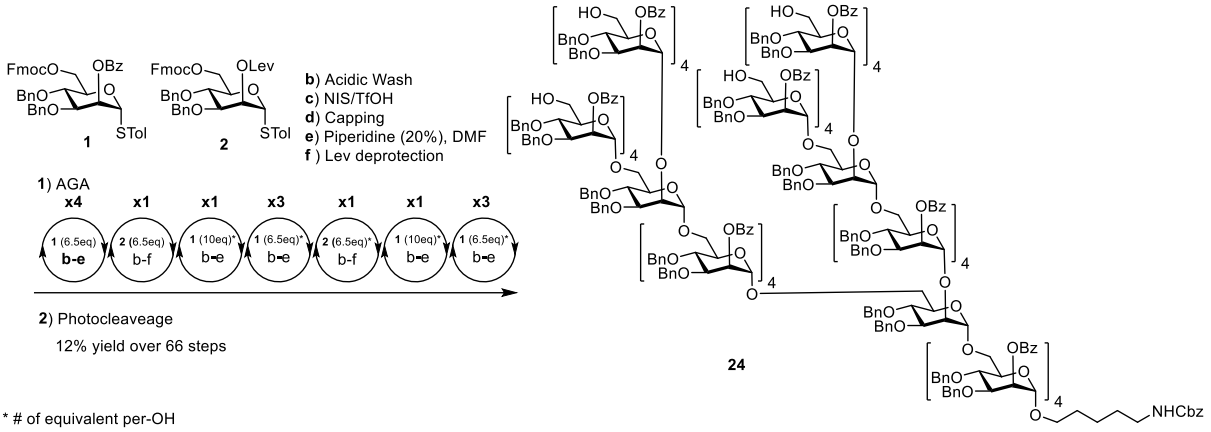

	Module	Conditions
	A: Resin Preparation for Synthesis	
4	B: Acidic Wash with TMSOTf Solution C: Thioglycoside Glycosylation D: Capping E: Fmoc Deprotection	BB1 (6.5 equiv)-20 °C for 5 min, 0 °C for 20 min
	B: Acidic Wash with TMSOTf Solution C: Thioglycoside Glycosylation D: Capping F: Lev Deprotection E: Fmoc Deprotection	BB2 (6.5 equiv)-20 °C for 5 min, 0 °C for 20 min
	B: Acidic Wash with TMSOTf Solution C: Thioglycoside Glycosylation D: Capping E: Fmoc Deprotection	BB1 (10 equiv) -20 °C for 5 min, 0 °C for 20 min
3	B: Acidic Wash with TMSOTf Solution C: Thioglycoside Glycosylation D: Capping E: Fmoc Deprotection	BB1 (6.5 equiv) -20 °C for 5 min, 0 °C for 20 min
	B: Acidic Wash with TMSOTf Solution C: Thioglycoside Glycosylation D: Capping F: Lev Deprotection E: Fmoc Deprotection	BB2 (6.5 equiv)-20 °C for 5 min, 0 °C for 20 min
	B: Acidic Wash with TMSOTf Solution C: Thioglycoside Glycosylation D: Capping E: Fmoc Deprotection	BB1 (10 equiv) -20 °C for 5 min, 0 °C for 20 min
3	B: Acidic Wash with TMSOTf Solution C: Thioglycoside Glycosylation D: Capping E: Fmoc Deprotection	BB1 (6.5 equiv) -20 °C for 5 min, 0 °C for 20 min

The product was cleaved from the solid support as described in the post-synthesizer manipulations followed by purification by using normal phase preparative HPLC with YMC diol column. (Method F) Linear gradient: Hex – 35% EtOAc as eluents [isocratic 35% EtOAc (5 min), linear gradient to 35% EtOAc (5 min), linear gradient to 60% EtOAc (30 min), linear gradient to 100% EtOAc (5 min)] 31-mer **24** eluted at 32.25 minutes.

HPLC of crude 31-mer **24** (280nm trace, Method E, t_R = 31.6 min)

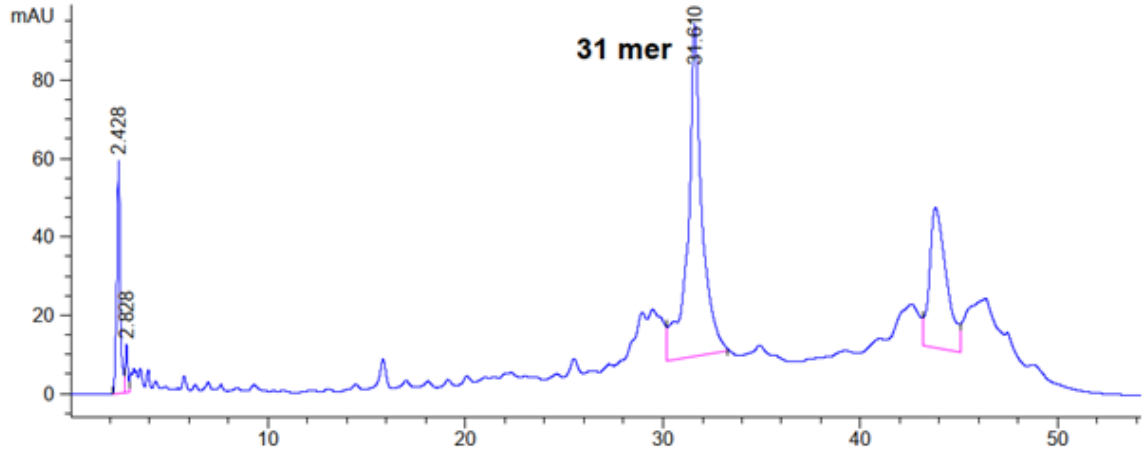

HPLC of 31-mer **24** (280nm trace, Method E, t_R = 32.2 min)

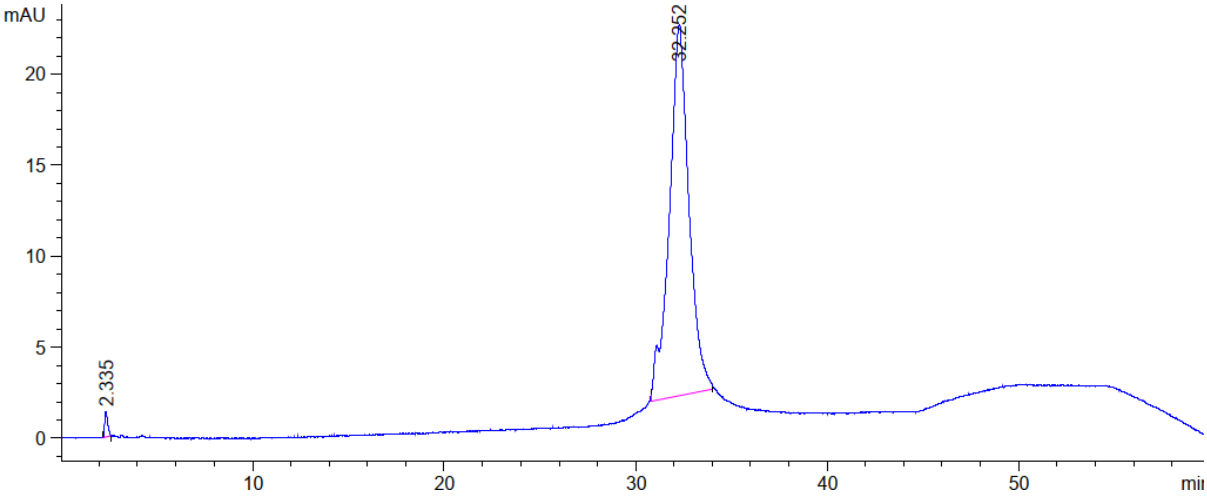

MALDI-TOF of 31-mer acceptor (**24**)

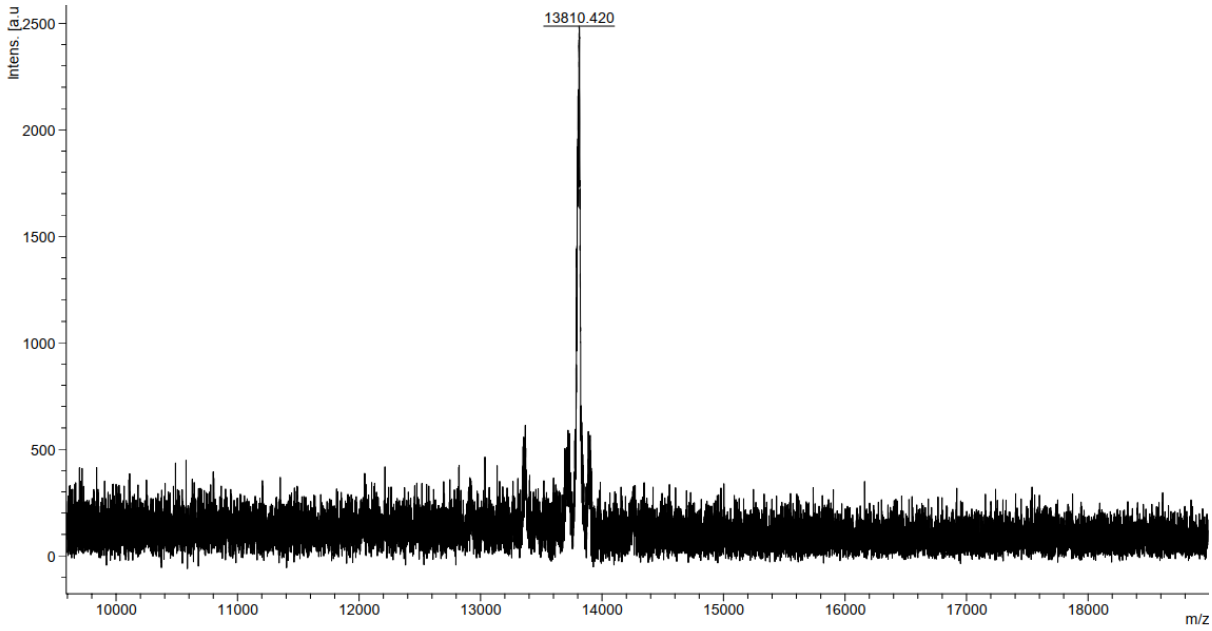

2.13.4. Synthesis of branched 151-mer polymannoside 25 via block coupling

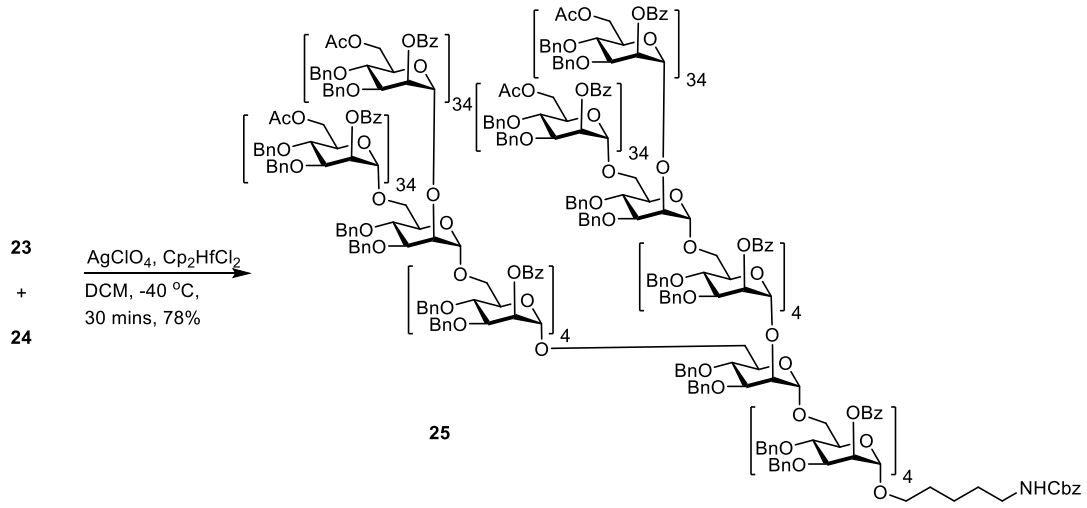

To a solution of glycosyl donor **23** (41 mg, 6 eq) and glycosyl acceptor **24** (7 mg, 1 eq) in 1mL of anhydrous CH_2Cl_2 was added activated 4Å molecular sieves (20 mg) at room temperature for 5 min protected from light. The reaction was cooled to -40 °C and silver perchlorate (2.8 mg, 5 eq) and bis(cyclopentadienyl) hafnium dichloride (2.5 mg, 3 eq) were added.[5] This mixture was allowed to stir at same temperature for 30 minutes, resulted completion of the reaction. This mixture was quenched with Et_3N diluted with CH_2Cl_2 and filtered through Celite. The filtrate was extracted with aqueous $NaHCO_3$(10 mL) and brine (10

mL) The organic layer was dried over $MgSO_4$ filtered, concentrated and purified by Preparative HPLC (Method H) with a YMC diol column. The pure compound **25** was isolated with (27 mg, 78%).

HPLC of crude 151-mer **25** (ELSD trace, Method G, t_R = 30.7 min)

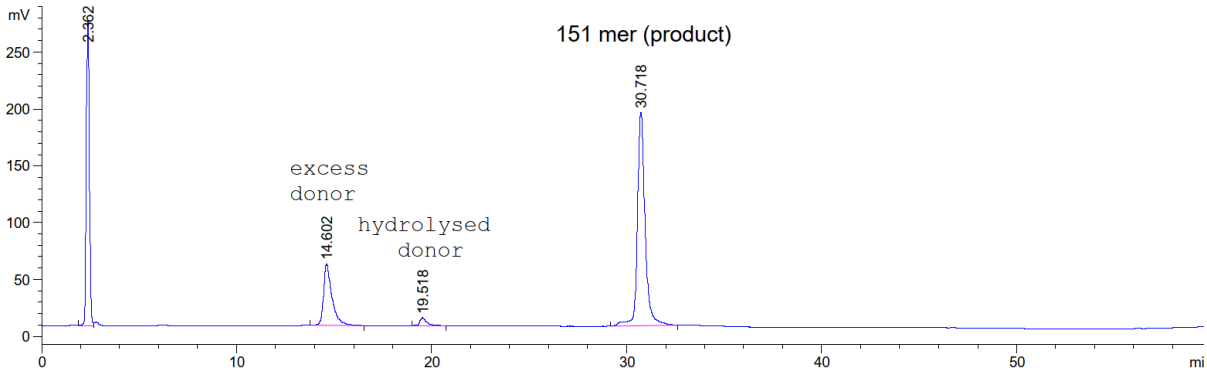

HPLC of 151-mer **25** (ELSD trace, Method G, t_R = 30.7 min)

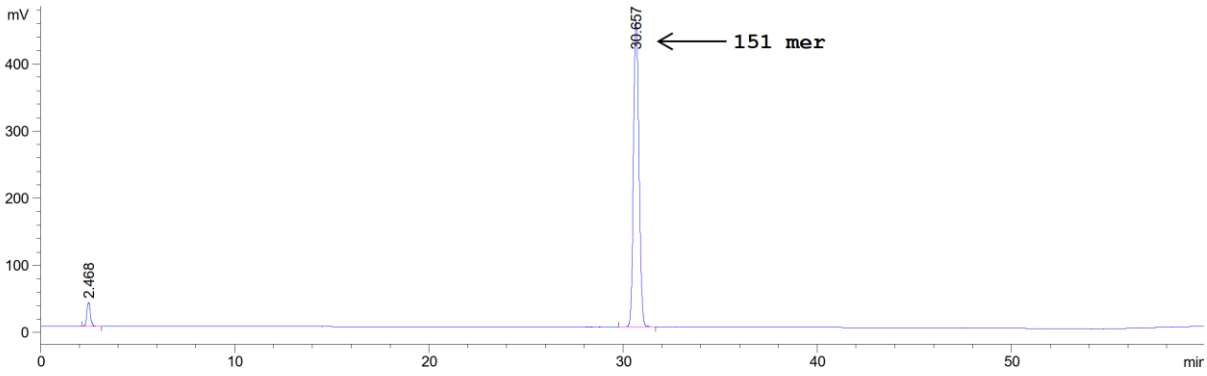

Analytical data for **25**: ^{1}H NMR (700 MHz, Chloroform-*d*) δ 8.18 (d, *J* = 7.6 Hz, 302H), 7.50 (dt, *J* = 13.3, 7.2 Hz, 453H), 7.23 – 7.04 (m, 1510H), 5.85 (d, *J* = 3.2 Hz, 151H), 5.05 (s, 151H), 4.88 (d, *J* = 11.6 Hz, 151H), 4.80 (d, *J* = 10.9 Hz, 151H), 4.43 (d, *J* = 11.0 Hz, 151H), 4.38 – 4.31 (m, 151H), 4.03 (dd, *J* = 9.3, 3.2 Hz, 151H), 3.98 (t, *J* = 9.5 Hz, 151H), 3.79 – 3.65 (m, 151H), 3.58 (d, *J* = 9.6 Hz, 151H), 3.46 – 3.37 (m, 151H), 2.38 (s, OAc, 12H); ^{13}C NMR (176 MHz, Chloroform-*d*) δ 165.54, 138.49, 137.51, 133.32, 130.01, 129.87, 128.65, 128.36,

128.34, 128.14, 127.69, 127.30, 127.02, 98.56, 78.20, 75.00, 73.72, 71.30, 70.90, 68.39, 65.72, 31.94, 29, 22.70; m/z (MALTI-TOF) 67133.363 $[M + Na]^+$ ($C_{4049}H_{3921}NO_{908}K$ requires 67116.0675).

MALDI-TOF of pure 151-mer (**25**)

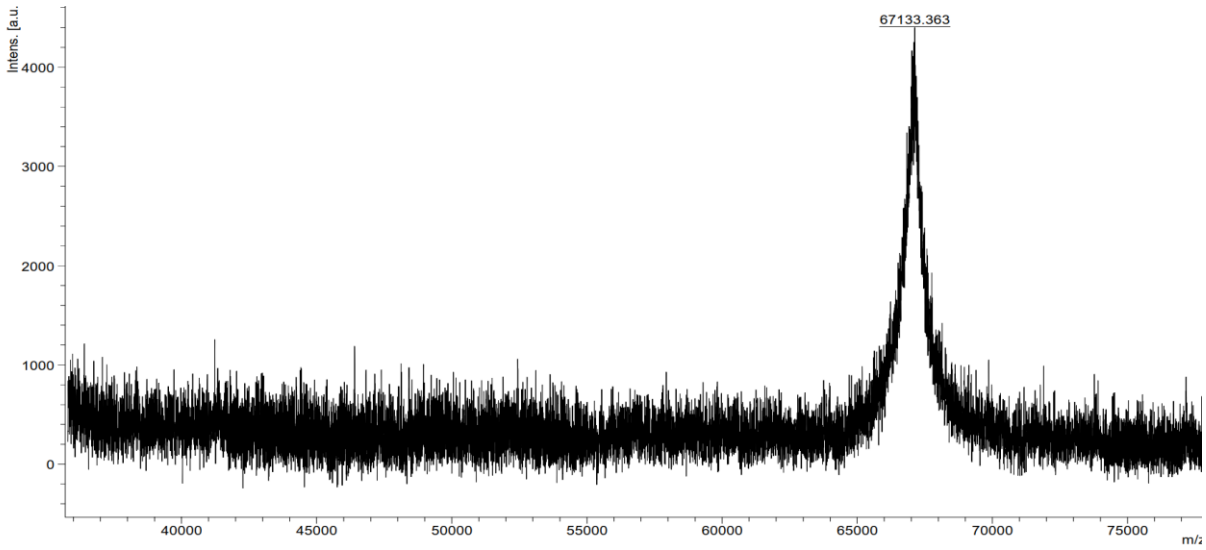

Deprotection of 151-mer polymannoside:

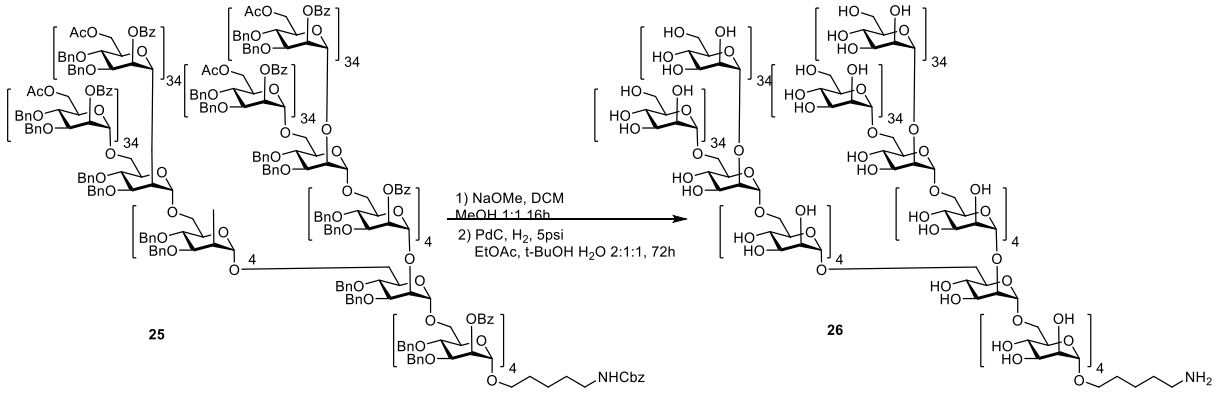

Zemplén Methanolysis. Sodium methoxide in methanol (0.5 M, pH 13) was added to a solution of protected oligosaccharide (12 mg) **26** in methanol:CH_2Cl_2 (1:1), and stirred at room temperature for 16 h, neutralized with Amberlite ion exchange (H+) resin, filtered and concentrated in vacuo and carried forward directly into hydrogenolysis without purification.

Hydrogenolysis. The Zemplén methanolysis product was dissolved in EtOAc:*t*-BuOH:H_2O (2:1:1) and transferred to cylindrical vials. Pd-C (10%) (100 weight %) was added and the reaction mixture was stirred in hydrogen reactor with 5 psi pressure for 72 h. The reaction mixture were filtered through Celite and washed with methanol and water. The filtrates were concentrated in vacuo and purified on Size exclusion chromatography (Method I) TSKgel G3000 PWXL column and lyophilized to give a pure compound **27** in 1.8 mg (41% yield over two steps).

HPLC of 151-mer **26** (ELSD trace, Method I, t_R = 15.7 min)

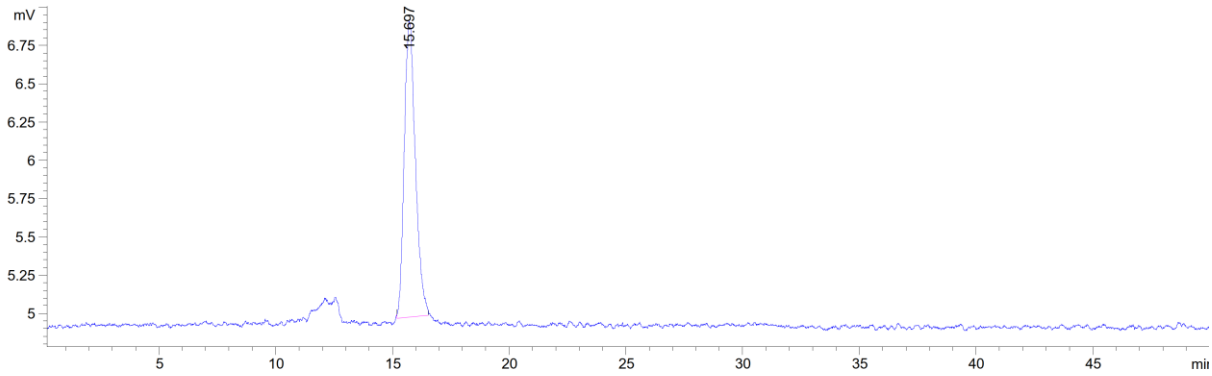

Analytical data for **26**: ^{1}H NMR (700 MHz, D_2O) δ 4.92 (s, 151H), 4.01 (s, 151H), 3.98 – 3.93 (m, 151H), 3.85 (d, *J* = 11.9 Hz, 302H), 3.80 (d, *J* = 11.2 Hz, 151H), 3.74 (t, *J* = 9.9 Hz, 151H), 3.06-3.04 (m, 2H), 3.02 (s, 2H), 2.0 (d, *J* = 6.9 Hz, 2H), 1.33 (d, *J* = 6.9 Hz, 2H); ^{13}C NMR (176 MHz, D_2O) δ 99.35, 70.84, 70.70, 69.99, 66.61, 65.52; m/z (MALTI-TOF) 24574.800 $[M+H]^+$ ($C_{911}H_{1524}NO_{756}$ requires 24574.076).

MALDI-TOF of 151-mer (**26**)

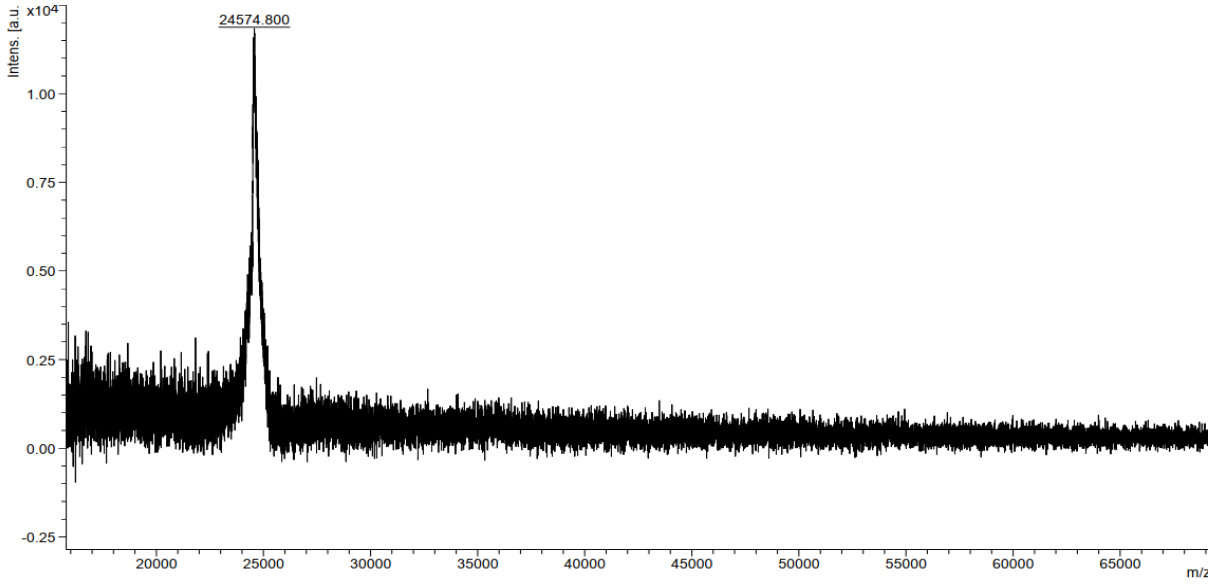

2.14. **Glycan Imaging - ES-IBD.**

For the ES-IBD experiment, the solution of the synthesized glycans (linear pentamannoside **16** and haxamannosides **11** and **17** were prepared by dissolving the powder in a water-ethanol 1:1 mixture with approx. 0.1% ammonia hydroxide to result in a concentration of ~10-4 mol/L. Subsequently, negative charged gas phase ions of the glycans were generated by our home-built ES-IBD apparatus (-1 for glycans **11, 16, 17**), 2-3 kV on the emitter, 20 µl/h flow rate, current up to ~200 pA, about 10 min of deposition time). Before the deposition in UHV, the composition of the ion beam is monitored by a time-of-flight (ToF) mass spectrometer and purified by RF quadrupoles. The deposition took place in the ultrahigh vacuum (UHV) chamber with a base pressure of 2 × 10-10 mbar. The landing energy of the molecular ion beam was below 5 eV to avoid fragmentation.

Before the deposition, the Cu (100) single crystal (Surface Preparation Laboratory, SPL) was cleaned via several cycles of Ar ion sputtering (1.2 kV, 20 min) and annealing (800 K, 10min). After the cleaning, the substrate was cooled down to ~120 K and transferred with a low temperature (LT) UHV suitcase (~120 K, 2 × 10-10 mbar) to the deposition chamber. During the deposition, the substrate was kept at ~120K.

STM measurements.

After the deposition, the sample was kept at ~120 K and transferred with the LT-UHV suitcase to the LT-STM for imaging. In all the chamber involved in the sample transfer, the base pressure is below 8 × 10-10 mbar. The STM experiments are performed in a home-built LT-STM operated at 4.5 K and controlled by a Nanonis RC5 electronics. All STM measurements were performed with a chemical etched W tip.

STM data analysis was performed using WSxM and OriginPro 2016. The interunit distance given in the paper is an average value taking into account only molecules where all features could be resolved in the STM measurement. For hexamannoside **11**, four molecules were taken into account with four (1-6) interunit distances each averaging to 0.49 ± 0.06 nm and two (1-2) interunit distance averaging to 0.62 ± 0.04 nm. For hexamannose **17**, three molecules were taken into account with four (1-6) interunit distances each averaging to 0.5 ± 0.04 nm and one (1-2) interunit distance averaging to 0.62 ± 0.02 nm.

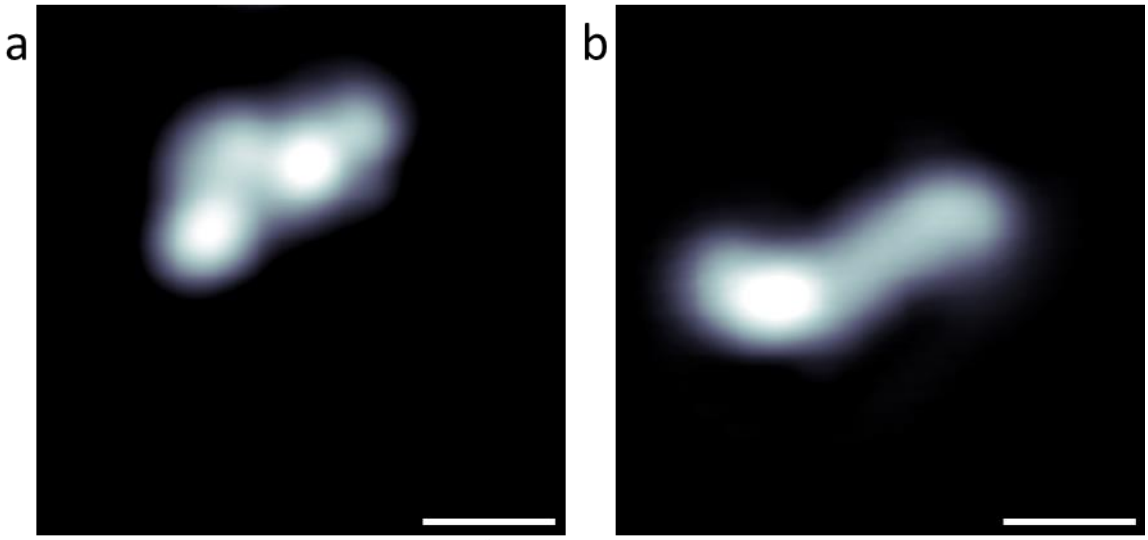

STM topography image of linear glycans. a,b STM images of pentamannoside **16** showing different conformations on the surface. Scale bars are 1 nm.

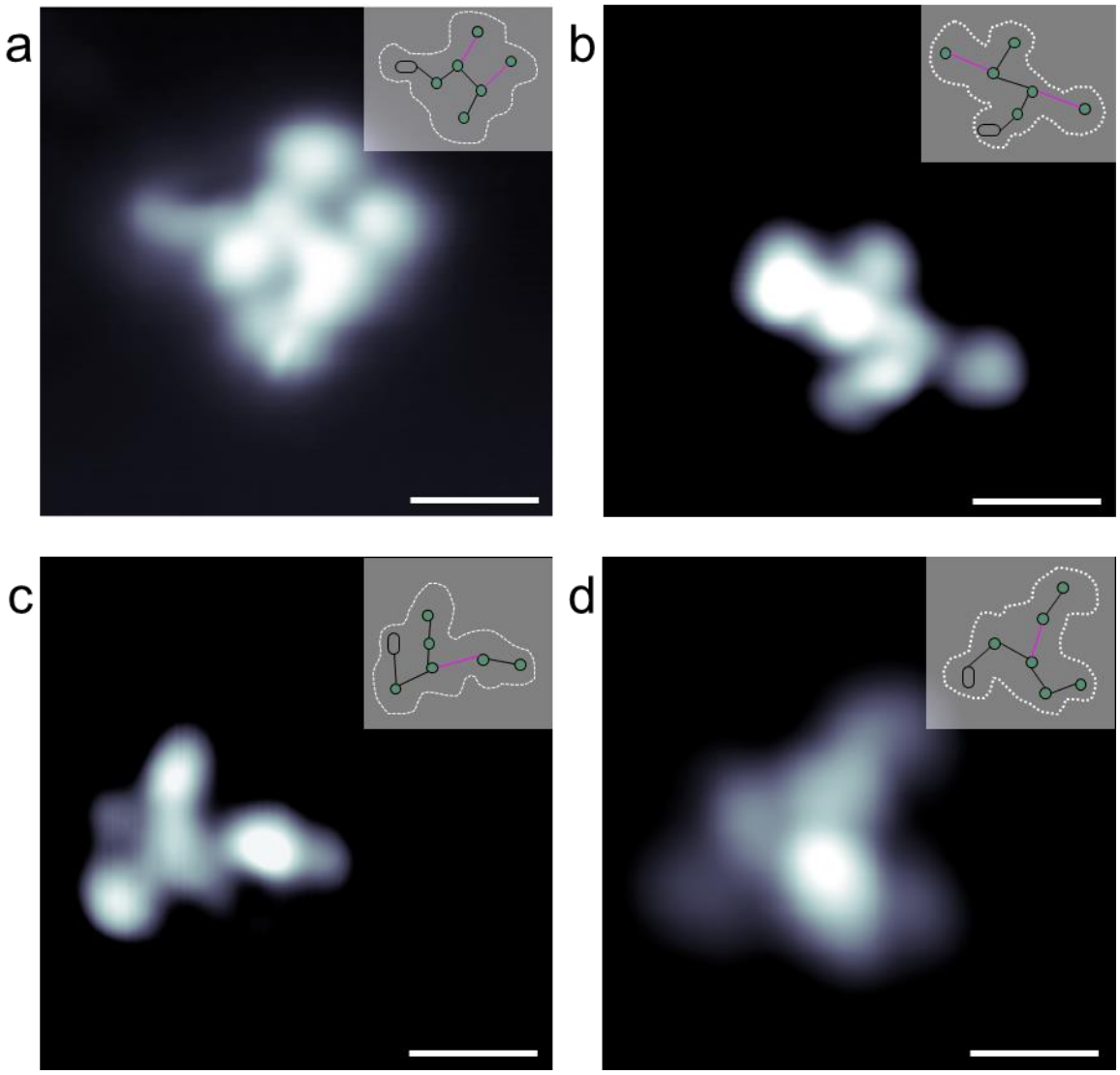

STM topography image of branched hexamannosides. **a,b** STM images of hexamannoside **11** showing different conformations on the surface. The branching is clearly visible. The assignment of the linkage is possible due to measurements of the interunit distance and is assigned in the inset ((1,2) linkage in pink)**. c, d** STM images of hexamannoside **17** showing different conformations on the surface. The branching is clearly visible. The assignment of the linkage is possible due to measurements of the interunit distance and is assigned in the inset ((1-2) linkage in pink). Scale bars are 1 nm.

3. Defined glycan structures as substrates to study marine hydrolases

This chapter has been modified in part from the following article:

Le Mai Hoang K., Pardo-Vargas A., Zhu Y., Yu Y., Loira M., Delbianco M., Seeberger P.H. **Traceless Photolabile Linker Expedites the Chemical Synthesis of Complex Oligosaccharides by Automated Glycan Assembly** *J. Am. Chem. Soc.* 2019, 141, 22, 9079-9086. DOI: 10.1021/jacs.9b03769

3.1. Abstract

Carbohydrate-degrading enzymes obtained from marine sources have been recognized as promising biocatalysts with high potential in biorefinery. Marine glycans with specific substitution patterns and length are required as substrates for the complete characterization of these enzymes. Automated Glycan Assembly (AGA) was employed to synthesize a collection of six linear α-(1,6)-mannosides and seven β-(1,3)-glucans with specific β-(1,6) and β-(1,4) substitution patterns. All of the compounds were obtained with a free reducing end using a traceless photolabile linker. The characterization of the putative mannanase GH76A from *Salegentibacter sp.* using synthetic glycans is also described. A detailed 3-D structure of the active site of GH76A was obtained after the co-crystallization of synthetic mannose tetramer with mutant mannanase GH76. Incubation of these synthetic α-(1,6)-mannosides with GH76A generated hydrolyzed glycans, this suggested that the enzyme GH76A function as an endo α-(1,6)- mannanase.

3.2. Algae bloom as source of Carbohydrate-Active Enymes (CAZymes)

Marine algae are major carbon sinks that convert carbon dioxide to carbohydrate materials such as laminarin.[124] These carbohydrates are nutrient sources for bacterial colonies in marine surface waters.[125] To digest these polysaccharides, bacteria use a vast number of carbohydrate-

degrading enzymes. For example, the marine flavobacterium *Formosa agariphila* degrades the main cell wall polysaccharide of marine algae *Ulva* to single monosaccharides using 12 different enzymes.[126] Thus, the expression and characterization of hydrolitic enzymes can turn an unexplored polysaccharides source into a valuable and ecologically renewable bioresource.[127]

Metagenomics studies of bacteria associated with the algal spring blooms, particularly *Bacteriodetes,* showed a high abundance of hydrolytic Carbohydrate-Active Enzymes (CAZymes).[128,129] There are over 400 putative genetic clusters (PULs), which encodes for hydrolytic CAZymes in the North Sea, and most of these clusters have not yet been studied.[130] Cloning and recombinant expression of CAZyme sequences permitted the elucidation of the degradation pathways for several polysaccharides such as rhamnogalacturonan,[131] xyloglucan and alpha-mannan.[132]

The enzymes belonging to the class of α-mannanase are of great interest because of their diverse functions such as glycoprotein maturation,[133] complex dietary polysaccharides processing by human gut microbiota[132] and fungal cell wall assembly.[134,135] One interesting putative genetic cluster is α-mannan PUL because most of the encoded enzymes are distantly related or their function is still completely unknown. Putative mannanase GH76A from *Salegentibacter sp.* may degrade α-mannans. Here the characterization of the putative mannanase GH76A using synthetic glycans is described. Automated Glycan Assembly (AGA) was employed to synthesize a collection of six linear α-(1,6)-mannosides with a free reducing end using a traceless photolabile linker.[114]

3.3. AGA of linear mannosides

The characterization of the putative mannanase GH76A required the synthesis of a collection of natural α-(1,6)-oligomannosides with a free reducing end. Therefore, BB **1**, bearing an Fmoc protecting group at C-6 for chain elongation, was coupled to a Merrifield resin equipped with a recently newly developed traceless photo-cleavable linker **28**. The oligosaccharide chain was assembled by using iterative optimized AGA cycles, which consisted of four modules (Figure 3.1). An acidic wash module B prepared the resin for the glycosylation by quenching any remaining base from the previous step. In the glycosylation module C, thioglycoside donor **1** was coupled to the resin upon activation with NIS and TfOH (from -20 °C to 0 °C) Next, a capping step D (30 min) prevented the formation of undesired side-products by acetylating any

incomplete glycosylation and finally module E removes the temporary Fmoc group (14 min) revealing a free hydroxyl group for subsequentent glycosylation.[108] After photocleaveage of the polysaccharide from the resin, a fully protected α-(1,6)-oligomannoside was obtained with a benzyl alchohol in the anomeric position that was later removed by hydrogenolysis during global deprotection.

A

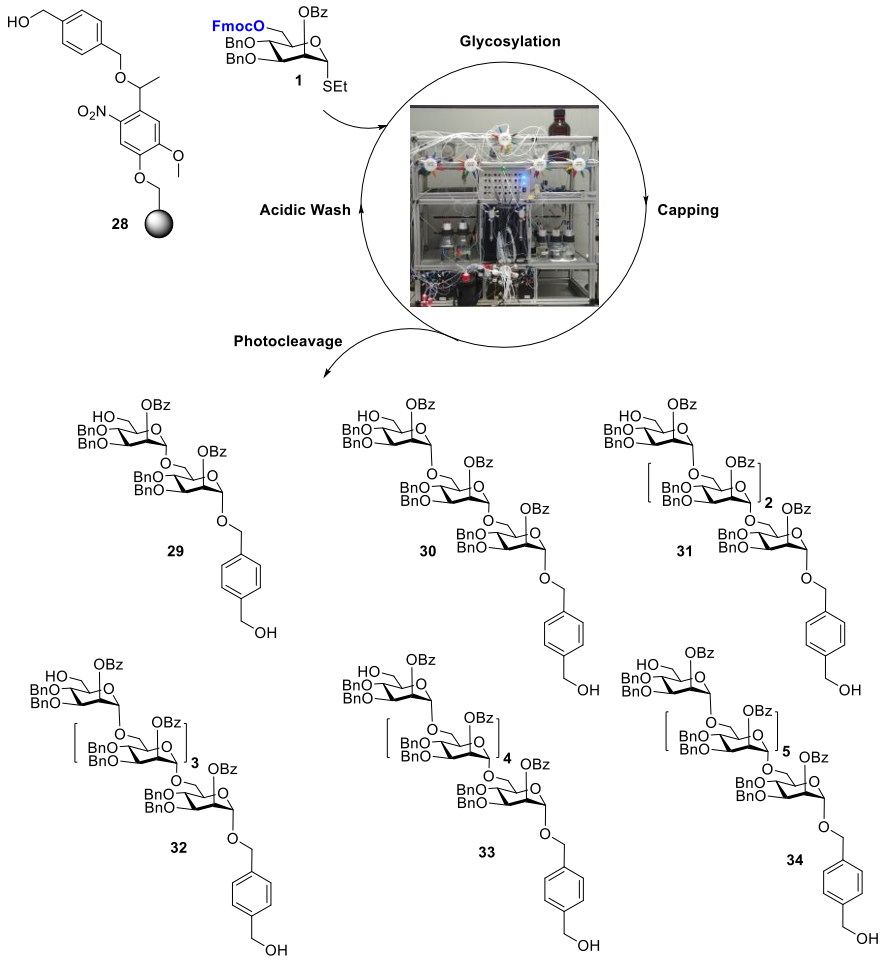

B

Cycles	Module	Conditions
	A: Resin Preparation for Synthesis	
n	B: Acidic Wash with TMSOTf Solution C: Thioglycoside Glycosylation D: Capping E: Fmoc Deprotection	BB**1** 6.5 eq, -20 °C for 5 min, 0 °C for 30 min

Figure 3.1 A) AGA scheme of α-(1,6)-mannosides **29-34** ranging from dimer (*n*=2) to heptamer (*n*=7) using a traceless photocleavable linker **28** and BB **1**. B) AGA sequence for α-(1,6)-mannosides **29-34.** Modules B-E were repeated *n* times until the desired sequence was obtained.

Linear α-(1,6)-dimannoside **29** was synthesized using two coupling cycles (*n=2*) and 6.5 equivalents of mannose BB **1**. During each cycle, no side products of incomplete glycosylation

were observed, and the crude product was purified using normal phase HPLC to obtain dimannoside **29** in 50% yield, based on resin loading. Following the same AGA procedure for compounds **30-34** no deletion sequence was observed even for the heptamer **34**. For the deprotection of **29**, the protected oligosaccharide was dissolved in a mixture MeOH and DCM, followed by the addition of 0.1 ml 1M solution of NaOMe in MeOH. After 12 h, the solution was neutralized with Amberlite IR-120. The crude compound was directly used for hydrogenolysis with Pd/C inside an H_2 bomb with 60 psi pressure for 16 hours. The reaction mixture was filtered, and washed with DCM, *t*BuOH and H_2O.

Compound	Yield
35	20%
36	33%
37	22%
38	18%
39	25%
40	30%

Table 3.1 Yields for linear oligomannosides **29** to **34** based on resin loading after AGA and two steps global deprotection.

All deprotected compounds **35** – **40** were purified using RP-HPLC. First attempts, using a C-18 synergy column, were not successful since mannoside **35** eluted with the injection peak. Purification using a Hypercarb column gave **35** in 20% yield after AGA and two steps deprotection. For deprotection of mannosides **30-34** the same protocol was followed to obtain the fully deprotected α-(1,6) mannosides **36-40** (Table 3.1) as a mixture of α and β isomers at the free reducing end.

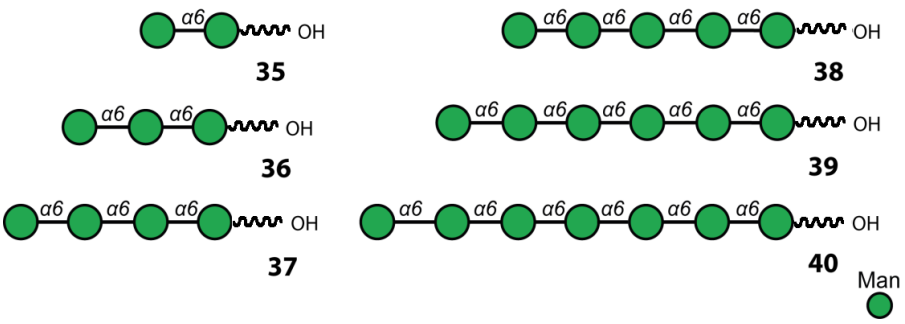

Figure 3.2 Schematic representation of linear α-(1,6)-oligomannosides **35-40** obtained by AGA.

With these optimized conditions, a total of six mannosides containing α-(1,6)-Man, linkages were synthesized by automated glycan assembly in high yields, using monosaccharide building block **1** and the new traceless linker **28** (Figure 3.2).

3.4. **Functional characterization of mannosylhydrolase GH76A**

3.4.1. GH76A crystal structures with synthetic mannosides

Dr Solanki (from the Max Planck Institute for Marine Microbiology) cloned, expressed and purified GH76AWild Type ($GH76A^{WT}$) using heterologous expression system for structural and functional characterization. To study interfacial binding in the absence of catalysis, a structurally intact but catalytically inactive GH76 mutant ($GH76^{mut}$) was expressed replacing the two aspartic acid residues D136 D137 at the active site for alanine 136A 137A. Co-crystallization trials were set in the presence of mannosides with different length (**35-40**) and $GH76^{mut}$. The D136A-D137A mutant in complex with tetramannoside **37** crystallized successfully and the structure was solved using a molecular replacement method using a WT structure as a search model. Figure 3.3 presents the crystal structure of $GH76A^{WT}$ (apo-form, resolution 2.0 Å) and Figure 3.4 shows the crystal structure of $GH76^{mut}$ with tetramannoside **37** at the active site with a 1.9 Å resolution. Both images show a typical $(\alpha/\alpha)_6$ fold, where six α-helices are forming a core covered by another layer of six α-helices around them. A similar structural fold was present in other homologs of GH76 from gut microbiota resident *Bacteroides thetaiotaomicron*[132] and the soil bacterium *Bacillus circulans*.[136] In both apo-form and substrate-bound form, a total of 12 α-helices and 6 β-strands are present.

The structural alignment and sequence alignment suggested that the catalytic residues Asp137 and Asp137 are conserved among the GH76 family.

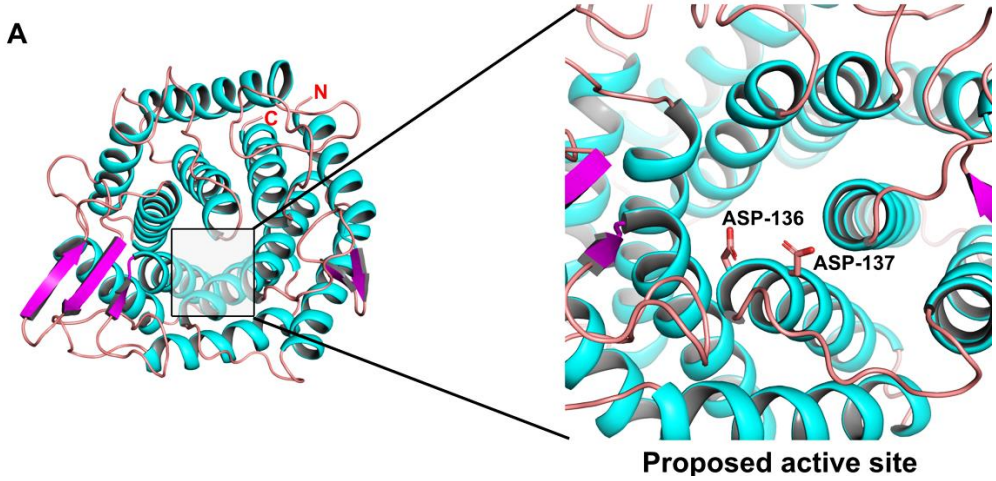

Figure 3.3 Cartoon representation of GH76A^{WT} crystal structure showing $(\alpha/\alpha)_6$ fold having the active site in the center (highlighted catalytic residues ASP136 and ASP137 in closer-view at right side panel).

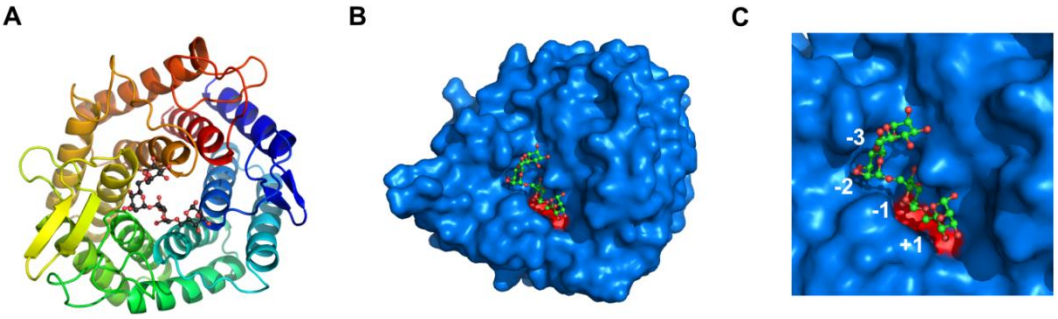

Figure 3.4 (A) 3D-Crystal structure of GH76A^{mut} in complex with tetramannoside **37** shows in a ball-stick representation. **(B)** Surface-view representation of GH76A^{mut} showing ligand pocket and catalytic residues mutated to Alanines (red). **(C)** Closer-view of active site revealing the distinct binding mode of tetramannoside **37.**

The ligand-bound form resulted in a RMSD of 0.228 Å, indicating no global change in the structure upon ligand binding. In the initial model, the electron density of tetramannoside **37** was visible and it is enough for four mannose molecules to fit into the active site (Figure 3.4). The surface view representation shows the active site cavity with **37** adopting a very sharp bent in the middle to occupy the active site (Figure 3.4). The attempts to co-crystallize different length/branched manno-oligosaccharides are still ongoing.

3.4.2. Recombinantly purified GH76A^{WT} has α-1,6-mannanase activity

The preliminary analysis by high-performance anion-exchange chromatography coupled with pulsed amperometric detection (HPAEC-PAD) showed that the GH76A^{WT} purified from heterologous host is functional and has α-1,6-mannanase activity. Yeast-mannan from *Saccharomyces cerevisiae* digested by this mannanase was hydrolyzed mainly into dimannoside **36** (Figure 3.5). The digested products were qualitatively analyzed on HPLC and identified by comparison with known synthetic oligosaccharides standard. Additionally, the presence of higher length mannan oligosaccharides in HPLC elution chromatogramm suggested an endo acting enzyme. For the next experiment, mannan-like oligosaccharides with α-1,6-linkages (**36-40**) were digested and analyzed by RP-HPLC. Different products with shorter lengths were identified (data from digestion of mannoside **40** is shown here as an example). When heptamannoside **40** was digested with GH76A^{WT}, the digested products were identified as dimannoside **36** and pentamannoside **38** (Figure 3.6). As the length of digested products is different, we propose that GH76A is an endo-acting enzyme. As expected, the double amino acid inactive mutant GH76^{mut} could not digest the yeast-mannan as well as the synthetic oligosaccharide **40** (Figure 3.5C, Figure 3.6C).

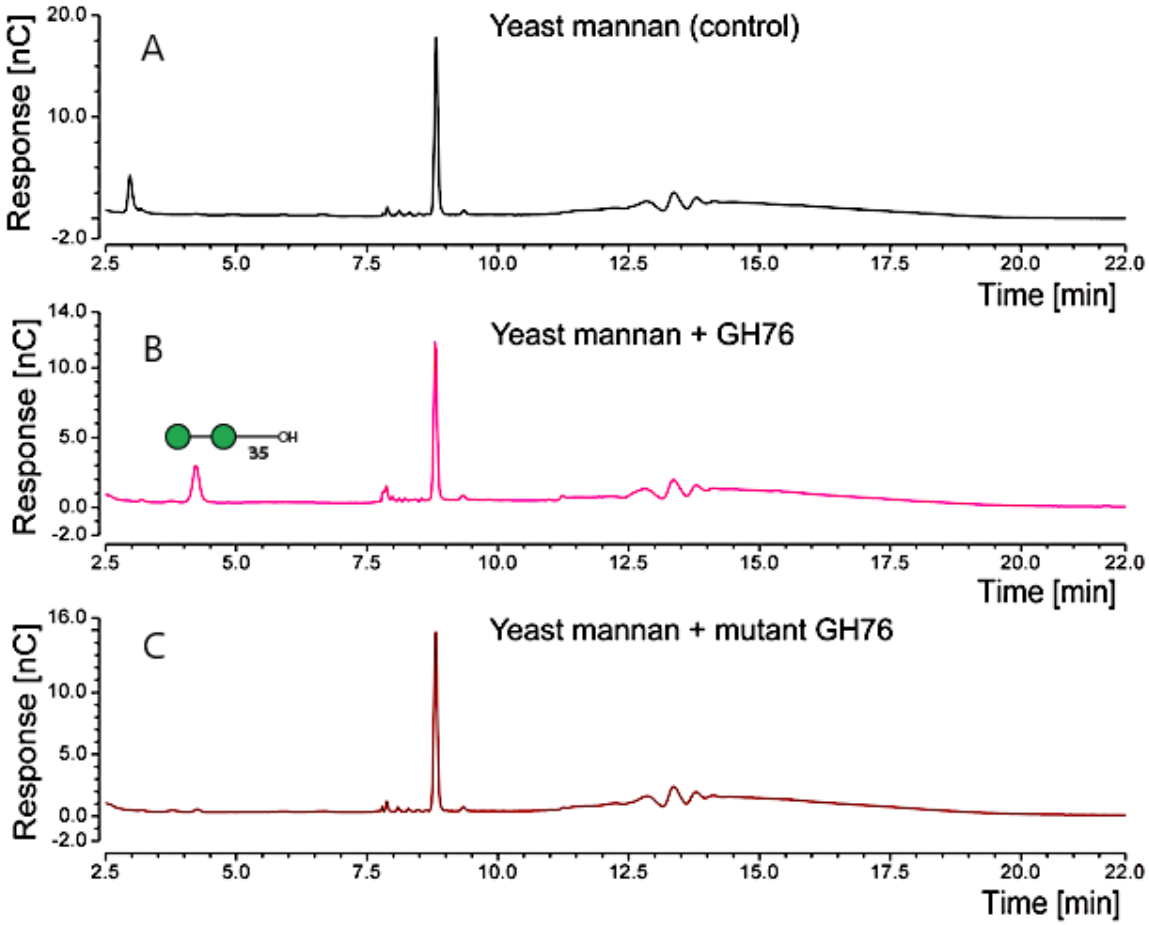

Figure 3.5 HPAEC-PAD chromatogramms of a) Control experiment: yeast-mannan and buffer b) Digestion of yeast-mannan with GH76A^{WT}. At 3.5 min dimannoside **35** was detected as reaction product c) Digestion of yeast-mannan with GH76A^{mut} no reaction observed.

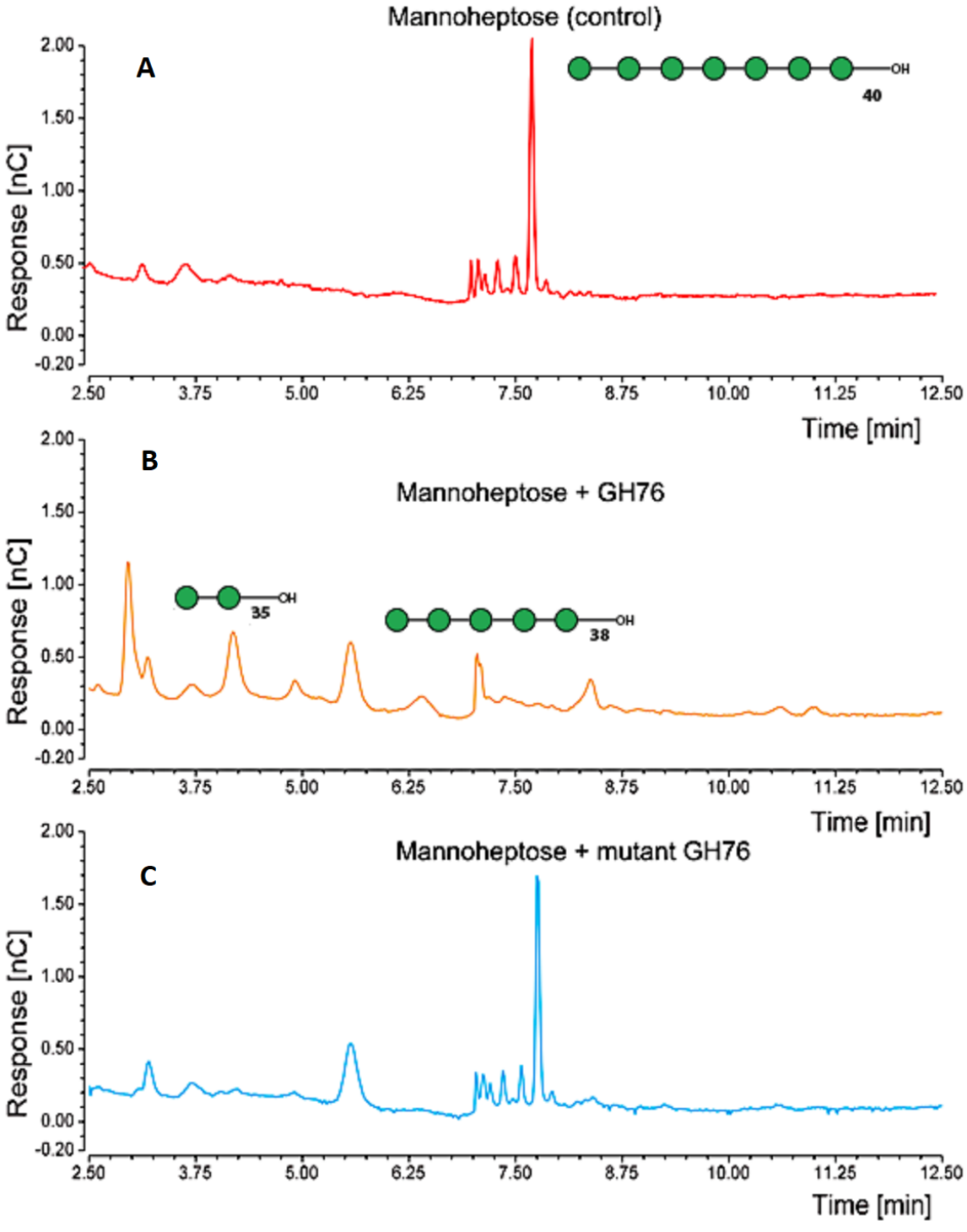

Figure 3.6 HPAEC-PAD of a) Control experiment: heptamannoside **40** and buffer b) Digestion of heptamannoside **40** with GH76A^{WT}. At 3.5 min was detected the dimannoside **35** along with pentamannoside **38** at 6.25 min as reaction products c) Digestion of heptamannoside **40** with GH76A^{mut}- no reaction observed.

3.5. AGA of linear and branched glucosides

β-(1,3)-glucans (laminarin) derivatives **44-50** (Figure 3.7) with specific β-(1,6) and β-(1,4) substitution patterns were chosen as model substrates to determine the specificity of three different *exo*-glucanases obtained from marine sources with probable β-(1,3), β-(1,4), β-(1,6) glucanase activity. To synthesize the laminarin series**,** three different glucose BBs **41 – 43** and a traceless photocleavable linker **21** based on the *o*-nitrobenzyl scaffold were used (Figure 3.7).[114] This linker, upon photo-cleavage, reveals an oligosaccharide with a free reducing end to obtain fully natural glycans.

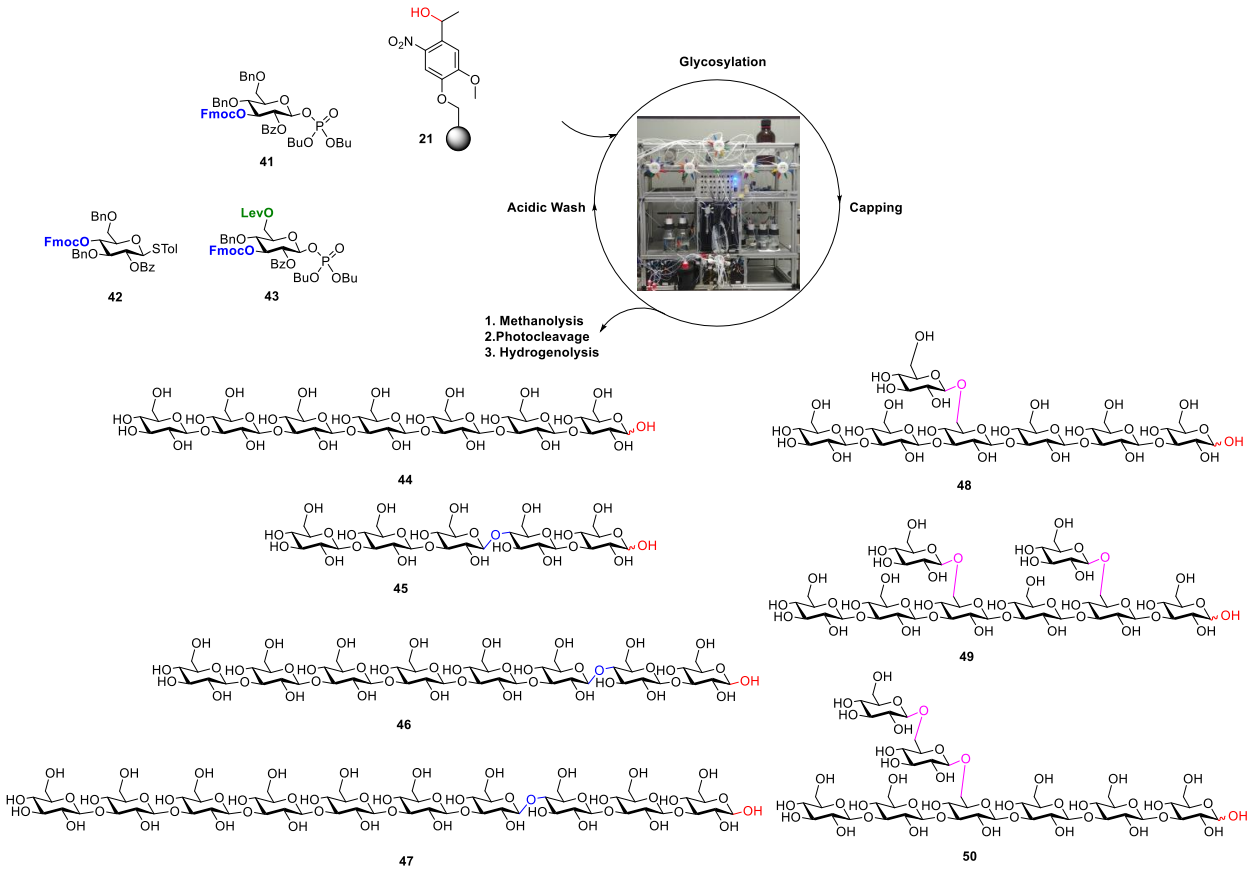

Figure 3.7 AGA of β-(1,3)-glucans with specific β-(1,6) and β-(1,4) substitution patterns **44-50** ranging from pentamer to decaglucoside using a traceless photocleavable linker **21**.

AGA of linear and branched β-(1,3)-glucans carrying an aminoalkyl spacer at the reducing end was reported before using glycosyl phosphate building blocks and a photolabile linker.[137] Convergent solution-phase syntheses of β-(1,3)-glucans were carachterized by low yields and aberrant α-linkage formation due to double-stereo differentiation effects as well as limitations in the chain length, position, and degree of branching.

Here, the core structure of laminarin structures was synthesized using BB **41** bearing Fmoc as a temporary protecting group for chain elongation at C-3 and Bz esters in the C2-position to ensure β-selectivity during glycosylation. The phosphate leaving group was selected since glycosyl phosphates provide the best coupling efficiencies, as previously described.[12] AGA cycles consisting of four modules (Figure 3.7) were utilized as mentioned in section 3.3. For the glycosylation, only 4.0 equivalents of phosphate donor **41** were required for coupling to the resin upon activation with TMSOTf (from -30 °C to -10 °C). These conditions permitted the assembly of linear β-(1,3)-heptaglucose **44** in 30% yield.

To obtain the mixed β-(1,3)-β-(1,4)-linked structures, an analogue of BB **41** bearing Fmoc as a temporary protecting group for chain elongation at C-4 (BB **42**) was synthesized**.** The thiol leaving group was selected since it was previously reported for its use in AGA[113] using 6.5 equivalents of BB per cycle. Several β-(1,3)-β-(1,4)-glucans such as pentaglucoside **45** as well as octaglucosides **46** and **47** were prepared using BB **41** and **42** with an overall yield of 22, 9 and 6% respectively (Table 3.2,).

Structures **48-50** are based on a β-(1,3) linear backbone with β-(1,6)-branches. The backbone was firstly built using the predefined sequence of glycosyl phosphates **41** and **43**. Building block **43** contains a C-3 Fmoc-protected hydroxyl group and a Lev ester on the C-6 hydroxyl. Upon completion of the backbone, selective removal of the levulinoyl ester allowed for the insertion of the β-(1,6)-branch. Module **E** (20% piperidine in DMF) was standardly used to remove Fmoc. However, in the presence of Lev, module **E2** (20% Et_3N in DMF) was employed, to avoid Lev migration. The methanolysis of base-labile protecting groups, as part of the global deprotection, was performed directly on the solid support and proved to be more effective than the more common solution phase methanolysis. The partially protected oligosaccharides were photocleaved from the resin and immediately debenzylated via hydrogenation using the Pd/C catalyst (60 psi in <1 h).

Compound	Yield
44	30%
45	22%
46	9%
47	6%
48	10%
49	8%
50	16%

Table 3.2 AGA of -(1,3)-glucans with specific β-(1,6) and β-(1,4) substitution patterns **44-50** based on resin loading after AGA and two steps global deprotection.

With this protocol, only a single purification with reverse-phase HPLC was needed to yield oligosaccharides **44** and **45** in 30% and 22% yields, respectively. Branched octasaccharides **48, 49** and **50**, as well as long linear structures **46** and **47** were isolated in lower quantities (6 – 16%) because these glycans unexpectedly partially fragmented during hydrogenation.

The application of these glucans as standards for determining the substrate specificities of the above-mentioned enzymes is still ongoing.

3.6. Conclusion

Synthetic α-(1,6)-oligomannosides are valuable standards for determining the substrate specificity of the mannose-degrading enzymes of the class of mannanases, as shown here for GH67A. A detailed 3D structure of the active site of GH76A was obtained via X-ray diffraction of the co-crystallized synthetic tetramannoside with mutant mannanase GH76. The structure of the active is conserved among the GH76 family. Digestion of the synthetic mannosides with GH76A indicated that mannanase GH76A is acting as an α-(1,6) endo-enzyme. Furthermore, the synthesis of seven β-(1,3)-glucans with specific β-(1,6) and β-(1,4) substitution patterns as long as 10-mer was successfully enabled by using phosphate glycosyl donors together with TMSOTf as promoter in AGA. Two new traceless photocleavable linkers were tested and successfully afforded glycans with free reducing ends. Laminarin analogs will be tested to determine the specificity of three different exo glucanases.

3.7. General Materials and Methods

All chemicals used were reagent grade and used as supplied unless otherwise noted. All building blocks used were purchased from *GlycoUniverse*, Germany. Automated syntheses were performed on a home-built synthesizer developed at the Max Planck Institute of Colloids and Interfaces.[108] Merrifield resin LL (100-200 mesh, Novabiochem^{TM}) was modified and used as solid support.[105] Analytical thin-layer chromatography (TLC) was performed on Merck silica gel 60 F254 plates (0.25 mm). Compounds were visualized by UV irradiation or dipping the plate in a p-anisaldehyde (PAA) solution. Flash column chromatography was carried out by using forced flow of the indicated solvent on Fluka Kieselgel 60 M (0.04 – 0.063 mm). Analysis and purification by normal and reverse phase HPLC was performed using an Agilent 1200 series. Products were lyophilized using a Christ Alpha 2-4 LD plus freeze dryer. ^{1}H, ^{13}C and HSQC NMR spectra were recorded on a Varian 400-MR (400 MHz), Varian 600-MR (600 MHz), or Bruker Biospin AVANCE700 (700 MHz) spectrometer. Spectra were recorded in $CDCl_3$ by using the solvent residual peak chemical shift as the internal standard ($CDCl_3$: 7.26 ppm ^{1}H, 77.0 ppm ^{13}C) or in D_2O using the solvent as the internal standard in ^{1}H NMR (D_2O: 4.79 ppm ^{1}H) and a D6-acetone spike as the internal standard in ^{13}C NMR (acetone in D_2O: 30.89 ppm ^{13}C) unless otherwise stated. High resolution mass spectra were obtained using a 6210 ESI-TOF mass spectrometer (Agilent) and a MALDI-TOF Autoflex^{TM} (Bruker). MALDI and ESI mass spectra were run on IonSpec Ultima instruments. HPAEC-PAD was performed in a Dionex ICS-5000 system (Thermo Fischer Scientific Inc., Waltham, MA, USA) with a working gold electrode and a pH (Ag/AgCl) reference electrode.

Solvents used for dissolving building block and preparing the activator, TMSOTf and capping solutions were taken from an anhydrous solvent system (jcmeyer-solvent systems). Other solvents used were HPLC grade. The building blocks were co-evaporated three times with toluene and dried 2 h under high vacuum before use. Activator, deprotection, acidic wash, capping and building block solutions were freshly prepared and kept under argon during the automation run. All yields of products obtained by AGA were calculated based on resin loading. Resin loading was determined by performing one glycosylation (Module C) with ten equivalents of building block followed by DBU promoted Fmoc-cleavage and determination of dibenzofulvene production by measuring its UV absorbance.

3.8. Preparation of stock solution.

- **Building block:** building block was dissolved in 1 mL dichloromethane (DCM).
- **Activator solution:** 1.56 g of recrystallized NIS was dissolved in 60 mL of a 2:1 mixture of anhydrous DCM and anhydrous dioxane. Then triflic acid (67 µL) was added. The solution is kept at 0 °C for the duration of the automation run.
- **Activator Solution 2**: 0.9 mL of TMSOTf was added to 40 mL of CH_2Cl_2
- **Fmoc deprotection solution:** A solution of 20% piperidine in dimethylformamide (DMF) (v/v) was prepared.
- **Fmoc Deprotection Solution 2**: 20 mL of Et_3N was added to 80 mL of anhydrous DMF
- **TMSOTf solution:** Trimethylsilyl trifluoromethanesulfonate (TMSOTf) (0.9 mL) was added to DCM (90 mL).
- **Capping solution:** A solution of 10% acetic anhydride (Ac_2O) and 2% methanesulfunic acid (MsOH) in anhydrous DCM (v/v) was prepared.

3.9. Modules for automated synthesis

3.9.1. Module A: Resin Preparation for Synthesis (20 min)

All automated syntheses were performed on 19 µmol scale. Resin was placed in the reaction vessel and swollen in DCM for 20 min at room temperature prior to synthesis. During this time, all reagent lines required for the synthesis were washed and primed. Before the first glycosylation, the resin was washed with the DMF, tetrahydrofuran (THF), and DCM (three times each with 2 mL for 25 s). This step is conducted as the first step for every synthesis.

3.9.2. Module B: Acidic Wash with TMSOTf Solution (20 min)

The resin was swollen in 2 mL DCM and the temperature of the reaction vessel was adjusted to -20 °C. Upon reaching the temperature, TMSOTf solution (1 mL) was added drop wise to the reaction vessel. After bubbling for 3 min, the acidic solution was drained and the resin was washed with 2 mL DCM for 25 s.

3.9.3. Module C: Thioglycoside Glycosylation (25 min)

The building block solution (0.150 mmol of BB in 1 mL of DCM per glycosylation) was delivered to the reaction vessel. After the set temperature (T1) was reached, the reaction was started by drop wise addition of the activator solution (1.0 mL, excess). The glycosylation was performed by increasing the temperature to T2 for 20-60 min (depending on oligosaccharide length). After completion of the reaction, the solution is drained and the resin was washed with DCM, DCM:dioxane (1:2, 3 mL for 20 s) and DCM (twice, each with 2 mL for 25 s). The temperature of the reaction vessel is increased to 25 °C for the next module.

3.9.4. Module C2: Glycosylation with Glycosylphosphate (55 min)

The building block solution (0.08 mmol of BB in 1mL of DCM) was delivered to the reaction vessel. After initiation temperature (**T1**) was reached, **Activator Solution 2** solution (1 mL) was added dropwise to the reaction vessel. Incubation temperature (**T2**) was set and the incubation duration (**t2**) was adjusted depending on the BB. The values for building block were shown in the table below. The solution was drained and the resin was washed with CH_2Cl_2, CH_2Cl_2/dioxane (1:2, 3 mL for 20 s) and CH_2Cl_2 (twice, each with 2 mL for 25 s). The temperature was increased to 25 °C.

3.9.5. Module D: Capping (30 min)

The resin was washed with DMF (twice with 2 mL for 25 s) and the temperature of the reaction vessel was adjusted to 25 °C. Pyridine solution 2 mL (10% in DMF) was delivered into the reaction vessel. After 1 min, the reaction solution was drained and the resin washed with DCM (three times with 3 mL for 25 s). The capping solution 4 mL was delivered into the reaction vessel. After 20 min, the reaction solution was drained and the resin washed with DCM (three times with 3 mL for 25 s).

3.9.6. Module E: Fmoc Deprotection (14 min)

The resin was washed with DMF (three times with 2 mL for 25 s) and the temperature of the reaction vessel was adjusted to 25 °C. Fmoc deprotection solution (2 mL) was delivered into the reaction vessel. After 5 min, the reaction solution was drained and the resin washed with DMF (three times with 3 mL for 25 s) and DCM (five times each with 2 mL for 25 s). The temperature of the reaction vessel is decreased to -20 °C for the next module.

3.9.7. Module E2: Fmoc Deprotection (14 min)

The resin was washed with DMF (three times with 2 mL for 25 s) and the temperature of the reaction vessel was adjusted to 25 °C. Fmoc deprotection solution **2** (2 mL 20% Et_3N in DMF) was delivered into the reaction vessel. After 5 min, the reaction solution was drained, and the resin washed with DMF (three times with 3 mL for 25 s) and DCM (five times each with 2 mL for 25 s). The temperature of the reaction vessel is decreased to -20 °C for the next module.

3.10. **Post-synthesizer Manipulations**

3.10.1. Cleavage from Solid Support

After automated synthesis, the oligosaccharides were cleaved from the solid support using a continuous-flow photo reactor. The Vapourtec E-Series UV-150 Photoreactor Flow Chemistry System with mercury lamp was employed. The resin, suspended in CH_2Cl_2, was loaded into a plastic syringe. The suspension was pumped using a syringe pump (PHD2000, Harvard Aparatus) at 1 mL/min through a 10 mL reactor, constructed of 1/8 inch o.d. FEP tubing. The temperature of the photoreactor was maintained at 20 °C.[108]

3.10.2. Purification

Crude products were analyzed and purified using analytical or preparative HPLC (Agilent 1200 Series System). All unprotected products were isolated as formate salt.

Module A (YMC-Diol-300 column, 150 x 4.6 mm): flow rate of 1.0 mL/min with 20% EtOAc/Hexane as eluents [isocratic (5 min), linear gradient to 55% EtOAc (30 min), linear gradient to 100% EtOAc (5 min)].

Module B (YMC-Diol-300 column, 150 x 20 mm): flow rate of 4.6 mL/min with 20% EtOAc/Hexane as eluents [isocratic (5 min), linear gradient to 55% EtOAc (30 min), linear gradient to 100% EtOAc (5 min)].

Module C (Synergi Hydro RP18 column, 250 x 2.6 mm): flow rate of 0.7 mL/min with H_2O (0.1% formic acid) as eluents [isocratic (5 min), linear gradient to 10% ACN (30 min), linear gradient to 100% ACN (5 min)].

Module D (Synergi Hydro RP18 column, 250 x 10 mm): flow rate of 3.7 mL/min with H_2O (0.1% formic acid) as eluents [isocratic (5 min), linear gradient to 10% ACN (30 min), linear gradient to 100% ACN (5 min)].

Method E: (Hypercarb column, 150 x 4.6 mm) flow rate of 0.7 mL / min with H_2O (0.1% formic acid) as eluents [isocratic (5 min), linear gradient to 30% ACN (30 min), linear gradient to 100% ACN (5 min)].

Method F: (Hypercarb column, 150 x 10 mm) flow rate of 1.3 mL / min with H_2O (0.1% formic acid) as eluents [isocratic (5 min), linear gradient to 30% ACN (30 min), linear gradient to 100% ACN (5 min)].

3.10.3. Oligosaccharide deprotection

Module G: Methanolysis

The protected oligosaccharide was dissolved in MeOH:DCM (1.5 mL,1:1). NaOMe in MeOH (0.1 mL of 0.5M solution) was added to the solution and stirred at room temperature. After 12 h, the solution was neutralized with Amberlite IR-120 (H^+ form) resin, filtered and concentrated *in vacuo.* The crude compound was used for hydrogenolysis without further purification.

Module H: Hydrogenolysis with Pd/C

The crude compound obtained from *Module G* was dissolved in 2 mL of DCM:*t*BuOH:H_2O (1:0.5:0.5) and Pd/C (10%) was added. The reaction was stirred in H_2 bomb with 60 psi pressure for 16 hours. The reaction was filtered, washed with DCM, *t*BuOH and H_2O. The filtrates were concentrated *in vacuo.*

3.11. AGA Synthesis of mannosides

3.11.1. Synthesis of α-(1,6) linear dimannoside (29)

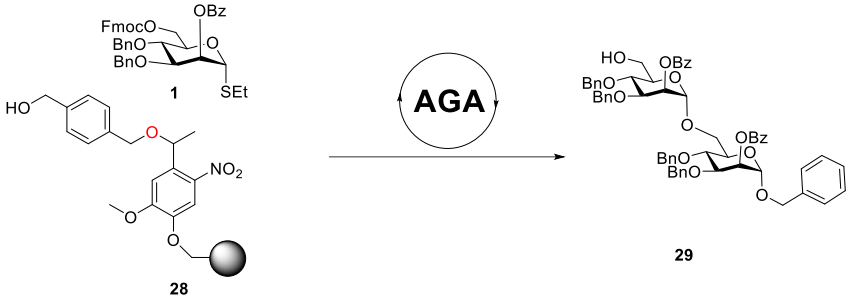

Cycles	Module	Conditions
	A: Resin Preparation for Synthesis	
2	B: Acidic Wash with TMSOTf Solution	
	C: Thioglycoside Glycosylation	BB1 6.5 eq, -20 °C for 5 min, 0 °C for 30 min
	D: Capping	
	E: Fmoc Deprotection	

Cleavage from solid support as described in section 4.4.2 Photocleavage, followed by purification using preparative HPLC (**Method B**) afforded compound **29** (5 mg, 31% from resin **28**).

Analytical data for **29**: 1H NMR (600 MHz, Chloroform-d) δ 8.09 (ddt, J = 9.5, 8.3, 1.3 Hz, 4H), 7.63 – 7.57 (m, 1H), 7.55 – 7.49 (m, 1H), 7.51 – 7.44 (m, 4H), 7.36 – 7.26 (m, 9H), 7.29 – 7.23 (m, 5H), 7.26 – 7.21 (m, 1H), 7.23 – 7.16 (m, 3H), 7.15 – 7.08 (m, 3H), 5.72 (dd, J = 3.1, 1.9 Hz, 1H), 5.67 (dd, J = 3.3, 1.8 Hz, 1H), 5.04 (d, J = 1.9 Hz, 1H), 4.97 (d, J = 1.8 Hz, 1H), 4.91 (d, J = 11.0 Hz, 1H), 4.87 (d, J = 11.1 Hz, 1H), 4.82 (d, J = 11.0 Hz, 1H), 4.72 (d, J = 11.5 Hz, 1H), 4.69 – 4.61 (m, 4H), 4.60 (s, 0H), 4.56 – 4.44 (m, 4H), 4.11 (ddd, J = 19.4, 9.2, 3.2 Hz, 2H), 3.97 (t, J = 9.5 Hz, 1H), 3.95 – 3.88 (m, 2H), 3.88 – 3.82 (m, 1H), 3.82 – 3.77 (m, 1H), 3.79 – 3.73 (m, 2H), 3.73 – 3.67 (m, 1H). ^{13}C NMR (151 MHz, cdcl$_3$) δ 165.87, 165.68,

140.94, 138.46, 138.34, 138.03, 137.82, 136.28, 133.43, 133.41, 130.06, 130.00, 129.98, 128.69, 128.65, 128.50, 128.48, 128.45, 128.29, 128.26, 128.09, 127.94, 127.86, 127.83, 127.81, 127.76, 127.30, 98.01, 97.09, 78.75, 77.97, 77.37, 77.16, 76.95, 75.41, 75.35, 74.43, 74.08, 72.26, 71.83, 71.47, 71.04, 69.30, 69.15, 68.93, 66.35, 65.23, 62.17. m/z (HRMS$^+$) 1053.408 $[M + Na]^+$ ($C_{62}H_{62}NaO_{14}^+$ requires m/z: 1053.403).

Deprotection of **29** as described in Module G , followed by purification using preparative HPLC (Method F) afforded compound **35** as a mixture of α and β isomers (1.0 mg, 3.2 µmol, 60% over two steps)

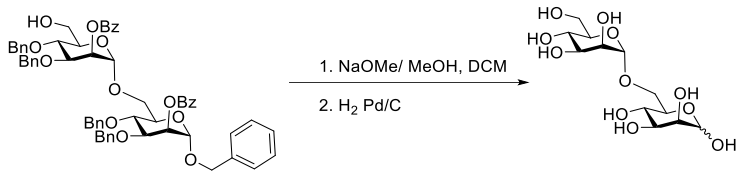

29 **35**

RP-HPLC of 35 (ELSD trace, Method E, t_R = 16.1 min)

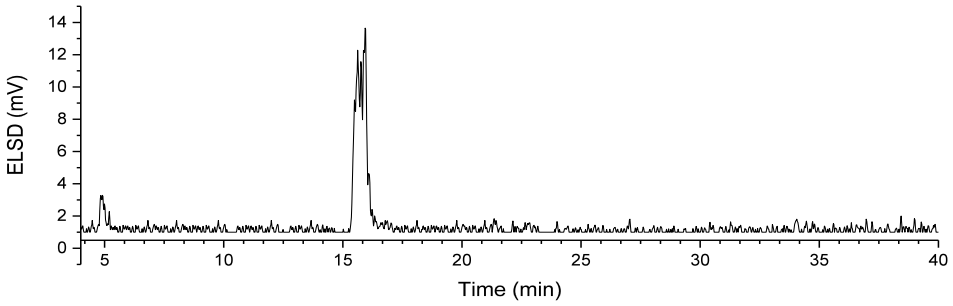

Analytical data for **35**: ^{1}H NMR (700 MHz, Deuterium Oxide) δ 8.59 (dd, *J* = 2.4, 1.2 Hz, 1H), 5.30 (d, *J* = 2.3 Hz, 1H), 5.06 – 5.02 (m, 3H), 4.13 (qt, *J* = 4.6, 2.7 Hz, 3H), 4.11 – 4.06 (m, 4H), 4.06 – 3.98 (m, 10H), 3.98 – 3.94 (m, 1H), 3.94 – 3.91 (m, 3H), 3.91 – 3.87 (m, 5H), 3.87 – 3.76 (m, 10H), 3.75 – 3.67 (m, 1H), 3.67 – 3.64 (m, 1H). ^{13}C NMR (176 MHz, D_2O) δ 99.93, 99.72, 94.31, 93.96, 74.43, 73.31, 72.84, 72.81, 71.29, 71.01, 70.79, 70.69, 70.58, 70.14, 70.06, 69.38, 69.11, 68.77, 66.90, 66.86, 66.65, 66.01, 63.37, 61.08. m/z (HRMS+) 365.1110 $[M + Na]^+$ ($C_{12}H_{22}NaO_{11}$+ requires m/z: 365.1054).

3.11.2. Synthesis of α-(1,6) linear trimannoside (30)

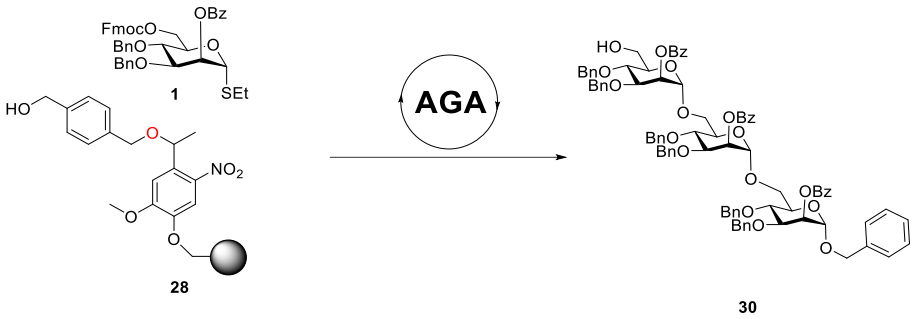

Cycles	Module	Conditions
	A: Resin Preparation for Synthesis	
3	B: Acidic Wash with TMSOTf Solution C: Thioglycoside Glycosylation D: Capping E: Fmoc Deprotection	BB1 6.5 eq, -20 °C for 5 min, 0 °C for 30 min

Cleavage from solid support as described in section 4.4.2 Photocleavage, followed by purification using preparative HPLC (**Method B**) afforded compound **30** (10.5 mg, 37% from resin **28**).

Analytical data for **30**: ^{1}H NMR (600 MHz, Chloroform-*d*) δ 8.14 (dd, *J* = 6.8, 2.9 Hz, 2H), 8.07 (ddd, *J* = 16.0, 8.2, 1.5 Hz, 4H), 7.53 – 7.42 (m, 8H), 7.34 – 7.26 (m, 8H), 7.26 – 7.21 (m, 16H), 7.21 – 7.11 (m, 11H), 5.77 (dd, *J* = 3.2, 1.9 Hz, 1H), 5.72 (t, *J* = 2.5 Hz, 1H), 5.66 (dd, *J* = 3.3, 1.9 Hz, 1H), 5.03 (dd, *J* = 19.2, 1.9 Hz, 1H), 4.96 (d, *J* = 1.8 Hz, 1H), 4.89 – 4.85 (m, 2H), 4.79 (dd, *J* = 15.9, 11.1 Hz, 2H), 4.69 (d, *J* = 10.8 Hz, 2H), 4.62 (s, 1H), 4.59 (d, *J* = 11.1 Hz, 1H), 4.52 (dd, *J* = 11.5, 9.6 Hz, 3H), 4.48 – 4.38 (m, 4H), 4.14 – 3.99 (m, 4H), 3.96 – 3.89 (m, 4H), 3.89 – 3.78 (m, 5H), 3.73 – 3.59 (m, 6H). ^{13}C NMR (151 MHz, $cdcl_3$) δ 165.89, 165.78, 165.60, 140.97, 138.60, 138.46, 138.06, 136.25, 133.40, 130.11, 130.07, 130.03, 129.99, 128.77, 128.70, 128.66, 128.64, 128.47, 128.45, 128.37, 128.30, 128.18, 128.15, 127.82, 127.79, 127.74, 127.63, 127.29, 98.33, 98.14, 97.09, 78.84, 78.37, 77.98, 77.37, 77.16, 76.95, 75.34, 74.43, 74.22, 73.99, 72.32, 71.85, 71.56, 71.43, 71.20, 71.00, 69.27, 69.21, 68.85, 68.74, 66.48, 65.99, 65.21, 62.09. m/z (HRMS^{+}) 1499.581 $[M + Na]^{+}$ ($C_{89}H_{88}NaO_{20}^{+}$ requires 1499.576).

Deprotection of **30** as described in Module G , followed by purification using preparative HPLC (Method F) afforded compound **36** as a mixture of α and β isomers (2.0 mg, 6.3 µmol, 40% over two steps)

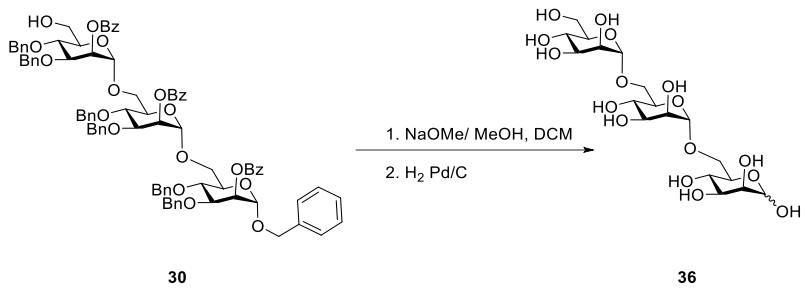

30 **36**

RP-HPLC of 36 (ELSD trace, Method E, t_R = 18.5 min)

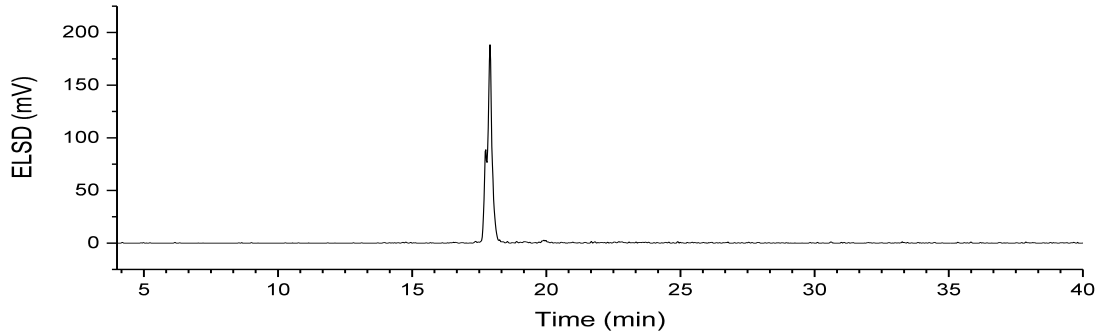

Analytical data for **36**:^{1}H NMR (700 MHz, Deuterium Oxide) δ 5.18 (s, 1H), 4.92 (s, 2H), 4.91 (s, 1H), 4.89 (s, 2H), 4.03 – 3.95 (m, 7H), 3.97 – 3.93 (m, 4H), 3.93 – 3.87 (m, 11H), 3.87 – 3.83 (m, 17H), 3.82 – 3.79 (m, 5H), 3.79 – 3.76 (m, 5H), 3.77 – 3.74 (m, 7H), 3.74 – 3.71 (m, 9H), 3.70 – 3.69 (m, 1H), 3.68 – 3.64 (m, 6H). ^{13}C NMR (176 MHz, D_2O) δ 100.01, 99.54, 72.86, 70.94, 70.71, 70.12, 69.37, 69.13, 69.02, 68.76, 66.90, 66.80, 65.82, 63.37, 61.09. m/z (HRMS^{+}) 527.1599 $[M + Na]^{+}$ ($C_{18}H_{32}NaO_{16}^{+}$ requires m/z: 527.1583).

3.11.3. Synthesis of α-(1,6) linear tetramannoside (31)

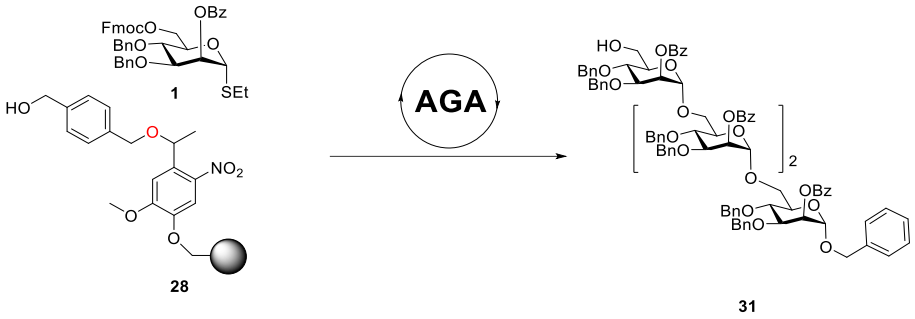

Cycles	Module	Conditions
	A: Resin Preparation for Synthesis	
4	B: Acidic Wash with TMSOTf Solution C: Thioglycoside Glycosylation D: Capping E: Fmoc Deprotection	BB1 6.5 eq, -20 °C for 5 min, 0 °C for 30 min

Cleavage from solid support as described in section 4.4.2 Photocleavage, followed by purification using preparative HPLC (**Method B**) afforded compound **31** (15.2 mg, 55% from resin **28**).

Analytical Data for **31**: ^{1}H-NMR (400 MHz, $CDCl_3$) δ 8.19-8.14 (m, 4H), 8.10 (s, 3H), 8.08 (d, *J* = 2.0 Hz, 2H), 8.06 (d, *J* = 1.5 Hz, 1H), 7.64 – 7.57 (m, 1H), 7.48 (ddd, *J* = 13.9, 6.9, 4.7 Hz, 11H), 7.33 – 7.18 (m, 28H), 7.18 – 7.09 (m, 9H), 5.82 (dd, *J* = 3.1, 1.9 Hz, 1H), 5.80 (dd, *J* = 3.1, 1.9 Hz, 1H), 5.77 – 5.70 (m, 1H), 5.68 (dd, *J* = 3.3, 1.8 Hz, 1H), 5.09 (d, *J* = 1.8 Hz, 1H), 5.06 (d, *J* = 1.7 Hz, 1H), 5.03 (d, *J* = 1.8 Hz, 1H), 4.96 (d, *J* = 1.8 Hz, 1H), 4.90 (d, *J* = 2.1 Hz, 1H), 4.87 (t, *J* = 1.8 Hz, 1H), 4.83 (s, 1H), 4.81 (s, 1H), 4.78 (s, 1H), 4.69 (dd, *J* = 14.5, 11.7 Hz, 2H), 4.63 (s, 2H), 4.59 (d, *J* = 11.1 Hz, 1H), 4.55-4.50 (m, 2H), 4.50 – 4.47 (m, 1H), 4.45 (d, *J* = 2.5 Hz, 2H), 4.42 (s, 1H), 4.41 – 4.32 (m, 1H) ppm; ^{13}C-NMR (100 MHz, $CDCl_3$) δ 137.58, 133.36, 133.30, 129.92, 129.89, 129.85, 128.66, 128.57, 128.53, 128.52, 128.38, 128.35, 128.32, 128.29, 128.22, 128.19, 128.06, 128.04, 127.72, 127.68, 127.64, 127.42, 127.38, 127.33, 127.13, 98.36, 98.18, 98.09, 96.86, 78.66, 78.27, 78.22, 75.21, 75.12, 74.21, 73.92, 73.81, 73.68, 72.10, 71.68, 71.38, 71.35, 71.19, 71.06, 70.92, 69.04, 68.96, 68.55, 68.51, 68.39, 66.22, 65.85, 65.51, 65.03, 61.83. m/z (HRMS^{+}) for $C_{116}H_{114}O_{26}Na$ $[M+Na]^{+}$ calcd. 1945.752, found: 1945.754.

Deprotection of **31** as described in Module G , followed by purification using preparative HPLC (Method F) afforded compound **37** as a mixture of α and β isomers (2.0 mg, 5.0 µmol, 40% over two steps)

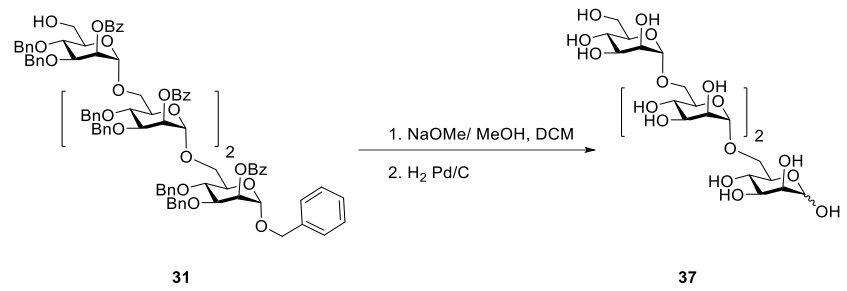

31 **37**

RP-HPLC of 37 (ELSD trace, Method E, t_R = 19.3 min)

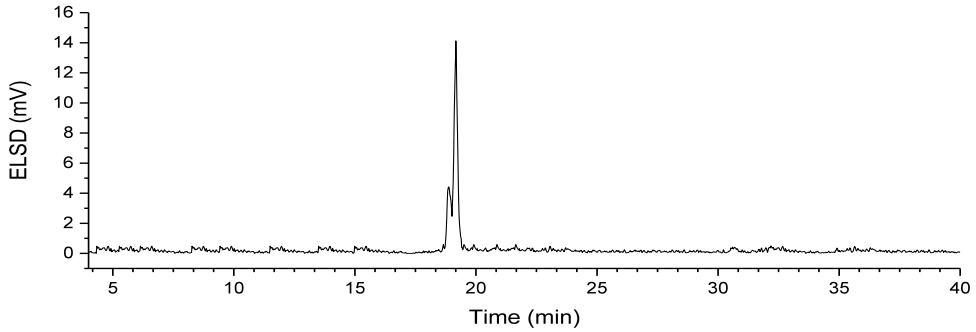

Analytical data for **37**: ^{1}H NMR (400 MHz, Deuterium Oxide) δ 5.12 (d, *J* = 1.8 Hz, 2H), 4.87 (s, 2H), 4.86 (s, 2H), 4.85 (d, *J* = 3.2 Hz, 10H), 3.99 – 3.92 (m, 13H), 3.89 (dq, *J* = 7.2, 4.7, 4.3 Hz, 9H), 3.84 (d, *J* = 1.6 Hz, 3H), 3.81 (dt, *J* = 3.7, 1.7 Hz, 8H), 3.79 – 3.76 (m, 10H), 3.76 – 3.72 (m, 7H), 3.71 – 3.67 (m, 11H), 3.65 (dd, *J* = 5.2, 1.5 Hz, 4H), 3.65 – 3.56 (m, 6H). ^{13}C NMR (101 MHz, D_2O) δ 99.49, 99.41, 99.18, 99.14, 94.10, 93.77, 74.06, 73.11, 72.62, 71.07, 70.71, 70.64, 70.58, 70.55, 70.41, 70.39, 70.37, 69.86, 69.81, 66.63, 66.53, 66.50, 66.46, 66.33, 65.62, 65.48, 65.38, 60.83. m/z (HRMS^{+}) 689.2140 $[M+Na]^{+}$ ($C_{24}H_{42}NaO_{21}$+ requires m/z: 689.2111).

3.11.4. Synthesis of α-(1,6) linear pentamannoside (32)

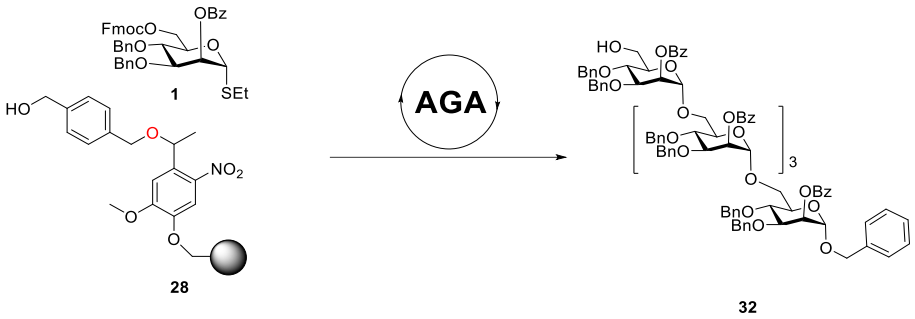

Cycles	Module	Conditions
	A: Resin Preparation for Synthesis	
5	B: Acidic Wash with TMSOTf Solution C: Thioglycoside Glycosylation D: Capping E: Fmoc Deprotection	BB1 6.5 eq, -20 °C for 5 min, 0 °C for 30 min

Cleavage from solid support as described in section 4.4.2 Photocleavage, followed by purification using preparative HPLC (**Method B**) afforded compound **32** (12 mg, 35% from resin **28**).

Analytical data for **32**: ^{1}H NMR (600 MHz, Chloroform-*d*) δ 8.14 (q, *J* = 5.0, 4.5 Hz, 5H), 8.11 – 8.05 (m, 5H), 7.48 (q, *J* = 3.2, 2.7 Hz, 11H), 7.44 (t, *J* = 8.5 Hz, 5H), 7.34 – 7.23 (m, 10H), 7.25 – 7.03 (m, 43H), 5.82 – 5.72 (m, 4H), 5.08 – 5.00 (m, 4H), 4.91 – 4.74 (m, 11H), 4.68 – 4.60 (m, 4H), 4.43 (dddd, *J* = 46.7, 42.8, 23.5, 11.7 Hz, 13H), 4.16 (d, *J* = 3.9 Hz, 2H), 4.13 – 3.77 (m, 14H), 3.72 (ddd, *J* = 34.6, 14.2, 7.5 Hz, 4H), 3.61 (t, *J* = 10.1 Hz, 2H), 3.49 (dd, *J* = 11.3, 5.8 Hz, 2H). ^{13}C NMR (151 MHz, cdcl$_3$) δ 165.69, 138.64, 133.41, 130.02, 128.78, 128.62, 128.47, 128.43, 128.38, 128.30, 127.83, 127.51, 127.36, 127.26, 98.35, 78.83, 78.43, 77.37, 77.16, 76.95, 75.19, 74.42, 74.15, 73.93, 73.49, 71.85, 71.54, 71.30, 71.17, 70.20, 69.22, 68.62, 65.95, 65.17. m/z (HRMS$^{+)}$ 2392.930 $[M + Na]^+$ ($C_{143}H_{140}NaO_{32}^+$ requires 2392.925).

Deprotection of **32** as described in Module G , followed by purification using preparative HPLC (Method F) afforded compound **38** as a mixture of α and β isomers (2.4 mg, 2.9 µmol, 60% over two steps).

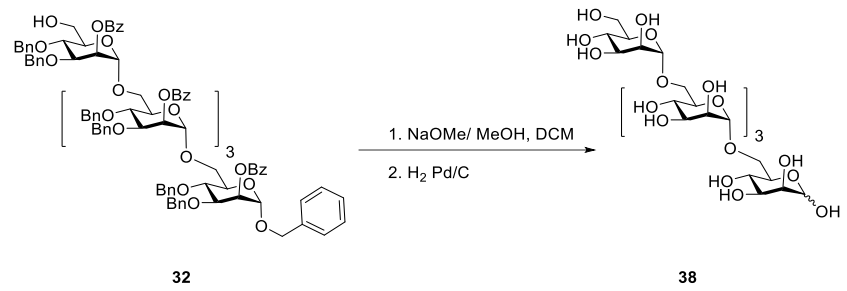

32 **38**

RP-HPLC of 38 (ELSD trace, Method E, t_R = 19.8 min)

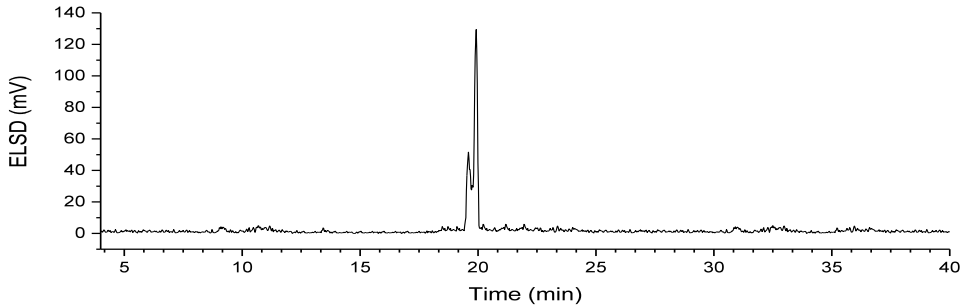

Analytical data for **38**: ^{1}H NMR (600 MHz, Deuterium Oxide) δ 5.18 (s, 1H), 4.94 – 4.89 (m, 8H), 4.01 (q, *J* = 4.2, 3.3 Hz, 8H), 3.96 (dq, *J* = 10.2, 6.4, 5.5 Hz, 11H), 3.92 (d, *J* = 2.0 Hz, 1H), 3.90 (d, *J* = 1.9 Hz, 1H), 3.91 – 3.82 (m, 16H), 3.81 (s, 2H), 3.79 (d, *J* = 5.8 Hz, 3H), 3.76 (d, *J* = 7.9 Hz, 3H), 3.73 (d, *J* = 10.0 Hz, 7H), 3.67 (s, 1H). ^{13}C NMR (151 MHz, d_2o) δ 99.51, 99.45, 99.26, 99.23, 99.20, 94.12, 93.78, 81.66, 74.09, 73.13, 72.64, 71.10, 70.74, 70.72, 70.68, 70.64, 70.62, 70.60, 70.57, 70.46, 70.44, 70.42, 69.90, 69.86, 69.83, 69.80, 66.67, 66.59, 66.55, 66.54, 66.52, 66.39, 65.67, 65.57, 65.53, 65.45, 60.86. m/z (HRMS^{+}) 851.2644 $[M + Na]^{+}$ ($C_{30}H_{52}NaO_{26}^{+}$ requires m/z: 851.2639).

3.11.5. Synthesis of α-(1,6) linear hexamannoside (33)

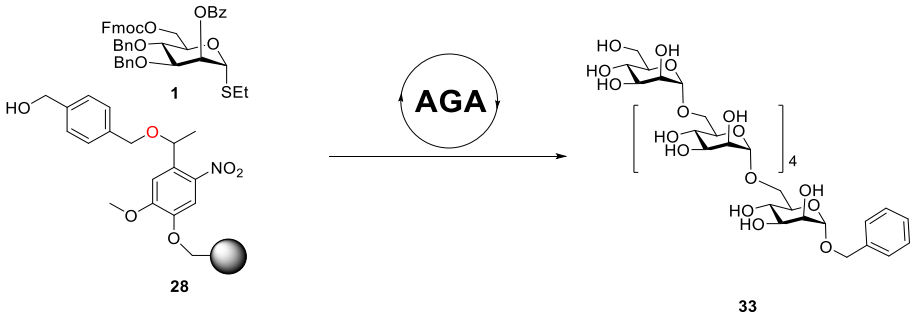

Cycles	Module	Conditions
	A: Resin Preparation for Synthesis	
6	B: Acidic Wash with TMSOTf Solution C: Thioglycoside Glycosylation D: Capping E: Fmoc Deprotection	BB1 6.5 eq, -20 °C for 5 min, 0 °C for 30 min

Cleavage from solid support as described in section 4.4.2 Photocleavage, followed by purification using preparative HPLC (**Method B**) afforded compound **33** (15 mg, 38% from resin **28**).

Analytical data for **33**: ^{1}H NMR (600 MHz, Chloroform-*d*) δ 8.18 – 8.13 (m, 8H), 8.08 (dd, *J* = 8.0, 5.8 Hz, 5H), 7.58 (t, *J* = 7.4 Hz, 1H), 7.53 – 7.42 (m, 19H), 7.33 – 7.27 (m, 10H), 7.26 – 7.22 (m, 6H), 7.22 – 7.14 (m, 27H), 7.13 – 7.08 (m, 11H), 5.84 – 5.74 (m, 6H), 5.67 (t, *J* = 2.6 Hz, 1H), 5.10 – 5.01 (m, 6H), 4.97 – 4.94 (m, 1H), 4.92 – 4.84 (m, 7H), 4.84 – 4.75 (m, 7H), 4.69 (dd, *J* = 30.6, 11.6 Hz, 3H), 4.64 – 4.57 (m, 4H), 4.57 – 4.32 (m, 15H), 4.16 – 3.85 (m, 18H), 3.85 – 3.68 (m, 7H), 3.68 – 3.56 (m, 6H), 3.56 – 3.51 (m, 2H), 3.46 (dd, *J* = 11.1, 5.4 Hz, 2H). ^{13}C NMR (151 MHz, cdcl$_3$) δ 165.87, 165.76, 165.68, 165.66, 165.56, 140.98, 138.67, 138.64, 138.61, 138.44, 138.35, 138.06, 137.77, 137.73, 137.72, 137.69, 137.67, 136.17, 133.44, 133.40, 130.13, 130.11, 130.04, 130.01, 129.97, 128.78, 128.69, 128.63, 128.49, 128.46, 128.43, 128.38, 128.37, 128.31, 128.29, 128.27, 128.18, 128.15, 127.83, 127.81, 127.79, 127.77, 127.75, 127.57, 127.52, 127.49, 127.48, 127.40, 127.32, 127.26, 127.24, 98.63, 98.61, 98.54, 98.33, 98.28, 97.07, 78.81, 78.41, 78.38, 78.34, 78.31, 77.83, 77.37, 77.16, 76.95, 75.32, 75.25, 75.23, 75.16, 75.14, 74.36, 74.10, 73.98, 73.91, 73.85, 72.25, 71.83, 71.53, 71.50, 71.46, 71.44, 71.34, 71.25, 71.17, 71.13, 71.07, 69.20, 69.15, 68.72, 68.61, 68.55, 68.53, 66.28, 65.99, 65.88, 65.60, 65.13, 61.97. m/z (HRMS^{+}) 2839.092[M + Na]$^{+}$ ($C_{170}H_{166}NaO_{38}^{+}$ requires 2839.098).

Deprotection of **33** as described in Module G , followed by purification using preparative HPLC (Method F) afforded compound **39** as a mixture of α and β isomers (3 mg, 3.6 µmol, 58% over two steps).

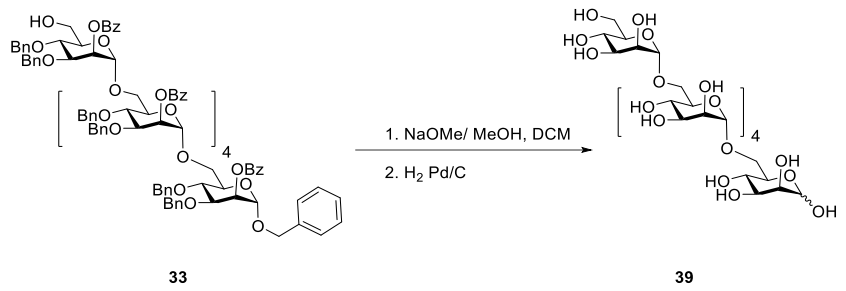

33 **39**

RP-HPLC of 39 (ELSD trace, Method E t_R = 20.5 min)

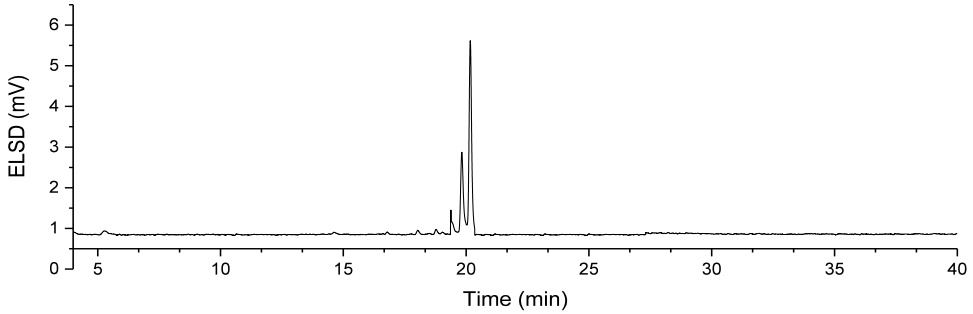

Analytical data for **39**: ^{1}H NMR (700 MHz, Deuterium Oxide) δ 5.31 (s, 1H), 5.07 – 5.02 (m, 10H), 4.15 – 4.12 (m, 10H), 4.12 – 4.05 (m, 13H), 4.05 – 4.00 (m, 3H), 4.00 – 3.95 (m, 21H), 3.95 – 3.90 (m, 6H), 3.92 – 3.88 (m, 3H), 3.90 – 3.84 (m, 10H), 3.83 – 3.77 (m, 4H). ^{13}C NMR (176 MHz, D_2O) δ 99.73, 99.67, 99.46, 94.32, 93.98, 74.34, 73.35, 72.86, 71.31, 70.97, 70.92, 70.90, 70.86, 70.71, 70.64, 70.13, 70.09, 70.07, 69.36, 66.92, 66.86, 66.80, 66.65, 65.95, 65.86, 65.81, 65.75, 65.73, 63.37, 61.09, 55.59.m/z (HRMS^{+}) 1013.318 $[M + Na]^{+}$ ($C_{36}H_{62}NaO_{31}$+ requires m/z: 1013.316).

3.11.6. Synthesis of α-(1,6) linear heptamannoside (34)

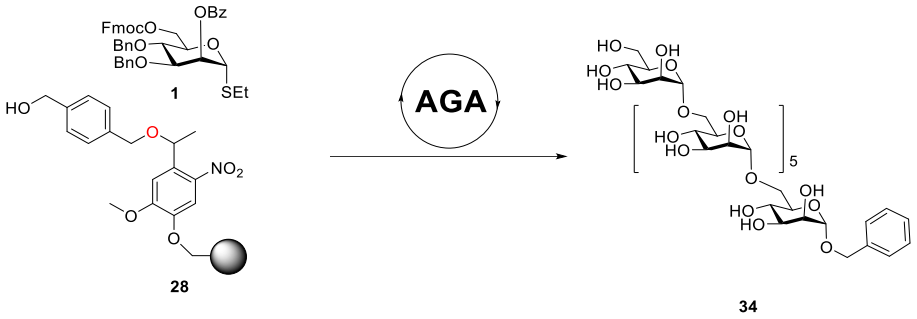

Cycles	Module	Conditions
	A: Resin Preparation for Synthesis	
7	B: Acidic Wash with TMSOTf Solution C: Thioglycoside Glycosylation D: Capping E: Fmoc Deprotection	BB1 6.5 eq, -20 °C for 5 min, 0 °C for 30 min

Cleavage from solid support as described in section 4.4.2 Photocleavage, followed by purification using preparative HPLC (**Method B**) afforded compound **34** (29 mg, 63% from resin **28**).

Analytical data for **34**: ^{1}H NMR (600 MHz, Chloroform-*d*) δ 8.16 (ddt, *J* = 7.9, 4.9, 3.0 Hz, 9H), 8.08 (ddt, *J* = 8.0, 6.0, 2.5 Hz, 4H), 7.62 – 7.55 (m, 1H), 7.48 (dqd, *J* = 15.3, 7.6, 5.0 Hz, 19H), 7.34 – 7.03 (m, 55H), 5.82 (dq, *J* = 7.5, 2.5 Hz, 4H), 5.80 – 5.77 (m, 1H), 5.76 (t, *J* = 2.5 Hz, 1H), 5.67 (dd, *J* = 3.3, 1.8 Hz, 1H), 5.10 – 5.01 (m, 6H), 4.95 (d, *J* = 1.8 Hz, 1H), 4.92 – 4.69 (m, 15H), 4.69 – 4.57 (m, 4H), 4.57 – 4.31 (m, 15H), 4.16 – 3.86 (m, 17H), 3.85 – 3.70 (m, 5H), 3.73 – 3.62 (m, 5H), 3.64 – 3.50 (m, 5H), 3.46 (td, *J* = 11.8, 1.9 Hz, 3H). ^{13}C NMR (151 MHz, cdcl$_3$) δ 165.87, 165.76, 165.68, 165.56, 140.98, 138.66, 138.61, 138.59, 138.45, 138.35, 138.06, 137.77, 137.74, 137.71, 137.69, 137.66, 136.17, 133.44, 133.39, 130.13, 130.11, 130.05, 130.00, 129.97, 128.79, 128.77, 128.69, 128.63, 128.62, 128.49, 128.47, 128.43, 128.38, 128.32, 128.29, 128.26, 128.18, 128.15, 127.83, 127.81, 127.79, 127.77, 127.75, 127.58, 127.51, 127.49, 127.43, 127.38, 127.29, 127.26, 127.24, 98.64, 98.55, 98.33, 98.29, 97.07, 78.81, 78.40, 78.38, 78.35, 78.31, 77.83, 77.37, 77.16, 76.95, 75.32, 75.26, 75.23, 75.17, 75.13, 74.36, 74.10, 73.98, 73.89, 73.85, 72.25, 71.83, 71.53, 71.49, 71.45, 71.34, 71.24, 71.18, 71.13, 71.07, 69.20, 69.15, 68.71, 68.61, 68.52, 66.28, 65.88, 65.59, 65.13, 61.97. m/z (HRMS$^{+)}$ 3286.275 $[M + Na]^+$ (: $C_{197}H_{192}NaO_{44}$+ requires 3286.274).

Deprotection of **34** as described in Module G , followed by purification using preparative HPLC (Method F) afforded compound **40** as a mixture of α and β isomers (2.8 mg, 3.3 µmol, 50% over two steps).

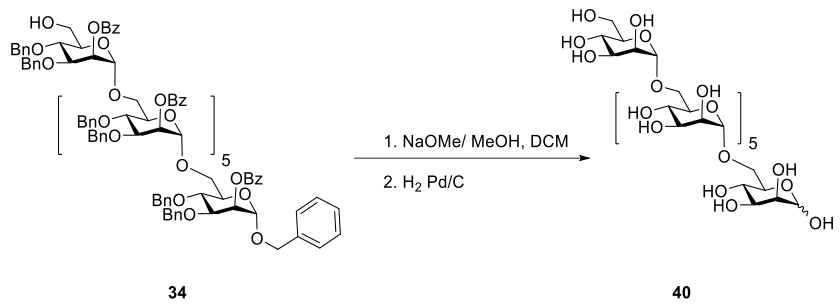

34 40

RP-HPLC of 40 (ELSD trace, Method E t_R = 21.6 min)

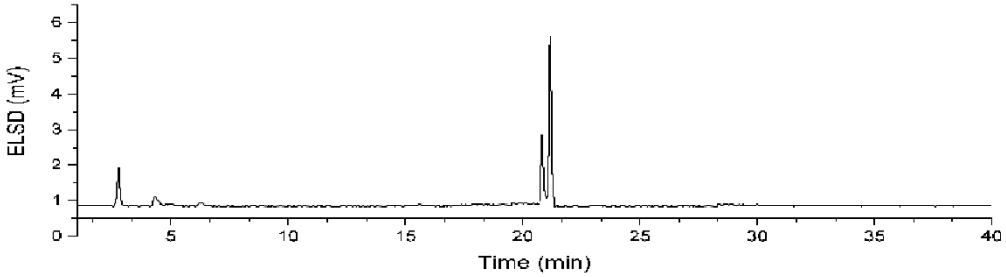

Analytical data for **40**: ^{1}H NMR (700 MHz, Deuterium Oxide) δ 5.20 – 5.14 (m, 2H), 4.94 – 4.90 (m, 14H), 4.03 – 3.99 (m, 21H), 4.00 – 3.93 (m, 28H), 3.93 – 3.84 (m, 35H), 3.85 – 3.74 (m, 27H), 3.73 (t, *J* = 10.0 Hz, 21H), 3.69 – 3.63 (m, 6H). ^{13}C NMR (176 MHz, D_2O) δ 99.57, 99.50, 99.29, 99.27, 99.25, 94.18, 93.84, 74.15, 73.19, 72.69, 71.15, 70.80, 70.74, 70.69, 70.66, 70.51, 70.48, 69.95, 69.91, 69.88, 69.85, 66.72, 66.63, 66.60, 66.58, 66.56, 66.43, 65.72, 65.61, 65.58, 65.49, 60.91. m/z m/z (HRMS$^+$) 1175,365 $[M + Na]^+$ ($C_{42}H_{72}NaO_{36}^+$ requires 1175,369).

3.12. AGA synthesis of glucosides

3.12.1. Synthesis of β-(1,3) linear heptaglucoside (44)

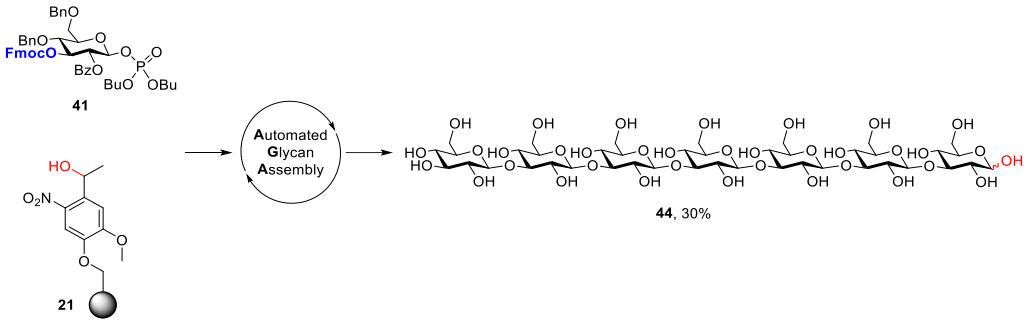

Automation sequence:

Cycles	Module	Conditions
	A: Resin Preparation for Synthesis	
7	B: Acidic Wash with TMSOTf Solution C: Phosphate Glycosylation D: Capping E: Fmoc Deprotection	BB**41** 4 eq, -30 °C for 10 min, -10 °C for 40 min

Post-Automation: **Module G – Methanolysis**, then **Photocleavage**, then **Module H – Hydrogenation**. The crude unprotected oligosaccharide was purified using reverse-phase preparative HPLC (**Method D**) to afford compound **44** (5.9 mg, 30%).

Analytical Data for **44**: ^{1}H-NMR (600 MHz, D_2O, both isomers) δ 5.10 (d, *J* = 3.7 Hz, 1H), 4.67 – 4.65 (m, 5H), 4.63 – 4.60 (m, 3H), 4.54 (d, *J* = 8.0 Hz, 1H), 3.80 (d, *J* = 2.0 Hz, 6H), 3.79 – 3.76 (m, 7H), 3.76 – 3.71 (m, 2H), 3.70 – 3.67 (m, 1H), 3.67 – 3.64 (m, 9H), 3.63 – 3.56 (m, 9H), 3.44 – 3.40 (m, 8H), 3.40 – 3.34 (m, 14H), 3.32 – 3.25 (m, 3H), 3.22 (dd, *J* = 9.4, 7.9 Hz, 2H) ppm; ^{13}C-NMR (150 MHz, D_2O) δ 102.74, 102.57, 102.46, 102.44, 95.61, 91.95, 84.41, 84.16, 83.99, 82.18, 75.93, 75.55, 75.51, 75.48, 73.77, 73.38, 73.23, 73.17, 71.16, 70.99, 69.50, 68.05, 68.01, 60.60, 60.46 ppm. m/z (HRMS+) for $C_{42}H_{72}O_{36}Na$ $[M+Na]^+$ calcd. 1175.3695, found: 1175.3660.

RP-HPLC of **44** (ELSD trace, **Method C**, t_R= 31.2 min)

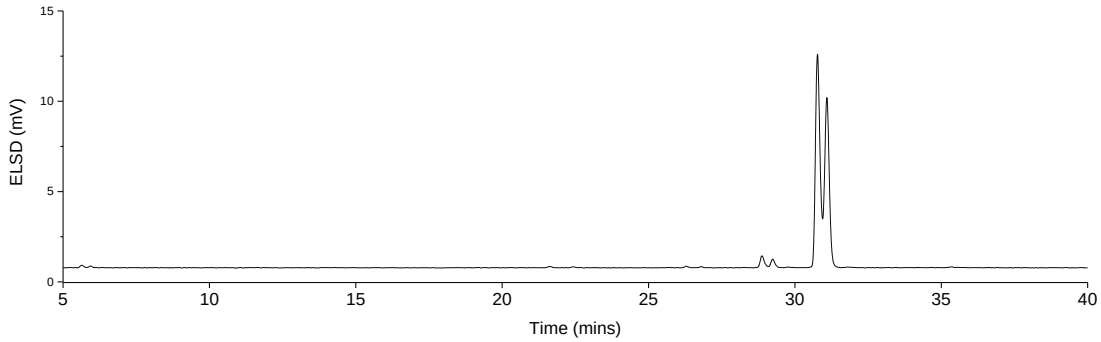

3.12.2. Synthesis of mix β-(1,3) and β-(1,4) pentaglucoside (45)

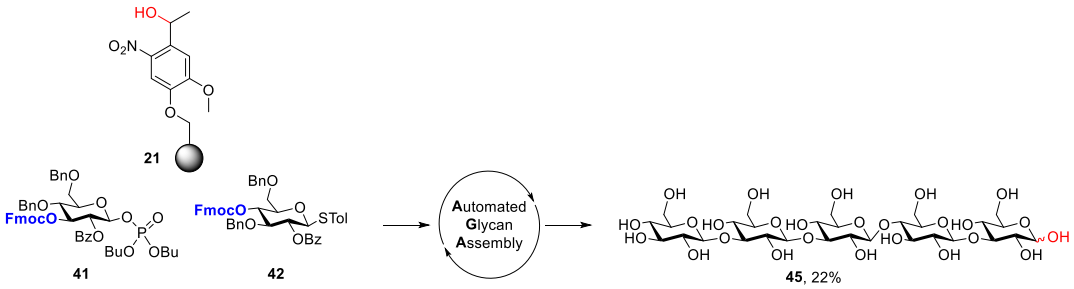

Automation sequence:

Cycles	Module	Conditions
	A: Resin Preparation for Synthesis	
	B: Acidic Wash with TMSOTf Solution	
	C: Phosphate Glycosylation	BB**41** 4 eq, -30 °C for 10 min, -10 °C for 40 min
	D: Capping	
	E: Fmoc Deprotection	
	B: Acidic Wash with TMSOTf Solution	
	C: 2x Thioglycoside Glycosylation	BB**42** 6.5 eq, -20 °C for 5 min, 0 °C for 20 min
	D: Capping	
	E: Fmoc Deprotection	
	B: Acidic Wash with TMSOTf Solution	
3	C: 2x Phosphate Glycosylation	BB**41** 4 eq, -30 °C for 10 min, -10 °C for 40 min
	D: Capping	
	E: Fmoc Deprotection	

Post-Automation: **Module G – Methanolysis**, then **Photocleavage**, then **Module H – Hydrogenation**. The crude unprotected oligosaccharide was purified using reverse-phase preparative HPLC (**Method D**) to afford compound **45** (2.6 mg, 22%).

Analytical Data for **45**: ^{1}H-NMR (700 MHz, D_2O, both isomers) δ 5.16 (d, *J* = 3.7 Hz, 1H), 4.73 – 4.65 (m, 2H), 4.59 (dd, *J* = 8.1, 1.6 Hz, 1H), 4.46 (d, *J* = 8.0 Hz, 2H), 3.92 (d, *J* = 2.2 Hz, 1H), 3.91 – 3.89 (m, 2H), 3.86 – 3.85 (m, 4H), 3.85 – 3.83 (m, 6H), 3.82 – 3.77 (m, 1H), 3.76 – 3.72 (m, 2H), 3.69 (dd, *J* = 8.3, 3.2 Hz, 2H), 3.65 (ddd, *J* = 16.3, 9.8, 4.0 Hz, 4H), 3.59 (dd, *J* = 6.5, 2.7 Hz, 4H), 3.57 – 3.53 (m, 4H), 3.49 – 3.45 (m, 3H), 3.45 – 3.42 (m, 8H), 3.40 (dd, *J* = 9.1, 6.9 Hz, 1H), 3.37 (d, *J* = 8.2 Hz, 1H), 3.34 (s, 1H), 3.30 – 3.25 (m, 2H) ppm; ^{13}C-NMR (176 MHz, D_2O) δ 102.81, 102.68, 102.59, 102.48, 102.35, 95.69, 84.50, 84.22, 83.77, 82.24, 78.54, 76.01, 75.61, 75.57, 75.56, 74.85, 74.15, 74.13, 73.82, 73.46, 73.23, 73.05, 71.04, 69.58, 68.13, 68.08, 67.97, 60.70, 60.68, 60.56, 60.00 ppm. m/z (HRMS+) for $C_{30}H_{52}O_{26}Na$ $[M+Na]^+$ calcd. 851.2639, found: 851.2628.

RP-HPLC of **45** (ELSD trace, **Method C**, t_R= 25.8 min)

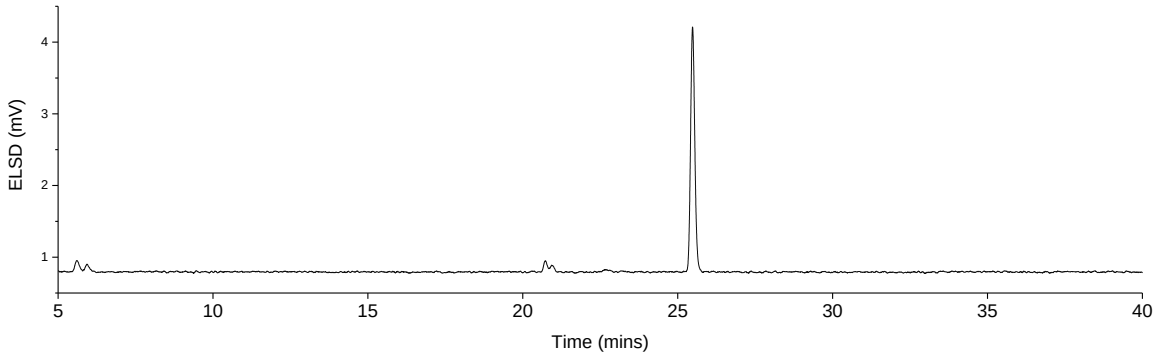

3.12.3. Synthesis of mix β-(1,3) and β-(1,4) octaglucoside (46)

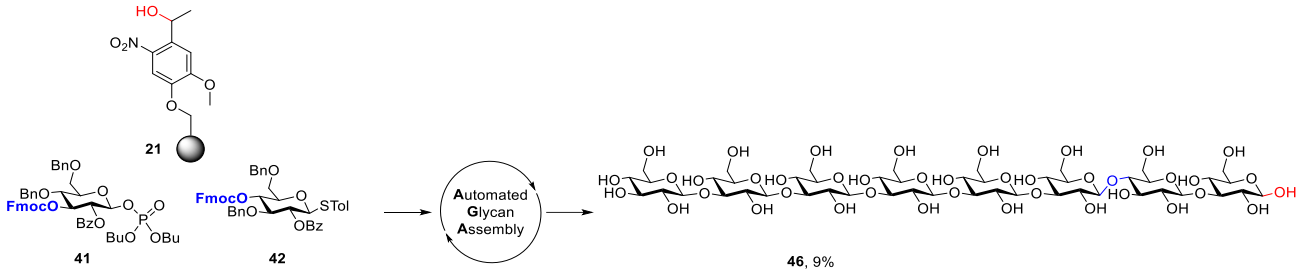

Automation sequence:

Cycles	Module	Conditions
	A: Resin Preparation for Synthesis	
	B: Acidic Wash with TMSOTf Solution C: Phosphate Glycosylation D: Capping E: Fmoc Deprotection	BB**41** 4 eq, -30 °C for 10 min, -10 °C for 40 min
	B: Acidic Wash with TMSOTf Solution C: 2x Thioglycoside Glycosylation D: Capping E: Fmoc Deprotection	BB**42** 6.5 eq, -20 °C for 5 min, 0 °C for 20 min
6	B: Acidic Wash with TMSOTf Solution C: 2x Phosphate Glycosylation D: Capping E: Fmoc Deprotection	BB**41** 4 eq, -30 °C for 10 min, -10 °C for 40 min

Post-Automation: **Module G – Methanolysis**, then **Photocleavage**, then **Module H – Hydrogenation**. The crude unprotected oligosaccharide was purified using reverse-phase preparative HPLC (**Method D**) to afford compound **46**

Analytical Data for **46**: ^{1}H-NMR (600 MHz, D_2O, both isomers) δ 5.11 (d, *J* = 3.7 Hz, 1H), 4.63 – 4.67 (m, 6H), 4.65 – 4.60 (m, 3H), 4.54 (d, *J* = 8.0 Hz, 1H), 3.80 (d, *J* = 2.0 Hz, 6H), 3.79 – 3.76 (m, 7H), 3.77 – 3.72 (m, 2H), 3.67 – 3.64 (m, 9H), 3.63 – 3.56 (m, 9H), 3.44 – 3.40 (m, 9H), 3.40 – 3.34 (m, 16H), 3.32 – 3.25 (m, 3H), 3.22 (m, 2H) ppm; ^{13}C-NMR (150 MHz, D_2O) δ 102.74, 102.57, 102.46, 102.44, 95.61, 91.95, 84.41, 84, 12, 84.16, 83.99, 82.18, 75.93, 75.55, 75.53, 75.48, 75,45, 73.80, 73.38, 73.23, 73.17, 71.16, 70.99, 69.50, 68.05, 68,03, 68.01, 60.60, 60.45 ppm. m/z (HRMS+) for $C_{48}H_{82}O_{41}Na$ $[M+Na]^+$ calcd. 1337.422, found: 1337.421.

RP-HPLC of **46** (ELSD trace, **Method C**, t_R= 36.6)

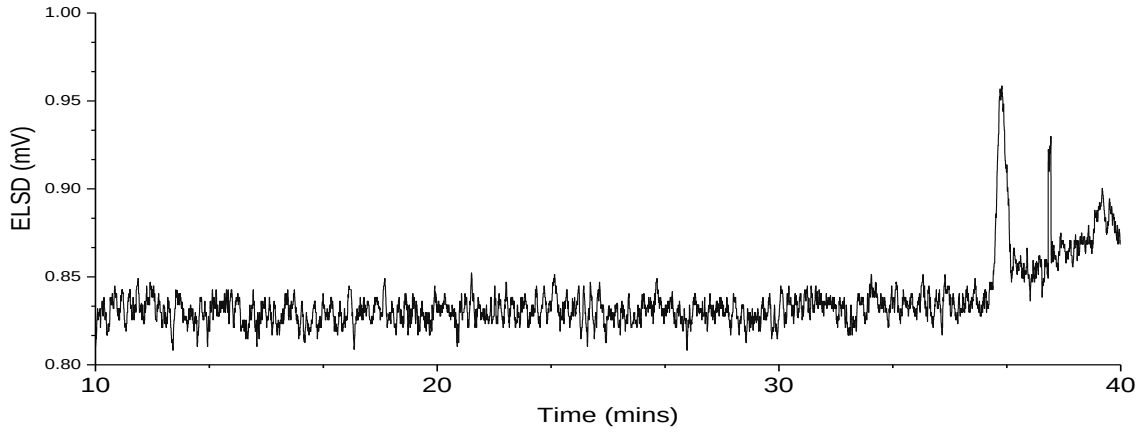

3.12.4. Synthesis of mix β-(1,3) and β-(1,4) decaglucoside (47)

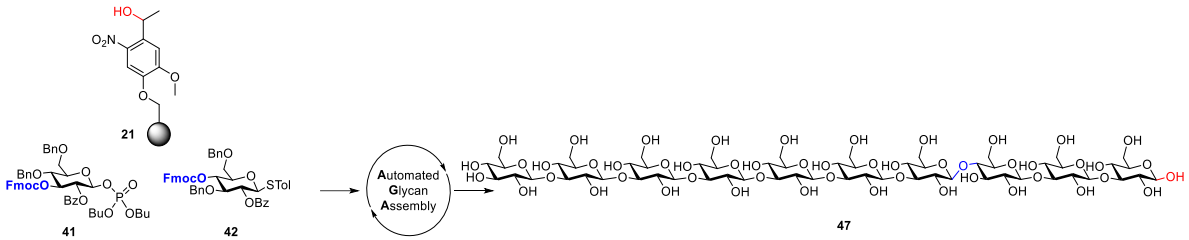

Automation sequence:

Cycles	Module	Conditions
	A: Resin Preparation for Synthesis	
2	B: Acidic Wash with TMSOTf Solution C: Phosphate Glycosylation D: Capping E: Fmoc Deprotection	BB**41** 4 eq, -30 °C for 10 min, -10 °C for 40 min
	B: Acidic Wash with TMSOTf Solution C: 2x Thioglycoside Glycosylation D: Capping E: Fmoc Deprotection	BB**42** 6.5 eq, -20 °C for 5 min, 0 °C for 20 min
7	B: Acidic Wash with TMSOTf Solution C: 2x Phosphate Glycosylation D: Capping E: Fmoc Deprotection	BB**41** 4 eq, -30 °C for 10 min, -10 °C for 40 min

Post-Automation: **Module G – Methanolysis**, then **Photocleavage**, then **Module H – Hydrogenation**. The crude unprotected oligosaccharide was purified using reverse-phase preparative HPLC (**Method D**) to afford compound **47**

Analytical Data for **47**: ^{1}H-NMR (600 MHz, D_2O, both isomers) δ 5.11 (d, *J* = 3.7 Hz, 1H), 4.63 – 4.67 (m, 6H), 4.65 – 4.60 (m, 3H), 4.54 (d, *J* = 8.0 Hz, 1H), 3.80 (d, *J* = 2.0 Hz, 6H), 3.79 – 3.76 (m, 9H), 3.76 – 3.73 (m, 2H), 3.68 – 3.63 (m, 12H), 3.62 – 3.56 (m, 11H), 3.45 – 3.40 (m, 11H), 3.40 – 3.33 (m, 20H), 3.32 – 3.25 (m, 1H), 3.22 (m, 2H) ppm; ppm. m/z (HRMS+) for $C_{60}H_{102}NaO_{51}^{+}$ $[M+Na]^{+}$ calcd. 1661.528, found: 1661.533.

Crude RP-HPLC of **47** (ELSD trace, **Method C**, t_R= 38.6 min)

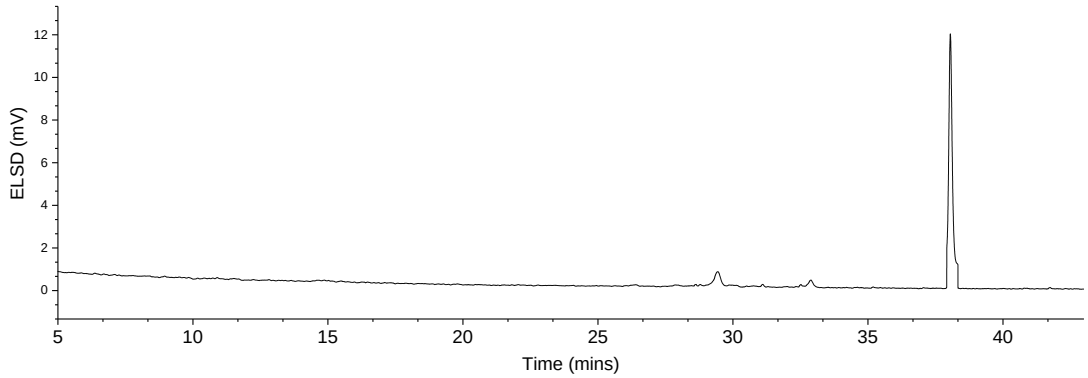

3.12.5. Synthesis of mix β-(1,3) and β-(1,6) heptaglucoside (48)

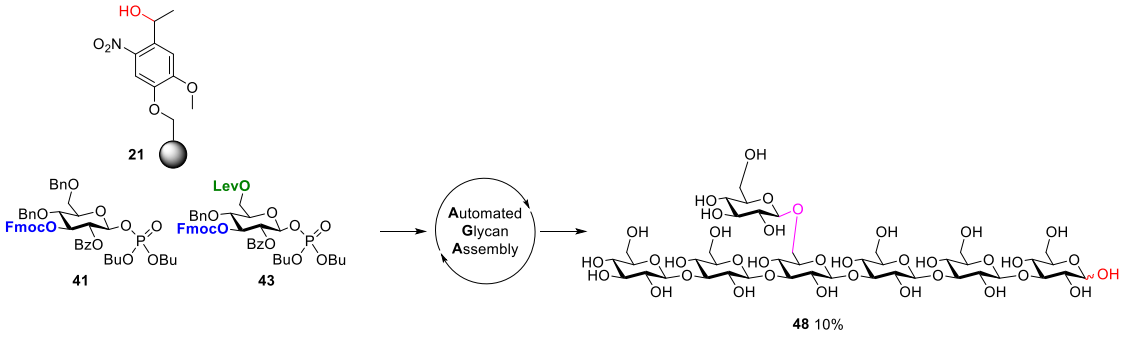

Automation sequence:

Cycles	Module	Conditions
	A: Resin Preparation for Synthesis	
3	B: Acidic Wash with TMSOTf Solution C: Phosphate Glycosylation D: Capping E: Fmoc Deprotection	BB**41** 4 eq, -30 °C for 10 min, -10 °C for 40 min
	B: Acidic Wash with TMSOTf Solution C: 2x Phosphate Glycosylation D: Capping E: Fmoc Deprotection	BB**43** 4 eq, -30 °C for 10 min, -10 °C for 40 min
2	B: Acidic Wash with TMSOTf Solution C: 2x Phosphate Glycosylation D: Capping E: Fmoc Deprotection	BB**41** 4 eq, -30 °C for 10 min, -10 °C for 40 min
	D: Capping F– 2x Lev Deprotection	
	B: Acidic Wash with TMSOTf Solution C: 2x Phosphate Glycosylation D: Capping E: Fmoc Deprotection	BB**41** 4 eq, -30 °C for 10 min, -10 °C for 40 min

Post-Automation: **Module G – Methanolysis**, then **Photocleavage**, then **Module H – Hydrogenation**. The crude unprotected oligosaccharide was purified using reverse-phase preparative HPLC (**Method D**) to afford compound.

Analytical Data for **48**: ^{1}H-NMR (700 MHz, D_2O, both isomers) δ 5.14 (d, *J* = 3.7 Hz, 1H), 4.75 – 4.68 (m, 6H), 4.57 (d, *J* = 8.1 Hz, 1H), 4.49 (d, *J* = 8.0 Hz, 2H), 4.45 (d, *J* = 7.9 Hz, 2H), 4.14 (m, 5H), 3.86 – 3.82 (m, 12H), 3.81 – 3.76 (m, 2H), 3.75 – 3.68 (m, 7H), 3.67 – 3.62 (m, 11H), 3.54 – 3.38 (m, 26H), 3.35 – 3.30 (m, 4H), 3.28 (t, *J* = 8.6 Hz, 2H), 3.24 (t, *J* = 8.6 Hz,

4H) ppm; ^{13}C-NMR (176 MHz, D_2O) δ 102.93, 102.81, 102.64, 102.55, 102.52, 95.69, 92.03, 84.49, 84.24, 84.14, 83.90, 76.11, 75.94, 75.62, 75.58, 75.53, 74.93, 74.58, 73.84, 73.46, 73.33 73.20, 73.18, 73.07, 71.46, 71.07, 69.64, 69.55, 69.42, 68.62, 68.15, 68.13, 68.09, 60.54 ppm. m/z (HRMS+) for $C_{42}H_{72}NaO_{36}$ $[M+Na]^+$ calcd. 1175.991, found: 1175.997.

RP-HPLC of **48** (ELSD trace, **Method C**, t_R= 34 min)

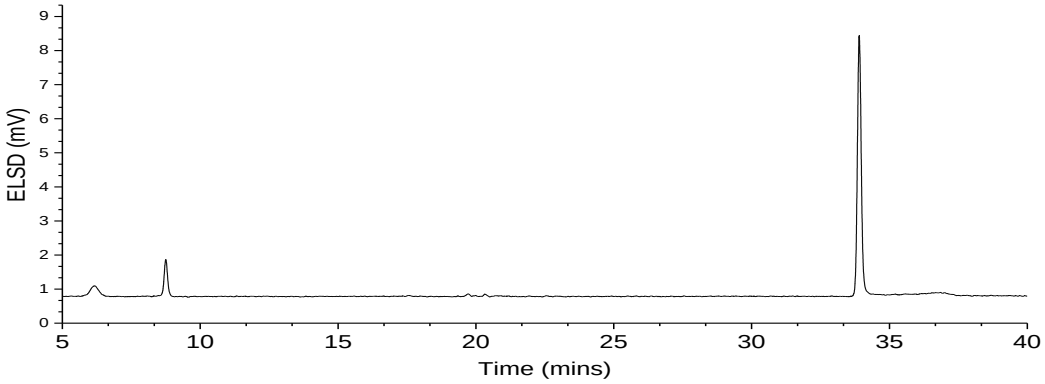

3.12.6. Synthesis of mix β-(1,3) and β-(1,6) octaglucoside (49)

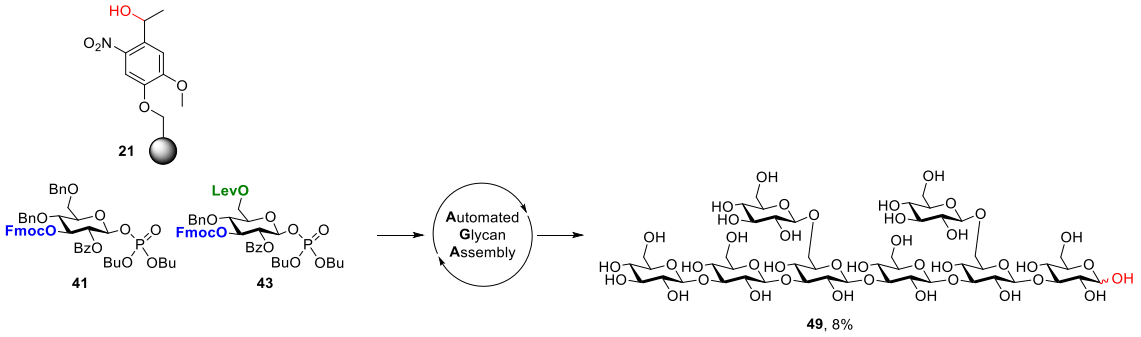

Automation sequence:

Cycles	Module	Conditions
	A: Resin Preparation for Synthesis	
2	B: Acidic Wash with TMSOTf Solution	
	C: 2x Phosphate Glycosylation	BB**41** 4 eq, -30 °C for 10 min, -10 °C for 40 min
	D: Capping	
	E: Fmoc Deprotection	
	B: Acidic Wash with TMSOTf Solution	
	C: 2x Phosphate Glycosylation	BB**43** 4 eq, -30 °C for 10 min, -10 °C for 40 min
	D: Capping	
	E: Fmoc Deprotection	
	B: Acidic Wash with TMSOTf Solution	
	C: 2x Phosphate Glycosylation	BB**41** 4 eq, -30 °C for 10 min, -10 °C for 40 min
	D: Capping	
	E: Fmoc Deprotection	
	F– 2x Lev Deprotection	
	C: 6x Phosphate Glycosylation	BB**41** 4 eq, -30 °C for 10 min, -10 °C for 40 min

Post-Automation: **Module G – Methanolysis**, then **Photocleavage**, then **Module H – Hydrogenation**. The crude unprotected oligosaccharide was purified using reverse-phase preparative HPLC (**Method D**) to afford compound **49** (1.7 mg, 8% from resin **5**).

Analytical Data for **49**: ^{1}H-NMR (700 MHz, D_2O, both isomers) δ 5.15 (d, *J* = 3.7 Hz, 1H), 4.75 – 4.64 (m, 6H), 4.59 (d, *J* = 8.1 Hz, 1H), 4.47 (d, *J* = 8.0 Hz, 2H), 4.43 (d, *J* = 7.9 Hz, 2H), 4.14 (dd, *J* = 18.1, 11.5 Hz, 5H), 3.86 – 3.82 (m, 14H), 3.81 – 3.76 (m, 2H), 3.75 – 3.68 (m, 9H), 3.68 – 3.60 (m, 13H), 3.55 – 3.36 (m, 32H), 3.35 – 3.31 (m, 4H), 3.28 (t, *J* = 8.7 Hz, 2H), 3.24 (t, *J* = 8.6 Hz, 4H) ppm; ^{13}C-NMR (176 MHz, D_2O) δ 102.95, 102.90, 102.81, 102.64, 102.55, 102.52, 95.69, 92.03, 84.69, 84.49, 84.24, 84.14, 84.10, 83.90, 76.01, 75.93, 75.66,

75.64, 75.62, 75.58, 75.56, 75.52, 74.93, 74.58, 73.84, 73.46, 73.33, 73.30, 73.26, 73.22, 73.14, 73.09, 71.23, 71.07, 69.64, 69.58, 69.42, 68.98, 68.62, 68.15, 68.13, 68.09, 60.70, 60.54 ppm. m/z (HRMS+) for $C_{48}H_{82}O_{41}Na$ $[M+Na]^+$ calcd. 1337.4224, found: 1337.4276.

Repurified RP-HPLC of **49** (ELSD trace, **Method C**, t_R= 33.7 min)

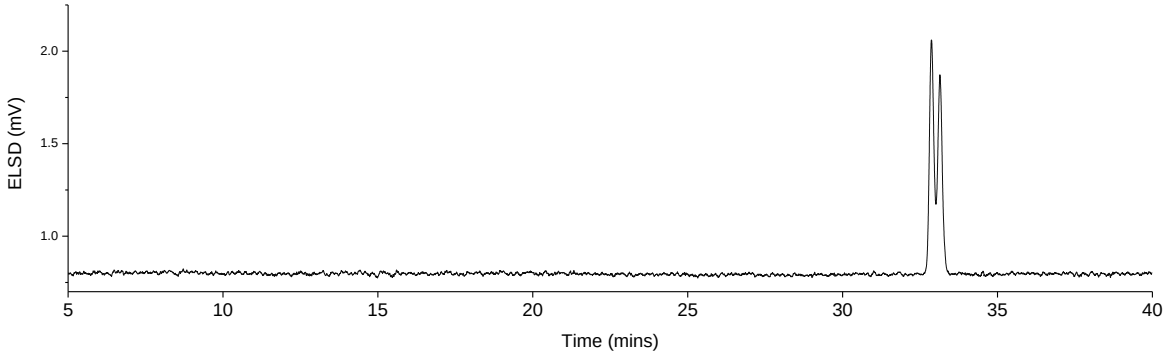

3.12.7. Synthesis of mix β-(1,3) and β-(1,6) octaglucoside (50)

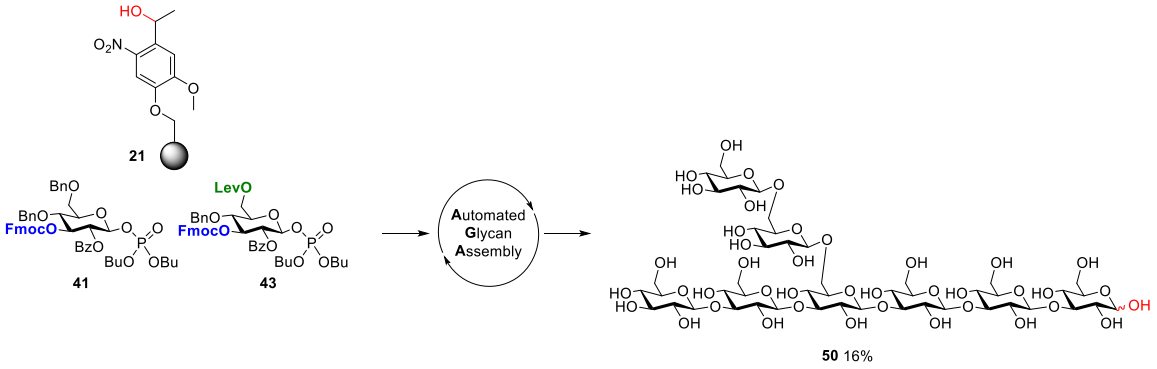

Automation sequence:

Cycles	Module	Conditions
	A: Resin Preparation for Synthesis	
3	B: Acidic Wash with TMSOTf Solution C: Phosphate Glycosylation D: Capping E: Fmoc Deprotection	BB**41** 4 eq, -30 °C for 10 min, -10 °C for 40 min
	B: Acidic Wash with TMSOTf Solution C: 2x Phosphate Glycosylation D: Capping E: Fmoc Deprotection	BB**43** 4 eq, -30 °C for 10 min, -10 °C for 40 min
2	B: Acidic Wash with TMSOTf Solution C: 2x Phosphate Glycosylation D: Capping E: Fmoc Deprotection	BB**41** 4 eq, -30 °C for 10 min, -10 °C for 40 min
	D: Capping F– 2x Lev Deprotection	
2	B: Acidic Wash with TMSOTf Solution C: 2x Phosphate Glycosylation D: Capping 2x Lev Deprotection	BB**43** 4 eq, -30 °C for 10 min, -10 °C for 40 min
	E: Fmoc Deprotection	

Post-Automation: **Module G – Methanolysis**, then **Photocleavage**, then **Module H – Hydrogenation**. The crude unprotected oligosaccharide was purified using reverse-phase preparative HPLC (**Method D**) to afford compound **50** (3.5 mg, 16% from resin **5**).

Analytical Data for **50**: ^{1}H-NMR (600 MHz, D_2O, both isomers) δ 5.11 (d, *J* = 3.7 Hz, 1H), 4.67 (d, *J* = 8.0 Hz, 5H), 4.64 – 4.59 (m, 8H), 4.55 (d, *J* = 8.0 Hz, 1H), 4.41 – 4.36 (m, 5H),

4.11 – 4.07 (m, 5H), 3.81 – 3.74 (m, 17H), 3.70 – 3.54 (m, 26H), 3.50 – 3.34 (m, 32H), 3.30 – 3.16 (m, 14H) ppm; ^{13}C-NMR (150 MHz, D_2O) δ 102.74, 102.72, 102.52, 102.43, 95.61, 91.91, 85.14, 84.63, 84.17, 83.75, 82.99, 75.93, 75.80, 75.53, 75.48, 75.45, 74.45, 74.38, 73.53, 73.38, 73.18, 73.14, 73.09, 72.99, 71.08, 70.75, 69.51, 68.67, 68.17, 68.15, 68.09, 68.06, 67.98, 60.63, 60.47 ppm. m/z (HRMS+) for $C_{48}H_{82}O_{41}Na$ $[M+Na]^+$ calcd. 1337.4224, found: 1337.4276.

RP-HPLC of **50** (ELSD trace, **Method C**, t_R= 33.5 min)

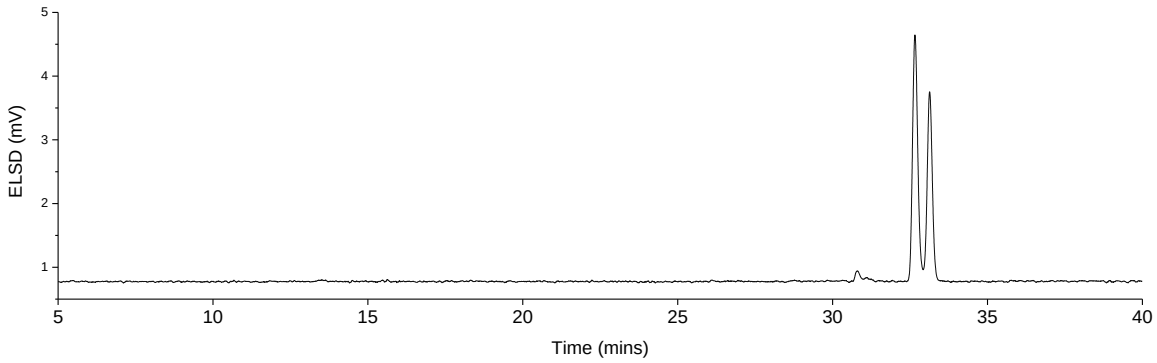

3.13. **Functional characterization of GH76**

3.13.1. Crystallization and structure determination GH76A^{WT} and GH76A^{mut}

For crystallization of GH76A^{WT}, 52 mg/mL concentration was used for setting up initial crystallization trial in three well crystallization plates using commercial crystallization screens. The plates were incubated at 16 °C. Initial hits were observed within 2-3 days of setting up the crystallization trials. The diffraction quality crystals were obtained using 0.2 M Magnesium chloride hexahydrate, 0.1 M Sodium acetate pH 5.0 and 20 % PEG 6000. Diffraction data was collected on beamline P14 at EMBL, DESY (Hamburg). A total of 3600 images were obtained. Each image was exposed for 0.1 seconds with 0.1° oscillation. Data were processed using XDS[136] and scaled using SCALA.[138] The structure was solved at 2 Å resolution using molecular replacement by searching Lin0763 protein from *Listeria innocua* (PDB ID 3K7X) as search model in PHASER,[139] respectively. For automatic model building, ARP/wARP[140] server was used. The initial model was refined using PHENIX.REFINE[141] and iterative rounds of the manual model building were carried out using COOT.[142] The final R/R_{free} of GH76A^{WT} structure is 18/22. There were no Ramachandran outliers in the build models.

For mutant, 5 mg/mL protein concentration was used to setup co-crystallization trays with 0.5 mg/mL of mannan-oligosaccharides in three well crystallization plates using commercial crystallization screens. The crystals were appeared after 2 months in 1.6 M tri-sodium citrate. Diffraction data was collected on beamline P11 at DESY (Hamburg). A total of 3600 images were obtained. Each image was exposed for 0.1 seconds with 0.1° oscillation. Data were processed using iMOSFLM[143] and scaled using SCALA. The structure was solved at 1.9 Å resolution using molecular replacement by searching $GH76A^{WT}$ as search model in PHASER, respectively. For automatic model building, phenix.autobuild[144] was used. The initial model was refined using PHENIX.REFINE and iterative rounds of the manual model building were carried out using COOT. The ligand mannotetrose was fitted using COOT and ligand refinement was performed in REFMAC5.[145] The final R/R_{free} of $GH76A^{mut}$ structure is 13/19. There were no Ramachandran outliers in the build models. Both WT and mutant protein structures were submitted to Protein Data Bank (PDB) and deposited as PDB ID: 6SHD and 6SHM, respectively.

3.13.2. Enzymatic digestion

10 μg of protein and 300 μg of oligosaccharide were mixed and incubated at 37 °C overnight. For yeast mannan, the incubation time was 30 min. The enzymatic reaction was stopped by heating at 95 °C for 10 min. The reaction mixture was filtered through 0.2 μm syringe filter and diluted 100 times with Milli-Q water. 100 μL of the diluted reaction mixture was injected to the HPLC. The individual mannosides **35-40** (25 μL) were injected in three different concentration as standards and their retention time were recorded.

3.13.3. HPAEC-PAD Analysis

Substrate digestion was analysed employing HPAEC-PAD with a Dionex CarboPac PA100 analytical column (2 × 250 mm). Using a binary pump, the flow rate was adjusted to 1 mL/min, starting from 100% Eluent A (100 mM NaOH in water) to 50% Eluent B (166mM NaOAc in water) following a linear gradient over 20.0 min.

4. References

1. A. Varki; R. Cummings; J. Esko; H. Freeze; P. Stanley; G. Hart; P.H. Seeberger,.; In *Essentials of glycobiology*, **2017**. *3rd ed*. pp 1-17.

2. Jane, J.; Lim, S.; Paetau, I.; Spence, K.; Wang, S., In *Polymers from Agricultural Coproducts*, **1994;** 575, pp 92-100.

3. Ghazarian, H.; Idoni, B.; Oppenheimer, S. B., *Acta Histochm* **2011,** *113* (3), 236-247.

4. Maverakis, E.; Kim, K.; Shimoda, M.; Gershwin, M. E.; Patel, F.; Wilken, R.; Raychaudhuri, S.; Ruhaak, L. R.; Lebrilla, C. B., *J Autoimmun* **2015,** *57*, 1-13.

5. Méndez-Huergo, S. P.; Blidner, A. G.; Rabinovich, G. A., *Curr. Opin. Immunol.* **2017,** *45*, 8-15.

6. Raman, R.; Raguram, S.; Venkataraman, G.; Paulson, J. C.; Sasisekharan, R., *Nat. Methods* **2005,** *2* (11), 817-824.

7. Stowell, S. R.; Arthur, C. M.; McBride, R.; Berger, O.; Razi, N.; Heimburg-Molinaro, J.; Rodrigues, L. C.; Gourdine, J.-P.; Noll, A. J.; von Gunten, S.; Smith, D. F.; Knirel, Y. A.; Paulson, J. C.; Cummings, R. D., *Nat. Chem. Biol.* **2014,** *10* (6), 470-476.

8. Taniguchi, N.; Miyoshi, E.; Jianguo, G.; Honke, K.; Matsumoto, A., *Curr. Opin. Struct. Biol.* **2006,** *16* (5), 561-566.

9. Mantelli, F.; Argüeso, P., *Curr Opin Allergy Cl.* **2008,** *8* (5), 477-483.

10. Akintayo, A.; Stanley, P., *Front Cell Dev Biol.* **2019,** *7*, 98-98.

11. Rajendran, L.; Simons, K., *J. Cell Sci.* **2005,** *118* (6), 1099.

12. Weintraub, A., *Carbohydr. Res.* **2003,** *338* (23), 2539-2547.

13. Daniels, C. C.; Rogers, P. D.; Shelton, C. M., *J Pediatr Pharmacol Ther.* **2016,** *21* (1), 27-35.

14. Steens, A.; Vestrheim, D. F.; Aaberge, I. S.; Wiklund, B. S.; Storsaeter, J.; Riise Bergsaker, M. A.; RØNning, K.; Furuseth, E., *Epidemiol Infect.* **2014,** *142* (12), 2471-2482.

15. Schumann, B.; Hahm, H. S.; Parameswarappa, S. G.; Reppe, K.; Wahlbrink, A.; Govindan, S.; Kaplonek, P.; Pirofski, L. A.; Witzenrath, M.; Anish, C.; Pereira, C. L.; Seeberger, P. H., *Sci Transl Med* **2017,** *9* (380).

16. Seeberger, P. H.; Pereira, C. L.; Govindan, S., *Beilstein J. Org. Chem.* **2017,** *13*, 164-173.

4 References

17. Amon, R.; Reuven, E. M.; Leviatan Ben-Arye, S.; Padler-Karavani, V., *Carbohydr. Res.* **2014,** *389*, 115-122.

18. Fujitani, N.; Furukawa, J.-i.; Araki, K.; Fujioka, T.; Takegawa, Y.; Piao, J.; Nishioka, T.; Tamura, T.; Nikaido, T.; Ito, M.; Nakamura, Y.; Shinohara, Y., *Proc. Natl. Acad. Sci.* **2013,** *110* (6), 2105.

19. Reis, C. A.; Osorio, H.; Silva, L.; Gomes, C.; David, L., *J Clin Path* **2010,** *63* (4), 322.

20. Ruhaak, L. R.; Miyamoto, S.; Lebrilla, C. B., *Mol Cell Proteom* **2013,** *12* (4), 846.

21. Danishefsky, S. J.; Shue, Y.-K.; Chang, M. N.; Wong, C.-H., *Acc. Chem. Res.* **2015,** *48* (3), 643-652.

22. Liu, Z.; Guo, J., *Carbohydr. Res.* **2017,** *452*, 78-90.

23. Huang, Y.-L.; Hung, J.-T.; Cheung, S. K. C.; Lee, H.-Y.; Chu, K.-C.; Li, S.-T.; Lin, Y.-C.; Ren, C.-T.; Cheng, T.-J. R.; Hsu, T.-L.; Yu, A. L.; Wu, C.-Y.; Wong, C.-H., *Proc. Natl. Acad. Sci.* **2013,** *110* (7), 2517.

24. Kelloff, G. J.; Hoffman, J. M.; Johnson, B.; Scher, H. I.; Siegel, B. A.; Cheng, E. Y.; Cheson, B. D.; Shaughnessy, J.; Guyton, K. Z.; Mankoff, D. A.; Shankar, L.; Larson, S. M.; Sigman, C. C.; Schilsky, R. L.; Sullivan, D. C., *Clin Cancer Res.* **2005,** *11* (8), 2785.

25. Scheen, A. J., *Diabetes Metab.* **1998,** *24* (4), 311-320.

26. Cheng, J. W. M., *Clin Ther.* **2002,** *24* (11), 1757-1769.

27. Tyers, M.; Mann, M., *Nature* **2003,** *422* (6928), 193-197.

28. Werz, D. B.; Ranzinger, R.; Herget, S.; Adibekian, A.; von der Lieth, C.-W.; Seeberger, P. H., *ACS Chem. Biol.* **2007,** *2* (10), 685-691.

29. Krasnova, L.; Wong, C.-H., *J. Am. Chem. Soc.* **2019,** *141* (9), 3735-3754.

30. Werz, D. B., In *Carbohydrate Microarrays: Methods and Protocols*, **2012**; pp 13-29.

31. Wu, Y.; Xiong, D. C.; Chen, S. C.; Wang, Y. S.; Ye, X. S., *Nat Commun* **2017,** *8*, 14851.

32. Zhu, X.; Schmidt, R. R., *Angew Chem Int Ed Engl* **2009,** *48* (11), 1900-1934.

33. Ranade, S. C.; Demchenko, A. V., *J. Carbohydr. Chem.* **2013,** *32* (1), 1-43.

34. Mucha, E.; Marianski, M.; Xu, F.-F.; Thomas, D. A.; Meijer, G.; von Helden, G.; Seeberger, P. H.; Pagel, K., *Nat. Commun.* **2018,** *9* (1), 4174.

35. van der Vorm, S.; Hansen, T.; van Hengst, J. M. A.; Overkleeft, H. S.; van der Marel, G. A.; Codée, J. D. C., *Chem. Soc. Rev.* **2019,** *48* (17), 4688-4706.

36. Mydock, L. K.; Demchenko, A. V., *Org. Biomol. Chem.* **2010,** *8* (3), 497-510.

37. Hahm, H. S.; Hurevich, M.; Seeberger, P. H., *Nat Commun* **2016,** *7*, 12482.

38. Crich, D.; Dai, Z., *Tetrahedron* **1999,** *55* (6), 1569-1580.

39. Ganesh, N. V.; Fujikawa, K.; Tan, Y. H.; Stine, K. J.; Demchenko, A. V., *Org. Lett.* **2012,** *14* (12), 3036-3039.

40. Satoh, H.; Hansen, H. S.; Manabe, S.; van Gunsteren, W. F.; Hünenberger, P. H., *J. Chem. Theory Comput.* **2010,** *6* (6), 1783-1797.

41. Kafle, A.; Liu, J.; Cui, L., *Can. J. Chem.* **2016,** *94* (11), 894-901.

42. Braccini, I.; Derouet, C.; Esnault, J.; de Penhoat, C. H. e.; Mallet, J. M.; Michon, V.; Sinaÿ, P., *Carbohydr. Res.* **1993,** *246* (1), 23-41.

43. Wu, C.-Y.; Wong, C.-H., In *Glycoscience: Biology and Medicine*, **2015**; pp 45-52.

44. Nokami, T.; Hayashi, R.; Saigusa, Y.; Shimizu, A.; Liu, C. Y.; Mong, K. K.; Yoshida, J., *Org. Lett.* **2013,** *15* (17), 4520-4523.

45. Manmode, S.; Sato, T.; Sasaki, N.; Notsu, I.; Hayase, S.; Nokami, T.; Itoh, T., *Carbohydr. Res.* **2017,** *450*, 44-48.

46. Nokami, T.; Isoda, Y.; Sasaki, N.; Takaiso, A.; Hayase, S.; Itoh, T.; Hayashi, R.; Shimizu, A.; Yoshida, J., *Org. Lett.* **2015,** *17* (6), 1525-1528.

47. Tang, S. L.; Pohl, N. L., *Org. Lett.* **2015,** *17* (11), 2642-2645.

48. Tang, S. L.; Pohl, N. L., *Carbohydr. Res.* **2016,** *430*, 8-15.

49. Tang, S. L.; Linz, L. B.; Bonning, B. C.; Pohl, N. L., *J. Org. Chem.* **2015,** *80* (21), 10482-10489.

50. Saliba, R. C.; Wooke, Z. J.; Nieves, G. A.; Chu, A. A.; Bennett, C. S.; Pohl, N. L. B., *Org. Lett.* **2018,** *20*, 3, 800-803.

51. Chai, Y. H.; Feng, Y. L.; Wu, J. J.; Deng, C. Q.; Liu, A. Y.; Zhang, Q., *Chin Chem Lett* **2017,** *28* (8), 1693-1700.

52. Meng, S.; Tian, T.; Wang, Y. H.; Meng, X. B.; Li, Z. J., *Org. Biomol. Chem.* **2016,** *14* (32), 7722-30.

53. Merrifield, R. B., *Science* **1965,** *150* (3693), 178-85.

54. Caruthers, M., *Science* **1985,** *230* (4723), 281-285.

55. Plante, O. J.; Palmacci, E. R.; Seeberger, P. H., *Science* **2001,** *291* (5508), 1523-1527.

56. Hahm, H. S.; Schlegel, M. K.; Hurevich, M.; Eller, S.; Schuhmacher, F.; Hofmann, J.; Pagel, K.; Seeberger, P. H., *Proc. Natl. Acad. Sci. U. S. A.* **2017,** *114* (17), E3385-E3389.

57. Seeberger, P. H., *Acc. Chem. Res.* **2015,** *48* (5), 1450-1463.

58. Routenberg Love, K.; Seeberger, P. H., *Angew Chem Int Ed Engl* **2004,** *43* (5), 602-605.

59. Krock, L.; Esposito, D.; Castagner, B.; Wang, C. C.; Bindschadler, P.; Seeberger, P. H., *Chem Sci* **2012,** *3* (5), 1617-1622.

60. Eller, S.; Collot, M.; Yin, J.; Hahm, H. S.; Seeberger, P. H., *Angew Chem Int Ed Engl* **2013,** *52* (22), 5858-5861.

61. Wilsdorf, M.; Schmidt, D.; Bartetzko, M. P.; Dallabernardina, P.; Schuhmacher, F.; Seeberger, P. H.; Pfrengle, F., *Chem Comm* **2016,** *52* (66), 10187-10189.

62. Le Mai Hoang, K.; Pardo-Vargas, A.; Zhu, Y.; Yu, Y.; Loria, M.; Delbianco, M.; Seeberger, P. H., *J. Am. Chem. Soc.* **2019,** *141* (22), 9079-9086.

63. Delbianco, M.; Kononov, A.; Poveda, A.; Yu, Y.; Jiménez-Barbero, J.; Seeberger, P. H. *J. Am. Chem. Soc.* **2018,** *140* (16), 5421-5426.

64. Yu, Y.; Kononov, A.; Delbianco, M.; Seeberger, P. H. *Chem.: Eur. J.* **2018,** *24* (23), 6075-6078.

65. Naresh, K.; Schumacher, F.; Hahm, H. S.; Seeberger, P. H., *Chem. Comm.* **2017,** *53* (65), 9085-9088.

66. Lai, C. H.; Hahm, H. S.; Liang, C. F.; Seeberger, P. H., *Beilstein J. Org. Chem.* **2015,** *11*, 617-621.

67. Fair, R. J.; Hahm, H. S.; Seeberger, P. H., *Chem Comm* **2015,** *51* (28), 6183-5.

68. Liang, C.-F.; Hahm, H. S.; Seeberger, P. H., In *Glycosaminoglycans: Chemistry and Biology*, **2015**; pp 3-10.

69. Hahm, H. S.; Broecker, F.; Kawasaki, F.; Mietzsch, M.; Heilbronn, R.; Fukuda, M.; Seeberger, P. H., *Chem* **2017,** *2* (1), 114-124.

70. Hahm, H. S.; Liang, C. F.; Lai, C. H.; Fair, R. J.; Schuhmacher, F.; Seeberger, P. H., *J. Org. Chem.* **2016,** *81* (14), 5866-5877.

71. Hofmann, J.; Hahm, H. S.; Seeberger, P. H.; Pagel, K., *Nature* **2015,** *526* (7572), 241-244.

72. Nagy, G.; Peng, T.; Pohl, N. L. B., *Anal Methods* **2017,** *9* (24), 3579-3593.

73. Geert Volbeda, A.; van Mechelen, J.; Meeuwenoord, N.; Overkleeft, H. S.; van der Marel, G. A.; Codee, J. D. C., *J. Org. Chem.* **2017,** *82* (24), 12992-13002.

74. Pistorio, S. G.; Nigudkar, S. S.; Stine, K. J.; Demchenko, A. V., *J. Org. Chem.* **2016,** *81* (19), 8796-8805.

75. Broecker, F.; Seeberger, P. H., *Methods Mol Biol* **2017,** *1518*, 227-240.

76. Seeberger, P. H., *Perspect Sci* **2017,** *11* (Supplement C), 11-17.

77. Weishaupt, M. W.; Hahm, H. S.; Geissner, A.; Seeberger, P. H., *Chem Comm* **2017,** *53* (25), 3591-3594.

78. Schmidt, D.; Schuhmacher, F.; Geissner, A.; Seeberger, P. H.; Pfrengle, F., *Chem Eur J* **2015,** *21* (15), 5709-13.

79. Dallabernardina, P.; Schuhmacher, F.; Seeberger, P. H.; Pfrengle, F., *Org. Biomol. Chem.* **2016,** *14* (1), 309-313.

80. Bartetzko, M. P.; Schuhmacher, F.; Hahm, H. S.; Seeberger, P. H.; Pfrengle, F., *Org. Lett.* **2015,** *17* (17), 4344-4347.

81. Ruprecht, C.; Bartetzko, M. P.; Senf, D.; Dallabernadina, P.; Boos, I.; Andersen, M. C. F.; Kotake, T.; Knox, J. P.; Hahn, M. G.; Clausen, M. H.; Pfrengle, F., *Plant Physiol.* **2017,** *175* (3), 1094-1104.

82. Dallabernardina, P.; Ruprecht, C.; Smith, P. J.; Hahn, M. G.; Urbanowicz, B. R.; Pfrengle, F., *Org. Biomol. Chem.* **2017,** *15* (47), 9996-10000.

83. Bartetzko, M. P.; Schuhmacher, F.; Seeberger, P. H.; Pfrengle, F., *J. Org. Chem.* **2017,** *82* (3), 1842-1850.

84. Dallabernardina, P.; Schuhmacher, F.; Seeberger, P. H.; Pfrengle, F., *Chem Eur J* **2017,** *23* (13), 3191-3196.

85. Senf, D.; Ruprecht, C.; de Kruijff, G. H.; Simonetti, S. O.; Schuhmacher, F.; Seeberger, P. H.; Pfrengle, F., *Chem Eur J* **2017,** *23* (13), 3197-3205.

86. Pfrengle, F., *Curr. Opin. Chem. Biol.* **2017,** *40*, 145-151.

87. Weishaupt, M. W.; Matthies, S.; Hurevich, M.; Pereira, C. L.; Hahm, H. S.; Seeberger, P. H., *Beilstein J. Org. Chem.* **2016,** *12*, 1440-1446.

88. Delbianco, M.; Bharate, P.; Varela-Aramburu, S.; Seeberger, P. H., *Chem Rev* **2016,** *116* (4), 1693-1752.

89. WHO, World Health Organization: Geneva, Switzerland, 2018.

90. Angala, S. K.; Palčeková, Z.; Belardinelli, J. M.; Jackson, M., *Nat. Chem. Biol.* **2018,** *14*, 193-198.

91. Besra, G. S.; Khoo, K.; McNeil, M. R.; Dell, A.; Morris, H. R.; Brennan, P. J., *Biochem.* **1995,** *34* (13), 4257-4266.

92 Shi, L.; Berg, S.; Lee, A.; Spencer, J. S.; Zhang, J.; Vissa, V.; McNeil, M. R.; Khoo, K.-H.; Chatterjee, D., *J. Biol. Chem.* **2006,** *281* (28), 19512-19526.

93 Briken, V.; Porcelli, S. A.; Besra, G. S.; Kremer, L., *Mol. Microbiol.* **2004,** *53* (2), 391-403.

94. Owens, N. A.; Young, C. C.; Laurentius, L. B.; De, P.; Chatterjee, D.; Porter, M. D., *Anal. Chim. Acta* **2019,** *1046*, 140-147.

95. Sigal, G. B.; Pinter, A.; Lowary, T. L.; Kawasaki, M.; Li, A.; Mathew, A.; Tsionsky, M.; Zheng, R. B.; Plisova, T.; Shen, K.; Katsuragi, K.; Choudhary, A.; Honnen, W. J.; Nahid, P.; Denkinger, C. M.; Broger, T., *J. Clin. Microbiol.* **2018,** *56* (12), e01338-18.

96. Chang, Y.; Meng, X.; Li, Y.; Liang, J.; Li, T.; Meng, D.; Zhu, T.; Yu, P., *MedChemComm* **2019,** *10* (4), 543-553.

97. Amin, A. G.; De, P.; Spencer, J. S.; Brennan, P. J.; Daum, J.; Andre, B. G.; Joe, M.; Bai, Y.; Laurentius, L.; Porter, M. D.; Honnen, W. J.; Choudhary, A.; Lowary, T. L.; Pinter, A.; Chatterjee, D., *Tuberculosis* **2018,** *111*, 178-187.

98. Choudhary, A.; Patel, D.; Honnen, W.; Lai, Z.; Prattipati, R. S.; Zheng, R. B.; Hsueh, Y. C.; Gennaro, M. L.; Lardizabal, A.; Restrepo, B. I.; Garcia-Viveros, M.; Joe, M.; Bai, Y.; Shen, K.; Sahloul, K.; Spencer, J. S.; Chatterjee, D.; Broger, T.; Lowary, T. L.; Pinter, A., *J. Immunol.* **2018,** *200* (9), 3053-3066.

99. Counoupas, C.; Pinto, R.; Nagalingam, G.; Britton, W. J.; Triccas, J. A., *Vaccine* **2018,** *36* (19), 2619-2629.

100. Lindenstrøm, T.; Agger, E. M.; Korsholm, K. S.; Darrah, P. A.; Aagaard, C.; Seder, R. A.; Rosenkrands, I.; Andersen, P., *J. Immunol.* **2009,** *182* (12), 8047-8055.

101. Maiti, K.; Syal, K.; Chatterji, D.; Jayaraman, N., *ChemBioChem* **2017,** *18* (19), 1959-1970.

102. Sahloul, K.; Lowary, T. L., *J. Org. Chem.* **2015,** *80* (22), 11417-11434.

103. Hölemann, A.; Stocker, B. L.; Seeberger, P. H., *J. Org. Chem.* **2006,** *71* (21), 8071-8088.

104. Wu, Y.; Xiong, D.-C.; Chen, S.-C.; Wang, Y.-S.; Ye, X.-S., *Nat. Commun.* **2017,** *8* (1), 14851-7.

105. Guberman, M.; Seeberger, P. H., *J. Am. Chem. Soc.* **2019,** *141* (14), 5581-5592.

106. Kandasamy, J.; Hurevich, M.; Seeberger, P. H., *Chem. Commun.* **2013,** *49* (40), 4453-4455.
107. Hahm, H. S.; Schlegel, M. K.; Hurevich, M.; Eller, S.; Schuhmacher, F.; Hofmann, J.; Pagel, K.; Seeberger, P. H., *Proc. Natl. Acad. Sci. U. S. A.* **2017,** *114* (17), E3385-E3389.

108. Pardo-Vargas, A.; Delbianco, M.; Seeberger, P. H., *Curr. Opin. Chem. Biol.* **2018,** *46*, 48-55.

109. Eller, S.; Collot, M.; Yin, J.; Hahm, H. S.; Seeberger, P. H., *Angew Chem Int Ed Engl* **2013,** *52* (22), 5858-61.

110. Yu, Y.; Kononov, A.; Delbianco, M.; Seeberger, P. H., *Chem.: Eur. J.* **2018,** *24* (23), 6075-6078.

111. Naresh, K.; Schumacher, F.; Hahm, H. S.; Seeberger, P. H., *Chem. Comm.* **2017,** *53* (65), 9085-9088.

112. Ma, S.; Tang, N.; Tian, J., *Curr. Opin. Chem. Biol.* **2012,** *16* (3-4), 260-7.

113. Delbianco, M.; Kononov, A.; Poveda, A.; Yu, Y.; Diercks, T.; Jimenez-Barbero, J.; Seeberger, P. H., *J. Am. Chem. Soc.* **2018,** *140* (16), 5421-5426.

114. Le Mai Hoang, K.; Pardo-Vargas, A.; Zhu, Y.; Yu, Y.; Loria, M.; Delbianco, M.; Seeberger, P. H., *J. Am. Chem. Soc.* **2019,** *141* (22), 9079-9086.

115. van der Vorm, S.; Hansen, T.; van Hengst, J. M. A.; Overkleeft, H. S.; van der Marel, G. A.; Codee, J. D. C., *Chem. Soc. Rev.* **2019,** *48* (17), 4688-4706.

116. Matsumoto, T.; Maeta, H.; Suzuki, K.; Tsuchihashi, l. G.-i., *Tetrahedron Lett.* **1988,** *29* (29), 3567-3570.

117. Hofmann, J.; Hahm, H.; Seeberger, PH, *Nature.* **2015** 526 (7572),241-244.

118. Mucha, E.; Marianski, M.; Xu, F.; Seeberger, PH.; Pagel, K. *Nat Commun* **2018,** 9, 4174

119. Mucha, E.; González Flórez, A. I.; Marianski, M.; Thomas, D. A.; Hoffmann, W.; Struwe, W. B.; Hahm, H. S.; Gewinner, S.; Schöllkopf, W.; Seeberger, P. H.; von Helden, G.; Pagel, K, *Angew. Chem. Int. Ed.* **2017**, *56*, 11248.

120. Rauschenbach, S.;Ternes, M.; Harnau, L.; Kern, K, *Annu Rev Anal Chem*. **2016,** 9.

121. Longchamp, J.; Rauschenbach, S.; Abb, S.; Escher, C.; Latychevskaia, T.; Kern, K.; *Proc. Natl. Acad. Sci. U.S.A* **2017**, 114, (7), 1474-1479.

122. Pardo-Vargas, A.; Bharate, P.; Delbianco, M.; Seeberger, P. H. *Beilstein J. Org. Chem.* **2019,** *15*, 2936–2940.

123. Abb. S.; Tarrat, N.; Cortés, J.; Andriyevsky, B.; Harnau, L.; Schön, J. C.; Rauschenbach, S.; Kern, K., *Angew. Chem. Int. Ed.* **2019**, *58*, 8336.

124. Field, C. B.; Behrenfeld, M. J.; Randerson, J. T.; Falkowski, P. *Science* **1998**, 281,237–240.

125. Becker, S.; Scheffel, A.; Polz, M. F.; Hehemann, J.-H. A*ppl. Environ. Microbiol.* **2017,** 83 (9) e03389-16.

126. Reisky, L.; Préchoux, A.; Zühlke, Becher, D.; M.; Schweder, T.; Bornscheuer, U.; Hehemann, J.; *et al. Nat Chem Biol* **2019,** 15, 803–812.

127. Wargacki, A. J.; Lakshmanaswamy, A.; Kashiyama, Y.; Baker, D.; Yoshikuni, Y. *Science* **2012**, 335, 308-313.

128. Pagarete, A.; Kusonmano, K.; Petersen, K.; Kimmance, S. A.; Martinez Martinez, J.; Wilson, W. H.; Hehemann J.-H.; Allen M. J., Sandaa, R.-A. *Virology*, **2014,** 466, 129–137.

129. Chen, J.; Robb, C.S.; Unfried, F.; Kappelmann, L.; Markert, S.; Song, T.; Harder, J.; Avcı, B.; Becher, D.; Xie, P.; Amann, R.I.; Hehemann, J.-H.; Schweder, T.; Teeling, H. *Environ Microbiol* **2018**, 20, 4127-4140.

130. Kappelmann, L.; Krüger, K.; Hehemann, J. *ISME J* **2019**, 13, 76–91.

131. Ndeh, D.; Rogowski, A.; Cartmell, A.; Davies, G.; Abbott, D.; Ralet, M.; Martens, E.; Henrissat, B.; Gilbert, H. *Nature* **2017**, 544, 65-70.

132. Cuskin, F.; Lowe, E.; Temple, M.; *Nature* **2015**, 517, 165-169.

133. Helenius, A.; Aebi, M. *Science* **2001**, 291, 2364-2369.

134. Spreghini, E.; Davis, D. A.; Subaran, R.; Kim, M.; Mitchell, A. P. *Eukaryot Cell* **2003**, 2, 746-755.

135. Kitagaki, H.; Ito, K.; Shimoi, H. *Eukaryot Cell* **2004**, 3, 1297-1306.

136. Kabsch, W. XDS. *Acta Crystallogr D Biol Crystallogr* **2010**, 66, 125-132.

137. Weishaupt, M. W.; Hahm, H. S.; Geissner, A.; Seeberger, P. H. *Chem. Commun.* **2017**, *53*, 3591– 3594.

138. Evans, P. *Acta Crystallogr D Biol Crystallogr* **2006**, 62, 72-82.

139. McCoy, A. J. *J Appl Crystallogr* **2007**, 40, 658-674.

140. Cohen, S. X. *Acta Crystallogr D Biol Crystallogr* **2008**, 64, 49-60.

141. Afonine, P. V. *Acta Crystallogr D Biol Crystallogr* **2012**, 68, 352-367.

142. Emsley, P., Lohkamp, B., Scott, W. G. & Cowtan, K. *Acta Crystallogr D Biol Crystallogr* **2010**, 66, 486-501.

143. Battye, T. G., Kontogiannis, L., Johnson, O., Powell, H. R. & Leslie, A. G.. *Acta Crystallogr D Biol Crystallogr* **2011**, 67, 271-281.

144. Terwilliger, T. C *Acta Crystallogr D Biol Crystallogr* **2008**, 64, 61-69.

145. Murshudov, G. N. *Acta Crystallogr D Biol Crystallogr* **2011**, 67, 355-367.